HUNGARIAN UNIVERSITY OF
AGRICULTURE AND LIFE SCIENCES

Hungarian University of Agriculture and Life Sciences

Experimental honey bee studies using non-invasive imaging methods

TAMÁS SIPOS

KAPOSVÁR

2026

Name of the doctoral school:	DOCTORAL SCHOOL OF AGRICULTURE AND FOOD SCIENCES
Discipline:	ANIMAL SCIENCE
The Head of Doctoral School:	PROF. DR. MELINDA KOVÁCS Professor, MHAS MATE, Institute of Animal Physiology and Nutrition
The Head of the Doctoral Program:	PROF. DR. ANDRÁS SZABÓ Professor, DSc MATE, Institute of Animal Physiology and Nutrition Department of Animal Physiology and Health
Supervisors:	PROF. DR. SÁNDOR KESZTHELYI Professor, PhD MATE, Institute of Agronomy Department of Agronomy
	DR. TAMÁS DONKÓ Honorary Associate Professor, PhD Medicopus Nonprofit Ltd.

....	……...
Approval of the Head of Doctoral School	Approval of the Supervisor(s)

Table of contents

LIST OF ABBREVIATIONS

ABPV	**Acute Bee Paralysis Virus**
AGID	**Agar Gel Immunodiffusion**
BQCV	**Black Queen Cell Virus**
CBPV	**Chronic Bee Paralysis Virus**
CCD	**Colony Collapse Disorder**
CLSM	**Confocal Laser Scanning Microscopy**
CT	**Computed Tomography**
DHC	**Differential Hemocyte Count**
DICOM	**Digital Imaging and Communications in Medicine**
DNA	**Deoxyribonucleic Acid**
DWV	**Deformed Wing Virus**
ELISA	**Enzyme-linked Immunosorbent Assay**
FRP	**Fibre-reinforced Composite Product**
FRPW	**Fibre-reinforced Composite Product with Wax**
Gy	**Gray**
HU	**Hounsfield Unit**
IAPV	**Israeli Acute Paralisis Virus**
IPM	**Integrated Pest Management**
IR	**Infrared**
IRAC MoA	**Insecticide Resistance Action Committee, Mode of Action**
KBV	**Kashmir Bee Virus**
MNR	**Mite Non Reproduction**
NB	**Nagyboczonádi**
NIFTI	**Neuroimaging Informatics Technology Initiative**
NMRI	**Nuclear Magnetic Resonance Imaging**
PCR	**Polymerase Chain Reaction**
Pdd	**Dark Brown-eyed Pupae with Dark Thorax**
Pdl	**Dark Brown-eyed Pupae with Light Pigmented Thorax**
PP	**Polypropylene**
Pr	**Red-eyed Pupa**
RNA	**Ribonucleic Acid**
RT-PCR	**Real Time Polymerase Chain Reaction**
SBPV	**Sacbrood Virus**

SBV	**Sacbrood Virus**
SMR	**Supressed Mite Reproduction**
THC	**Total Hemocyte Count**
VP	**Viral Protein**
VSH	**Varroa Sensitive Hygene**
µ-CT	**Micro Computed Tomography**

1. INTRODUCTION

One of the major global ecological challenges of our time is the drastic decline in pollinator species diversity and population size. Among the affected groups, one of the most well-known and at the same time most vulnerable species from a human perspective is the Western honey bee (*Apis mellifera* L., 1758), (Hymenoptera: Apidae) (henceforward: *A. mellifera*), which is also registered as a managed livestock species. As a key component in maintaining ecological cycles, this insect species is currently exposed to numerous negative pressures, including the decline in floral resource diversity, intoxication resulting from inappropriate chemical use, and, not least, the transcontinental spread and increasing damage pressure of honey bee specific parasites (both microbial and arthropod) (Rosenkranz *et al*., 2010; Martin *et al*., 2012; Mordecai *et al*., 2015; Morfin *et al*., 2020). Within this complex, the Varroa mite (*Varroa destructor* Anderson and Trueman, 2000), (Arachnida: Varroidae) (henceforward: *V. destructor*) originating from the Far East, can be highlighted as the most significant threat, by the severe damage it causes to *A. mellifera* colonies (Anderson and Trueman, 2000; Evans and Chen, 2021; Warner *et al*., 2024).

Following the global spread of the parasite, apicultural research has extensively focused on the biology and morphology of *V. destructor,* as well as on understanding the possible infestation pathways of *A. mellifera* colonies (Rosenkranz *et al*., 2010; Dietemann *et al*., 2012). The primary objective of these studies was to identify potential control strategies and effective acaricidal treatments to reduce damage. By now, it can be stated that these applied and practice-oriented research efforts have reduced the occurrence of large-scale or total colony losses caused by the parasite; however, a comprehensive solution has not yet been achieved (Rosenkranz *et al*., 2010; Kolics *et al*., 2021; Warner *et al*., 2024). The use of conventionally applied acaricidal products is currently declining due to increasingly strict honey quality standards, expectations related to healthy lifestyles, and the development of resistance (Jack and Ellis, 2021; Mitton *et al*., 2022). At present, neither conventional nor alternative acaricidal products, nor biological methods, can guarantee the complete elimination of parasite damage in practice, and selective breeding efforts have also failed to provide a fully effective solution for commercial beekeeping operations (Le Conte *et al*., 2020; Jack and Ellis, 2021). The emergence of acaricide resistance places increasing pressure on the demand for novel control agents (Kolics *et al*., 2021; Mitton *et al*., 2022). As a practicing beekeeper, I consider research aimed at addressing this severe problem to be of particular importance; therefore, the *V. destructor* was selected as the target organism, and the exploration of imaging-based approaches in honey bee health research became the focus of my doctoral thesis.

The pathologies induced by the mite manifest at both individual and social levels and are difficult to quantify due to its hidden lifestyle. *V. destructor* exhibits two major life cycles: a phoretic phase, enabling transmission between colonies, and a reproductive cycle responsible for population maintenance (Rosenkranz *et al*., 2010; Warner *et al*., 2024). Damage primarily occurs at the individual level during *A. mellifera* development within sealed brood cells, which may escalate to disturbances in the social behavior of the superorganism-level colony (Rosenkranz, 2010; Ramsey *et al*., 2019; Warner *et al*., 2024). Feeding on the developing pupae fat body and hemolymph leads to reduced lipid synthesis, impairing energy metabolism and consequently affecting protein synthesis quality (Ramsey *et al*., 2019; Han *et al*., 2024). Reduced lipid and protein synthesis compromises metabolic turnover and increases susceptibility of the immune system. Additional consequences include decreased tolerance to pesticides (Bowen-Walker and Gunn, 2001; van Dooremalen *et al*., 2013; Ramsey *et al*., 2019; Morfin *et al*., 2022).

Reduced body mass and abdominal deformities are clearly observable in adult bees at the end of development. In worker bees, body mass reduction averages approximately 7% compared to intact adults (De Jong *et al*., 1982; Bowen-Walker and Gunn, 2001). This reduction is more pronounced in drones, reaching 11-19% depending on the degree of parasitism (Duay *et al*., 2003). Reduced body mass or impaired wing development – particularly in cases of Deformed Wing Virus (DWV) infection – leads to diminished functionality of worker bees (Martin *et al*., 2012). In workers, this results in an earlier shift to foraging tasks or, in some cases, failure to initiate flight activity, significantly shortening lifespan and generating energetically inefficient investment for the colony (De Jong *et al*., 1982; Amdam *et al*., 2004). Additionally, impaired orientation abilities have been observed in workers damaged during development, contributing further to colony weakening through increased loss of disoriented individuals (Martin *et al*., 2012; Mordecai *et al*., 2015). Overall, the severity of varroatosis – *i.e.*, the disease complex induced by the mite – is mostly influenced by mite population size and the viruses transmitted by the parasite. These effects may be further exacerbated by environmental stressors, such as reduced pollen quality, harmful effects of plant protection products, and energy deficits caused by periodic nectar shortages (van Dooremalen *et al*., 2013; Corby-Harris *et al*., 2019; Morfin *et al*., 2020).

There is an urgent need for to develop novel diagnostic methods enabling improved characterization of the hidden lifestyle, biology, and damage of *V. destructor*. Within entomological research – and particularly in apicultural sciences – the application of digital imaging techniques remains limited (Facchini et al., 2019). These diagnostic technologies such as diagnostic computed tomography (CT), micro-computed tomography (micro-CT), and infrared thermography are novel in this field and, in certain cases, allow deeper insights into the superorganism-level of the *A. mellifera* colony, anatomy and biology, as well as the biology and the damage of *V. destructor* (Alba-Tercedor and Alba-Alejandre, 2017; Castejón *et al*., 2018; Facchini *et al*., 2019; De Paula *et al*., 2022). The initial application of X-ray radiation in entomological research was primarily aimed at developing pest control strategies, such as the sterile insect technique (Hallman, 2013). Although the radiation doses applied in diagnostic CT and micro-CT examinations do not reach the gray (Gy) levels used in such control experiments, they may nevertheless influence individual vitality. Therefore, to investigate the tolerance of *A. mellifera* and *V. destructor* to X-ray radiation is important, thereby establishing foundational knowledge for the application of ionizing radiation-based imaging techniques in apicultural research (Wipfler *et al*., 2016; Hall and Martín-Vega, 2019; Facchini *et al*., 2019).

Based on these considerations, the primary objectives of the doctoral research were to address several previously unanswered questions, using a completely novel, non-invasive methodological approach. In line with this hypothesis, the specific aims of the study were as follows:

1. To evaluate the applicability and to establish objective parameters of imaging techniques (human diagnostic CT, micro-CT, and infrared imaging) for the detection of *V. destructor* and comb cell deformations.
2. To assess the presence of *Varroa destructor* within brood cells and to evaluate its effects on preimaginal developmental stages of honey bees, with particular emphasis on body deformities and changes in tissue density.
3. To further investigate and confirm the indirect relationship between the presence of *V. destructor* and social fever using infrared thermography under field conditions.
4. As a complementary objective, to examine the effect of comb wear, expressed as available brood cell volume, on normal and deformed *A. mellifera* pupae.
5. To evaluate the potential effects of ionizing radiation associated with CT diagnostic procedures on the host *A. mellifera* and parasite *V. destructor* viability, as well as to assess possible histological alterations in the host organism.

The long-term goal of these investigations is to develop research methodologies applicable to apicultural research that can support practical and theoretical efforts in the ongoing struggle against *V. destructor*, which has persisted for over 70 years.

2. LITERATURE REVIEW

2.1. Factors affecting the beekeeping sector adapted to Hungarian conditions

One of the fundamental pillars of sustainable crop production is the protection of pollinator organisms, with particular emphasis on honey bees and the support of their beneficial ecosystem services. These objectives necessarily include the objective assessment of biotic and abiotic stressors affecting the beekeeping sector, which is of strategic importance in Hungary despite its relatively small economic volume, as well as the development and practical implementation of technological solutions that minimize harm to these beneficial organisms (USDA, 2016; Potts *et al*., 2016; Hung *et al*., 2018). A stable beekeeping sector is in the shared interest of crop production, agriculture as a whole and society. It relies on maintaining colony health, improving production systems and ensuring economically viable production (Leonhardt *et al*., 2013; Feketéné Ferenczi *et al*., 2023).

The emergence of biotic agents, including invasive species, alongside abiotic stressors caused by global climate change, poses a significant challenge to modern agriculture and the beekeeping industry. The greatest threat to beekeeping worldwide and in Hungary is the *V. destructor* ectoparasites, which has been spreading since the 1970s. (Rosenkranz *et al*., 2010; Traynor *et al*., 2020). Its impact raises serious honey bee health concerns and economic losses, with annual colony losses reaching 20-30% in some regions. In parallel, weather anomalies associated with global climate change constitute an additional major concern for beekeeping, most manifested in prolonged mild autumn periods and highly variable, unpredictable temperature fluctuations (Belsky and Joshi, 2019; Neoy *et al*., 2019). These effects influence the pollen and nectar production of major honey plants and bee pastures (e.g., black locust, linden, oilseed rape, sunflower, phacelia), thereby affecting forage availability (Farkas and Zajácz, 2007). Furthermore, climatic stressors impact foraging activity, colony foraging potential, worker and colony vitality, developmental dynamics, behavioural traits, and the adaptive capacity *A. mellifera* colonies to changing environmental conditions (Polatto *et al*., 2014; Benett *et al*., 2022).

The European honey market is the second-largest honey-producing region globally, and among participating countries, Hungary holds a leading position with an annual honey production of approximately 25-28 thousand tonnes (Popescu *et al*., 2021). Owing to its favourable natural conditions, Hungary is capable of high honey yields; however, the sector is strongly export-oriented and therefore highly dependent on global honey market dynamics (Farkas and Zajácz, 2008; Feketéné Ferenczi *et al*., 2023). Financial deficits arising from marketing difficulties represent a serious challenge for producers and indirectly exert negative effects on honey bee health and the overall development of the beekeeping sector (Feketéné Ferenczi *et al.*, 2024).

The challenges facing the Hungarian beekeeping sector are comprehensively summarised by a study conducted in 2024 based on the responses of 632 producers, which assessed the perceived severity of various stress factors. Among biotic factors, *V. destructor* and nosemosis were identified as the most impactful threats, while among abiotic factors, pesticide-related production losses represented the most severe problem. These challenges are further compounded by marketing difficulties and unfavourable honey market conditions, which together pose substantial concerns for producers (Neov *et al.*, 2019; Feketéné Ferenczi *et al*., 2024). Collectively, these factors justify the need for objective, non-invasive assessment of stressors affecting *A. mellifera* colonies, with particular emphasis on revealing the concealed damage caused by *V. destructor* and achieving a more comprehensive understanding of the *V. destructor*-*A. mellifera* complex.

2.2. Biology and ecology of *Apis mellifera*

2.2.1. Taxonomical and general biological features of *Apis mellifera*

The *A. mellifera* is one of the most extensively studied and cosmopolitan species among eusocial insects. Its long-standing and close relationship with humans is well illustrated by its prominent role as a sacred animal in several historical periods and advanced civilisations (Crane, 1999; Foster, 2020). The oldest known depiction of human-honey bee interaction dates back approximately 15,000 years and originates from a rock painting in the Cuevas de la Arana cave in Spain, which portrays human figures engaged in the plundering of a honey bee colony and the collection of honey (Dams, 1978). Archaeological evidence of organised apicultural activity, represented by material remains dating to the 9th-10th centuries BC was discovered near the ancient city of Tel Rehov in present-day Israel, where the remains of a complete production-scale apiary were uncovered (Mazar and Paintz-Cohen, 2022). In early forms of beekeeping, honey harvesting imposed a substantial burden on colonies due to the absence of movable-frame systems (Crane, 1999). The principles and advantages of modern frame-based beekeeping, which are compatible with contemporary apicultural requirements, were not recognised until the mid-18th century, when they were gradually adopted (Crane, 1999).

The honey bee is a species of insect that belongs to the group of true social insects and forms colonies. There are 33 recognised subspecies, which differ in their suitability for apicultural use due to variations in biological traits and productivity (Ilyasov *et al.*, 2020). In Hungary, the

Carniolan honey bee (*Apis mellifera carnica* Pollmann, 1879) is the predominant subspecies; owing to its favourable characteristics, it represents the second most widely kept honey bee subspecies globally (Plate *et al*., 2020). Colony size exhibits pronounced seasonal dynamics, most clearly reflected in fluctuations in population size. During winter, the overwintering population typically consists of approximately 5,000-10,000 individuals, whereas by mid-summer colony size may increase to 60,000-70,000 individuals, depending on the range of environmental and biological factors (Seeley, 2009). The success of a honey bee colony fundamentally relies on coordinated division of labour, altruistic behaviour, and collective organization (Shik *et al*., 2012; Seeley, 2019).

A honey bee colony cannot be reduced to individual bees, castes, or discrete tasks, as the functioning of the colony depends on the integrated contributions of all individuals and castes. Consequently, the honey bee colony is widely regarded as a superorganism (Seeley, 1989). Both the queen and her worker offspring contribute jointly to the establishment and maintenance of a viable colony, while seasonally present males (drones) also play an essential role in colony success through reproduction (Winston, 1987; Seeley, 2009).

2.2.2. Development and ontogenetical stages of *Apis mellifera*

The development of *A. mellifera* is characterised by complete metamorphosis (holometabolism) and occurs within brood cells. The duration of development differs among castes (Winston, 1987). The duration of development is influenced by several factors, including hive temperature – whose regulatory mechanisms are discussed in detail in Section 2.2.2. as well as the quantity and quality of available nutritional resources (Seeley, 2009). Unfavourable conditions related to these factors may result in prolonged developmental periods (Tautz *et al*., 2003; Brodschneider and Crailsheim, 2010). Among the three castes, the queen exhibits the shortest developmental time, completing development within approximately 16 days, followed by workers after 21 days, while drones require the longest developmental period of approximately 24 days.

In all castes, the egg stage lasts for approximately three days and is followed by a larval stage of about six days. During this period, larvae pass through five distinct larval instars, during which they are fed by young nurse workers with food corresponding to their respective developmental stage (Haydak, 1970). Although queens and workers share an identical genetic background, differences in larval nutrition and brood cell size induce epigenetic and gene expression differences, resulting in pronounced physiological and behavioural divergence between these two castes (Evans and Wheeler, 1999; Kolics *et al*., 2020).

Following the larval stage, brood cells are sealed by adult worker bees with a thin wax cap, marking the onset of the capped brood stage. During this phase, no additional food is supplied to the cell, and concomitantly, the opportunities for pathogen and pest entry are reduced. The capped larval stage is followed by the prepupal and pupal stages, the latter of which can be subdivided into seven morphologically distinct phases (Odemer, 2020). Pupation culminates around day 21 of the developmental timeline, at which point the fully developed adult insect emerges (Rembold *et al*., 1980; Winston, 1987).

During development, negative biotic (viral, bacterial, fungal and arthropod bioagents), abiotic (temperature, humidity *etc*.) and other anthropogenic factors (*e.g*. brood cell size, pesticides, nutritional status, beekeeping technology) influence on the vitality of the emerging imagoes (Klein *et al*., 2017; Neov *et al*., 2019). The most visible consequences of these adverse effects are reflected in changes to body mass and size, as well as altered behavioural patterns (Tautz *et al*., 2003; Medrzycki *et al*., 2010). In addition to the above factors, deficiencies arising from apicultural practices may negatively affect individual development and consequently colony vitality. The accumulation of cocoon residues, pollen, and other contaminants within brood cells can create unfavourable conditions for developing individuals and may also contribute to the transmission of various pathogens (Taha and Al-Kahtani, 2020). Brood combs used in apicultural frames undergo gradual deterioration over successive production cycles; as a result, both the diameter and depth of brood cells continuously decrease over time (Al-Kahtani and Taha, 2021). Due to the narrowing of brood cells, worker body mass may be reduced by an average of up to 38%, while the storage capacity of the cells may decrease by approximately 39% (Al-Kahtani and Taha, 2021). Wild living *A. mellifera* colonies compensate for these effects through swarming and the removal of aged combs; however, under managed conditions, such processes would result in substantial production losses (Seeley, 2019). According to apicultural practice, the negative effects associated with comb aging can be mitigated by replacing frames every 3-4 years, thereby maintaining colony health and uninterrupted development (Taha and Al-Kahtani, 2020; Meng *et al*., 2025).

In addition to these factors, the negative effects of certain pesticides play a significant role in development. Among these, the impacts of neurotoxin zoocides [carbamides (IRAC Moa:1A), organic phosphates (IRAC Moa:1B), neonicotinoids (IRAC Moa: 4A), butanolides (IRAC Moa:4D), sulfoxamides (IRAC Moa: 4C) *etc*.] on the development of the central nervous system are considered the most severe (Walsh *et al*., 2020; Tome *et al*., 2021; IRAC, 2026). Many of the conventional acaricides used against *V. destructor* are synthetic pesticides, among which coumaphos (organic phosphates: IRAC Moa:1B) is most frequently detected in recycled beeswax.

In this context, coumaphos concentrations of up to 132 mg kg^{-1} measured in beeswax have been shown to result in increased brood mortality (Kast *et al.*, 2023). One of the most significant and still insufficiently understood phenomena in honey bee health is pesticide-induced disruption of the gut microbiome, which leads to reduced immunity not only in developing individuals but also at the colony level (Kakumanu *et al.*, 2016; Papp et al., 2022).

From the perspective of biotic stressors, the most severe damage affecting developing *A. mellifera* caused by *V. destructor*, which is discussed in detail in Section 2.3. In addition to the ectoparasite, several pathogens and pests - some of which are subject to quarantine regulations - may attack developing individuals. However, in most cases, these stressors result in mortality during development. Among bacterial diseases, American foulbrood (*Paenibacillus larvae* Genersch, 2006) (Bacilli: Paenibacillaceae) and European foulbrood (*Melissococcus plutonius*, Bailey and Collins, 1983) (Bacilli: Enterococcaceae), both of which primarily affect larval and prepupal stages, are categorised as quarantine diseases in Hungary (Daisley *et al.*, 2023; Mallory *et al.*, 2024). In these bacterial infections, the pupal stage is typically not affected, as pathogens attack developing individuals at early larval stages, preventing them from reaching pupal development (Tucker, 1978; Pasho *et al.*, 2021). In addition to bacterial pathogens, a entomopathogenic fungi, including chalkbrood (*Ascosphaera apis* L.S. Olive and Spiltoir, 1955) (Ascomycota: Ascosphaeraceae) and stonebrood (*Aspergillus flavus* Link, 1809) (Ascomycota: Aspergillaceae), likewise primarily damage larval stages (Tucker, 1978; Pasho *et al.*, 2021). Beyond these microorganisms, a leading role is played by various entomopathogenic viruses vectored by *V. destructor,*

2.2.3. Colony temperature regulation of *Apis mellifera*

Many eusocial insects have evolved advanced mechanisms to provide optimal environmental conditions for the development of their offspring and to survive unfavourable winter periods (Stabentheiner *et al.*, 2010; Stabentheiner *et al.*, 2022). The *A. mellifera* exhibits a highly developed thermoregulatory system both in summer and winter, which is considered one of the most well-characterised among eusocial insects (Southwick and Heldmaier, 1987; Cook *et al.*, 2016). Proper thermoregulation plays a key role in maintaining the homeostasis of the superorganism. Developing eggs, larvae, and pupae are extremely sensitive to changes in environmental conditions, particularly to fluctuations in temperature and humidity (*et al*). The optimal environmental temperature range for brood development lies between 32 °C and 36 °C, which ensures healthy development (Stabentheiner *et al.*, 2010; Seeley, 2009).

Eggs and larvae tolerate temperatures below the optimal range better than pupae, whereas pupae show greater tolerance to elevated temperatures near the upper pessimum range (refers to the extreme upper limit of *A. mellifera* tolerance for a heat stress). This difference is explained by variations in protein composition and heat shock protein expression among developmental stages (Becher *et al.*, 2010). Exposure of pupae to temperatures below 32 °C for as little as 30 minutes significantly increases the likelihood of developmental abnormalities. Several studies have demonstrated reduced memory and orientation abilities in workers who developed under suboptimal temperature conditions (Groh *et al.*, 2004; Jones *et al.*, 2005). In larvae, low temperatures reduce resistance to pathogenic microorganisms attacking the brood (Southwick and Heldmaier, 1987).

Preimaginal stages are considered poikilothermic and lack intrinsic thermoregulatory mechanisms; therefore, they are unable to generate sufficient thermal energy for proper development on their own (Southwick and Heldmaier, 1987; Seeley, 2009). Numerous studies have shown that newly emerged workers younger than two days are ectothermic, whereas workers aged 4-12 days functioning as nurse bees are already capable of endothermic heat production when required, with older workers also contributing to the stabilization of hive temperature. Thermal energy is primarily generated by middle-aged (4-12 day old) adult workers through the activity of their thoracic muscles, achieved by vibrating their wings. The wing muscles can increase thoracic temperature to above 45 °C (Bujok *et al.*, 2002; Stabentheiner *et al.*, 2010). Workers that have warmed their thorax transfer heat to the brood via direct contact, using two distinct mechanisms. Concentrated heating of a single brood cell, known as the hotspot heating phenomenon, involves workers releasing thermal energy directly onto the brood surface of an individual cell in a circular pattern (Bujok *et al.*, 2002). Another mechanism contributing to brood heating is the so-called empty hot brood cell concept, in which workers enter empty cells with a heated thorax and thereby warm the neighbouring brood cells (Kleinhenz *et al.*, 2003).

Several subspecies of *A. mellifera* are adapted to warmer climates, such as those found in Italy or Turkey, while other subspecies can tolerate extreme cold conditions down to -40 °C. Consequently, thermal tolerance varies among subspecies (Kovac *et al.*, 2014; Norrström *et al.*, 2022). For the *A. mellifera carnica*, external temperatures above 35 °C represent severe heat stress, whereas temperatures as low as -30 °C can be well tolerated during overwintering (Kovac *et al.*, 2014; Alghamdi and Alattal, 2023). To maintain hive temperature at optimal levels, colonies employ numerous thermoregulatory mechanisms associated with high energetic costs, both for heating and cooling. Fresh air supply within the hive is ensured through active ventilation performed by worker bees arranged in chains at various points extending from the hive entrance, effectively forming air channels (Seeley, 2019). By fanning their wings, workers generate continuous airflow toward the exit, thereby facilitating the removal of metabolic products from developing brood and adult bees (Seeley, 2009). A fundamental component of active cooling is the dispersing of collected water across comb surfaces; evaporation of water is an endothermic process that removes heat from the environment, thereby cooling the combs and the whole hive (Southwick and Moritz, 1987; Seeley, 2019). The intensity of water collection depends on nectar availability, the nectar water content in the surrounding forage area, the amount of brood in the hive, and environmental conditions. Above 30 °C, active cooling follows an exponential trend, requiring progressively increasing effort (Kühnholz and Seeley, 1997; Seeley, 2009).

Survival of unfavourable winter conditions is only possible through harmonious cooperation within the colony and undisturbed natural conditions. During the active brood-rearing season, colonies employ different heating strategies than during winter. In winter, the colony adjusts the brood area in accordance with cluster size to minimise heat loss or suspends brood rearing entirely during prolonged cold periods (Stabentheiner *et al.*, 2003). When external temperatures fall below 15 °C, the formation of the winter cluster starts (Southwick and Heldmaier, 1987). Flight activity decreases at temperatures below 8-10 °C, which induces brood laying to stop, and the bees form an overwintering cluster (Abou-Shaara *et al.*, 2017; Glass and Harrison, 2024). Within the cluster, the bees form a spherical structure by aggregating tightly in layered groups. The density of this structure increases as the temperature decreases (Sumpter and Broomhead, 2000). Severson and Erickson (1990) conducted measurements that showed the extent of cluster compactness, which showed that cluster size decreased by 55% and surface area by 40% between 4 °C and -24 °C, independently of colony size (Severson and Erickson, 1990). Long-term measurements indicate that broodless colonies maintain an average central cluster temperature of 21.3 °C at temperatures below 0 °C, which requires substantial heat production (Fahrenholz *et al.*, 1989). Bees within the cluster warm each other through contact: those on the outer edge, with body temperatures of 10-15 °C, form an insulating layer that acts as a living thermal barrier, while endothermic bees in the centre actively generate heat (Stabentheiner *et al.*, 2010). The bees on the outer shell and within the core of the cluster continuously exchange positions. The winter cluster consists of two main functional categories: around 15% of the population are endothermic workers that produce heat through thoracic muscle vibrations, and the remaining bees are ectothermic and occupy the central region to recover. On the outer surface, insulating bees continuously rotate from the outer shell toward the cluster centre (Stabentheiner *et al.*, 2003). Bees on the outer surface lock their legs, thereby enhancing insulation and reducing heat loss (Seeley, 2009).

2.2.4. Defence mechanisms and immunity of *Apis mellifera*

For all living organisms, defence against pathogens and parasites is of fundamental importance, as it directly determines survival and evolutionary success (Rosengaus *et al*., 1999). In the case of *A. mellifera*, understanding both individual immune responses and colony-level defense mechanisms is essential. This is especially true for socially organised insects, such as *Apis* spp., where thousands or even tens of thousands of individuals live together in a single hive. Such high population density creates numerous opportunities for pathogen transmission; therefore, both horizontal (within-generation) and vertical (between-generation) transmission routes are distinguished (Fries and Camazine, 2001). In the case of *Apis* spp., close physical contact resulting from communication, grooming behaviour, and trophallaxis – an essential component of both communication and nutrition – can further accelerate the spread of infections (Fries and Camazine, 2001; Naug, 2008).

Table 1. Modes of pathogen transmission within and between *A. mellifera* colonies (Fries and Camazine, 2001)

	Horizontal	Vertical
Intracolony	Worker to brood, worker or drone Drone to worker, or drone	Queen to daughter (worker) Queen to daughter (queen) Queen to son (drone)
Intercolony	Worker to worker or drone Drone to worker or drone (Drifting, robbing)	Swarming

Compared to solitary species, the immune system of the *A. mellifera* is characterised not only by individual immune responses but also by colony-level behavioural and organizational elements, which together function as constitutive and inducible defence mechanisms (Simone-Finstrom, 2017).

Examples of constitutive defence mechanisms include the propolis envelope covering the walls of the hive or tree cavity, which provides protection against a wide range of fungal and bacterial pathogens through its antimicrobial properties. Genetic diversity ensured by polyandry represents another key constitutive defence mechanism: differences among subfamilies or microcolonies originating from multiple drones may provide protection against certain diseases due to variation in susceptibility (Hamilton, 1987; Simone-Finstrom, 2017). Additionally, individual differences may occur in the production of specific immune cells (Morfin *et al.*, 2021). Overall, a positive correlation has been demonstrated between genetic diversity and fitness. This indicates that genetic diversity is an essential component of maintaining colony health (Mattila and Seeley, 2007; Tarpy *et al.*, 2013).

In addition, task allocation within the colony provides protection through age-related division of labour and functional specialization (Naug, 2008; Armitage *et al.*, 2010; Evans and Spivak, 2010). Although workers perform different tasks as they age, they are largely protected from environmental stressors until they are approximately 20-21 days old because they are restricted to in-hive activities during this period (Bloch *et al.*, 2001; Johnson, 2008). Constitutive colony-level defence mechanisms are essential for maintaining the colony health. However, the present dissertation focuses on inducible defence mechanisms triggered by pathogens. Therefore, only the latter are discussed in detail in the following sections.

Inducible defence mechanisms comprise a complex system of behavioural and organisational traits. The execution of these traits may involve workers of different age classes or specific age groups. A key characteristic of these defence mechanisms is that they are activated exclusively in response to the presence of a pathogen or parasite (Simone-Finstrom, 2017). The first line of defence is the hive entrance, where older worker bees attempt to prevent the entry of potential pests and pathogens. In the spread of pathogens, as well as economically important parasites such as *V. destructor*, drifting behaviour plays a significant role and is closely associated with colony aggressiveness. Several studies have shown that colonies exhibiting higher levels of aggressive behaviour may experience reduced rates of mite infestation, primarily through enhanced defence against robbing bees (Breed *et al.*, 1990; Arechavaleta-Velasco, 2003).

Grooming also constitutes a key defence mechanism of the colony against invading microorganisms and parasites (Zhukovskaya *et al.*, 2013). Two main behavioural forms can be distinguished: auto-grooming (self-grooming) and allo-grooming (grooming of nestmates). Within the framework of social immunity, grooming acts as a barrier preventing the entry and establishment of ectoparasites in the colony, such as the tracheal mite *Acarapis woodi* Rennie 1921 (Arachnida: Tarsonemidae) and *V. destructor*. From a social immunization perspective, worker bees can sense immune-challenged individuals. This hypothesis has been tested in *A. mellifera* workers, and experimental evidence suggests that individuals injected with bacteria receive significantly more allo-grooming than non-injected bees. Allo-grooming may therefore play an essential role in trans-generational immune priming through social immunization among workers (Sadd *et al.*, 2005; Hernández *et al.*, 2014; Ory *et al.*, 2022).

Because cleaning behaviour is critical to limiting the spread of diseases and parasites, it is considered one of the most important selection criteria for colony health. It can slow the transmission of infections such as nosemosis, chalkbrood, and American foulbrood. Hygienic behaviour refers specifically to behavioural patterns associated with the detection and removal of diseased brood from the colony (Evans and Spivak, 2010). One of the most important defence mechanisms against *V. destructor* infestation is Varroa-sensitive hygiene (VSH), a specialised form of hygienic behaviour (Panziera *et al*., 2017). In colonies expressing the VSH trait, workers can discriminate parasitised brood cells from healthy brood cells. Parasitised cells are uncapped and, in some cases, the developing parasitised individuals are removed from the cells (Spivak and Danka, 2021). As a consequence, the biological cycle of mites developing within these cells is disrupted, either immediately following uncapping or due to brood removal, resulting in a reduced reproductive index of female mites and a subsequent decline in mite population size (Ibrahim and Spivak, 2006).

Mite non-reproduction (MNR) refers to a phenomenon in which reproduction of female mites is partially or completely absent. Previously described as suppressed mite reproduction (SMR), MNR represents a still not fully understood aspect of mite biology in relation to VSH (Harbo and Harris, 1999a; Sprau *et al*., 2024a). Brood cells in which no offspring are present, only male offspring are detected, or offspring remain at underdeveloped stages are all considered to fall within the MNR category. Both MNR and VSH are desirable traits in breeding programs aimed at improving Varroa tolerance; however, numerous studies have demonstrated that the heritability of both traits is relatively low (Sprau *et al*., 2024a, b).

Social fever represents a less well-known inducible defence mechanism of *A. mellifera* colony, during which workers deliberately elevate nest or brood temperature in response to pathogen presence (Starks *et al*., 2000; Goblirsch *et al*., 2023). The temperature increase is generated not by a single individual but rather by the coordinated activity of many workers, primarily heater bees, making social fever a true colony-level adaptive response to certain diseases. Elevated temperatures primarily inhibit the development of heat-sensitive pathogens such as *Ascosphaera apis* and reduce the spread of infection within the combs. Although a direct disease-reducing effect of elevated temperature was not conclusively demonstrated by Goblirsch *et al*. (2020), pathogen-specific thermal response mechanisms have been confirmed by several studies (Starks *et al*., 2000; Campbell *et al*., 2010; Goblirsch *et al*., 2020). Based on the work of Palmer-Young *et al*. (2023), inhibition of Deformed Wing Virus (DWV) replication occurs only at pupal temperatures elevated above the developmental optimum; however, such temperatures simultaneously compromise host viability (Palmer-Young *et al*., 2023). Bauer *et al*. (2018) found that, in the case of an artificial infestation of a brood cell with one or two mites, the temperature of the cell increased by 0.1-0.19 °C. They concluded that this increase may be due to the higher energy demand of the developing pupae caused by the infestation or the replication of the viruses vectored by the mite (Bauer *et al*., 2018).

These mechanisms serve as a complex defence system that allows the colony to be regarded as a superorganism capable of overcoming pathogens and parasites through coordinated collective action. Consequently, colony population size and nutritional status are critical factors because disruption or impairment of these defence mechanisms may increase susceptibility to pathogens and contribute to colony collapse (Simone-Finstrom, 2017; Seeley, 2020; Evans and Chen, 2021).

Individual immunity:

The immune system of *A. mellifera* relies exclusively on innate mechanisms; nevertheless, its level of organization and functional complexity enables effective defence against pathogens and parasites. Individual immune responses can be divided into two closely related components: humoral and cellular immunity. While humoral defence is primarily mediated through enzymatic cascades and antimicrobial peptides, cellular immune responses provide direct protection against infectious agents via the activity of circulating hemocytes (Evans *et al*., 2006; Chen *et al*., 2006a; Morfin *et al*., 2021).

Hemocytes are central to the cellular immune response and include several functional cell types, such as those specialised in phagocytosis, encapsulation, and melanisation. These cells can recognise and encapsulate foreign material. In the case of larger pathogens, they form multicellular structures that isolate and neutralize invading organisms. The activity of hemocytes varies depending on the type and intensity of infection, as well as the physiological state of the individual (Negri *et al*., 2016; Hystad *et al*., 2017).One of the key processes of the immune response is melanisation, during which the phenoloxidase cascade is activated and pathogens or damaged tissues become encapsulated by a melanin layer. This mechanism not only forms a physical barrier but also exerts direct toxic effects on pathogens through reactive intermediates. The intensity of the melanisation response often reflects the immunological status of the individual (Gábor *et al*., 2020; Morfin *et al*., 2021).

The efficiency of the cellular immune response is closely linked to the age, nutritional status, and physiological role of individuals. It has been demonstrated that younger workers – particularly nurse bees – exhibit stronger cellular immune responses, whereas immune functions gradually decline in older foragers. This age-related immunological variation is tightly associated with division of labor within the colony and the differing levels of risk exposure experienced by individuals (Hystad *et al*., 2017).

Parasites, particularly *V. destructor*, exert a substantial impact on individual cellular immune responses. Parasitisation may lead not only to a reduction in hemocyte numbers but also to alterations in their functional activity, thereby increasing susceptibility to secondary infections and viral diseases. Consequently, impairment of individual immune responses is directly linked to deterioration of overall colony health (Koleoglu *et al*., 2018; Morfin *et al*., 2023).

Overall, individual cellular immune responses represent a fundamental pillar of the colony defence system, and their function is closely associated with the physiological condition, age, and environmental stress exposure of the individual. The effectiveness of these mechanisms influences not only individual survival but also indirectly determines the resilience and stability of the colony as a whole superorganism.

2.3. Parasitological characteristics of *Varroa destructor*

2.3.1. Historical overview of *Varroa destructor* description and spread

Species belonging to the genus *Varroa* are recognised as some of the most widespread and well-known parasites affecting *A. mellifera* populations worldwide. Originally, three species were assigned to the genus *Varroa*, all of which feed on the hemolymph of their hosts. *Varroa jacobsoni* Oudemans, 1904 (Arachnida: Laelapidae) was first described in 1904 on individuals of the Eastern honey bee (*Apis cerana* Fabricius 1793) (Hymenoptera: Apidae) on the island of Java, Indonesia (Oudemans, 1904). Subsequently, it was also observed on *Apis nigrocincta* Smith 1861, (Hymenoptera: Apidae) in Indonesia (Hadisoesilo and Otis, 1998). Another species within the genus, *Varroa underwoodi* Delfinado-Baker and Aggarwal 1987 (Arachnida: Laelapidae) was first identified on *A. cerana* in Nepal in 1987 (Delfinado-Baker and Aggrawal, 1987). *Varroa rindereri* De Guzman and Delfinado-Baker, 1996 (Arachnida: Laelapidae) was later described from colonies of the red honey bee (*Apis koschevnikovi* Enderlein 1906) (Hymenoptera: Apidae) on Borneo in 1996 (De Guzman and Delfinado-Baker, 1996). This species list was expanded by Anderson and Trueman (2000) with the description of a fourth species, *V. destructor*, which currently represents one of the greatest challenges for researchers and beekeepers working with the *A. mellifera* worldwide. The occurrence of this mite on *A. mellifera* was first reported from the Philippines, after which it became evident that certain populations previously identified as *V. jacobsoni* were genetically distinct from one another (Anderson, 1994). The evolutionary origin of *V. destructor* is linked to Japan and Korea, as only haplotypes from these regions have been shown to successfully infest both *A. mellifera* and *Apis cerana* colonies. Comparative analyses of mitochondrial cytochrome c oxidase subunit 1 (COI) gene sequences have revealed greater genetic divergence within the Japanese haplotype than within the Korean haplotype; however, due to its higher pathogenicity and adaptive capacity, the Korean haplotype has become one of the most dominant globally (Traynor *et al*., 2020; Bai *et al*., 2021). The species-level distinction of *V. destructor* and the understanding of its global spread are of fundamental importance for interpreting the biology of the parasite, host-parasite interactions, and its complex effects on colonies.

In Hungary, the first documented cases of varroosis were originally attributed to *V. jacobsoni*. However, based on current taxonomic and genetic knowledge, it is highly likely that these early observations already corresponded to the presence of *V. destructor*, marking the beginning of active control efforts. Reports of the parasite first emerged from countries neighbouring Hungary, particularly Romania, where the presence of the mite was documented in 1976 by Pál Zoltán Örösi (Csaba, 1983). In Hungary, the parasite was first detected in an apiary located in the village of Pocsaj, near the Slovak border (Csaba, 1983).

2.3.2. Morphology of *Varroa destructor*

V. destructor is characterised by pronounced sexual dimorphism; however, body segmentation is similar in both sexes and can be divided into two main regions: the idiosoma and the gnathosoma (Rosenkranz *et al*., 2010). In females, both the dorsal and ventral shields are strongly sclerotised and exhibit a reddish-brown coloration in mature individuals. The dorsal shield of females is flattened and ellipsoidal in shape, with an average length of approximately 1063.0 µm (±26.4 µm) and a width of 1506.8 µm (±6.0 µm) (Rosenkranz *et al*., 2010). Males are considerably smaller than females, display a pear-shaped body form, and show markedly weaker sclerotization, lacking the characteristic reddish-brown coloration. Their legs are proportionally much longer relative to body size and are specialised for mating. Additional morphological differences have been described between winter and summer mite populations, with greater morphological variability observed in summer populations (Akimov *et al*., 2004).

The chelicerae of *V. destructor* consist of three main components: a basal segment, an intermediate segment, and a distally located, movable, finger-like structure. In females, the distal movable part bears two teeth that play a crucial role in penetrating the host’s exocuticle. In males, the distal third of the mouthparts is reduced to a tubular structure involved in copulation and sperm transfer (Rosenkranz *et al*., 2010). The female reproductive system is divided into two principal units. The first comprises the ovary, uterus, and genital opening, with the external genital pore located between the second pair of legs (Piou *et al*., 2021). The second unit is responsible for sperm reception and maturation and consists of the spermatheca and the lyrate organ (Alberti, 1986; Piou *et al*., 2021).

The entire body surface of female mites, including the legs and mouthparts, is covered with sensory setae (Rosenkranz *et al*., 2010). Most of these sensory hairs function as mechanoreceptors and chemoreceptors (Eliash *et al*., 2014). Females rarely use the first pair of legs for locomotion; instead, these appendages primarily serve a sensory function and house the pit sensory organ, which is considered analogous to Haller's organ in ticks. It has been demonstrated that methyl palmitate, ethyl palmitate, and methyl linolenate the volatile compounds associated with royal jelly are induces electrophysiological responses in the olfactory sensilla of the parasite, playing an important role in host detection (Rosenkranz *et al*., 2010; Eliash *et al*., 2014; Nazzi and Le Conte, 2016). The morphological and sensory specializations of *V. destructor* are closely linked to its parasitic lifestyle and fundamentally determine host recognition, feeding behaviour, and reproductive success (Traynor *et al*., 2020).

2.3.3. Life cycles and host selection of *Varroa destructor*

V. destructor finds the conditions required for its survival exclusively within honey bee colonies, as its reproduction is strictly associated with brood cells. Consequently, it is considered an obligate ectoparasite (Rosenkranz *et al*., 2010). The life cycles of the two sexes differ markedly, and their lifespans also show substantial differences as a result. Males complete their entire life cycle within capped brood cells, which is explained by the haplodiploid mode of inheritance, as their sole function is fertilization (Traynor *et al*., 2020). Their morphology is highly adapted to a lifestyle in the capped brood due to the lack of cuticular sclerotization, males do not tolerate conditions outside the brood cell and are unable to feed independently (Rosenkranz *et al*., 2010).

In contrast, the life cycle of female mites can be divided into two well-defined phases, the understanding of which is essential for interpreting parasite transmission and maintaining colony health (Fries *et al*., 1994; Dietemann *et al*., 2012). These phases include the so-called phoretic phase and the reproductive phase, which takes place within capped worker and drone brood cells (Peck, 2021). The phoretic phase facilitates parasite dispersal, during which female mites attach to adult bees and spread both between colonies and among brood cells serving as sites of reproduction (Fries *et al*., 1994). During this phase, 88.5% of female mites are typically located on the ventral abdominal region of adult bees, hiding between the abdominal sternites, which provides mechanical protection (Kirrane *et al*., 2012). Female mites observed on the thorax exhibit behaviour distinct from those located on the abdomen. These individuals have been observed raising their first pair of sensory legs into the air and actively moving across the bee's body while refraining from feeding, suggesting an intention to transfer to another host (Ramsey *et al*., 2019). Phoretic mites have been predominantly identified in young nurse bees, with a lesser prevalence in older worker bees. These host groups play a key role in enabling mites to locate intact brood cells and access new colonies (Rosenkranz *et al*., 2010; Ramsey *et al*., 2019). The ability of phoretic mites to locate brood cells is influenced by multiple factors, including their ability to detect vibrations and light (Reams and Rangel, 2022). Beyond chemical orientation, temperature sensing plays a particularly important role in host selection. Laboratory studies have demonstrated that the general physiological optimum for female *V. destructor* lies between 26 and 33 °C (Pätzold and Ritter, 1989; Le Conte *et al*., 1990). However, subsequent field experiments conducted within capped brood cells indicate that reproductive success peaks at temperatures between 33.5 and 35.5 °C, corresponding to the natural thermal conditions of brood (Becher, 2009; Rosenkranz *et al*., 2010). Above these optimal temperatures, mite tolerance is lower than that of developing pupae, which has led to the acceptance of elevated temperatures as a physical control method, although this approach remains limited in practical application (Porporato *et al*., 2022). Chemical orientation represents the most significant factor in host selection, primarily mediated by cuticular hydrocarbon (CHC) profiles emitted by the brood (Del Piccolo *et al*., 2010; Reams and Rangel, 2022). Phoretic female mites are capable of discriminating among adult bees based on their age and colony task (Liu *et al*., 2022). Rather than remaining on newly emerged workers, female mites actively migrate within the hive toward nurse bees and, to a lesser extent, toward older workers during the phoretic phase (Kuenen and Calderone, 1997). Both laboratory and field studies indicate that nurse bees aged 3-12 days constitute the primary host group for mites, whereas newly emerged bees and foragers carry mites with significantly lower probability (Xie *et al*., 2016). This host preference is adaptive for the parasite, as nurse bees frequently visit developing larvae, thereby facilitating mite access to brood cells that serve as reproductive sites (Reams and Rangel, 2022). The fat body content of workers is not constant throughout life but changes continuously from the larval stage through adulthood. Nurse bees possess the largest and most densely structured fat bodies, which contribute to their preferential selection as hosts during the phoretic phase. The fat body represents an essential nutritional resource for mites during this stage, explaining the high prevalence of phoretic mites on nurse bees between reproductive cycles (Ramsey *et al*., 2019; Han *et al*., 2024). Significant differences are also observed in the types of brood cells selected for reproduction. It is well established that reproductive rates of mites are higher in drone brood, reaching an average of 2.6 sexually mature female offspring per cell, while infestation levels in drone brood may be three to ten times higher than in worker brood (Fuchs, 1990; Calderone, 2001). Preference for drone brood is largely explained by differences in the duration of the invasion window. Worker brood cells are susceptible to infestation approximately 15-20 hours prior to capping, whereas the susceptible period for drone brood exceeds twice this duration, with infestation occurring up to 40-50 hours before capping (Ifantidis *et al*., 1988; Boot *et al*., 1992).

Historically, the higher infestation rates observed in drone brood were often attributed to increased feeding frequency and more intensive contact between nurse bees and brood. However, recent investigations by Reams *et al*. (2024) demonstrated that differences in feeding activity alone are insufficient to explain mite preference. Instead, host selection is more closely associated with the cuticular hydrocarbon profile of drone brood and the extended invasion window, indicating that preference results from a combination of biochemical and age-related factors rather than increased nurse bee feeding behaviour alone (Reams *et al*., 2024). Beekeepers exploit this preference in biological control strategies based on drone brood removal, through which up to 80% of the mite population can be eliminated in early summer (Fuchs, 1990; Haizhou *et al*., 2019; Peck, 2021).

2.3.4. Biology of *Varroa destructor*

The reproductive cycle of *V. destructor* takes place only within brood cells. Female mites primarily parasitize brood cells containing larvae in the fifth larval instar that are frequently visited by nurse bees. In worker brood, invasion occurs during the final 15-20 hours prior to capping, whereas in drone brood infestation may take place 40-50 hours before cell sealing (Nazzi and Le Conte, 2016). After entering the brood cell, the female mite moves through the narrow space between the brood and the cell wall to the bottom of the cell, where larval food composed of royal jelly, honey, and pollen is located. The mite then hides within this food mass and remains concealed until the brood cell is capped (Rosenkranz *et al*., 2010). Five to eight hours after capping, the larva consumes all remaining food at the bottom of the cell, thereby releasing the mite from its concealed position. At this point, the mite begins feeding on the larva (Ifantidis, 1988). This feeding activity initiates oogenesis, which is followed by vitellogenesis (Garrido *et al*., 2000). Approximately 70 hours after cell capping, the female lays her first egg, which is haploid; consequently, following the haplodiploid reproductive system, this first offspring develops into a male (Ifantidis, 1983). Subsequent eggs are laid at intervals of 20-32 hours and give rise exclusively to female offspring (Martin, 1994; Garrido and Rosenkranz, 2003). In worker brood, a single female mite typically produces three to four viable, mature female offspring. In contrast, the longer 24-day developmental period of drone brood allows reproductively healthy female mites to produce an additional offspring (Garrido and Rosenkranz, 2003).

Newly emerged offspring acquire the nutrients required for development through the feeding wound created by their mother. This wound is located on the second abdominal sternite of the pupa and, due to the position of the brood within the cell, lies close to the zone where feces accumulate at the bottom of the brood cell (Kanbar, 2003; Dietemann *et al.*, 2013; Han *et al.*, 2024). Within a few hours after egg deposition, larvae hatch and subsequently pass through two developmental stages proto- and deutonymph, prior to reaching adulthood. Each of these stages is preceded by an immobile phase, referred to as the protochrysalis and deutochrysalis stages, respectively (Ifantidis, 1983; Donzé and Guerin, 1994). Regarding developmental duration, female mites reach maturity in approximately 5.8 days on average, whereas males require about 6.6 days to become fully developed (Ifantidis, 1990; Rosenkranz *et al.*, 2010; Dietemann *et al.*, 2013).

V. destructor exhibit pronounced sexual dimorphism throughout their entire development. Male individuals remain smaller than females at all stages, and their legs are proportionally much longer relative to body size (Rosenkranz *et al.*, 2010). Female mites undergo continuous morphological changes during development, with body size increasing progressively. However, they acquire their characteristic oval body shape only after the deutochrysalis stage, after which cuticular pigmentation and sclerotization begin, ultimately resulting in the final reddish-brown coloration (Dietemann *et al.*, 2012). Both male and female mites reach sexual maturity following their final molt. Males remain within the fecal accumulation zone of the brood cell, where they await the emergence of sexually mature females, and mating occurs within this confined space (Ziegelmann *et al.*, 2013).

The average reproductive rate of female mites is approximately 1.3-1.45 in worker brood, whereas in drone brood it increases to 2.2-2.6 due to the extended developmental period (Martin, 1994; Rosenkranz *et al.*, 2010). Under laboratory conditions, female mites may complete up to six to seven reproductive cycles during their lifetime; however, under natural conditions, an average of only two to three cycles is typically observed (Reams and Rangel, 2022). The strictly timed reproductive strategy of *V. destructor* is closely linked to capped brood, that is fundamental to determining the growth of the parasite population. This strategy plays a central role in the development of effective control strategies and the level of infestation observed.

2.3.5. Host depending phenology of *Varroa destructor*

Density is a fundamental driver of the spread of pests and pathogens. This population dynamic principle has been well-demonstrated in the case of *V. destructor* (Dynes *et al*., 2019). Experimental studies indicate that higher spatial densities of colonies significantly increase the population growth rate of mites (Frey and Rosenkranz, 2014; Jack and Ellis, 2021). In regions with high colony density and in apiaries with large numbers of colonies, the probability of reinfestation (reinvasion) is highly elevated (Peck and Seeley, 2019). Several behavioural mechanisms contribute to reinvasion, among which drone drifting between colonies during the May-July period and worker bee drifting play a dominant role (Goodwin *et al*., 2006; Utaipanon *et al*., 2019). Additionally, consider robber behaviour that occurs during periods of nectar deficiency. During such periods, colonies weakened by varroosis become sources of parasites that are transferred to stronger colonies by robbing workers, a phenomenon commonly referred to as the “mite bomb” effect (Peck and Seeley, 2019). Strong colonies can be capable of robbing other colonies up to 1 km away. Therefore, the distance between apiaries is a critical factor influencing mite spread (Frey and Rosenkranz, 2014; Jack and Ellis, 2021). This phenomenon is particularly prevalent during nectar-poor periods, when colonies deprived of forage begin exploiting the honey stores of neighbouring colonies, a process further facilitated by crowded apiary conditions. Under the combined influence of Hungary’s variable climatic conditions and heterogeneous forage availability, mid-July as well as September and early October represent periods of elevated risk for *A. mellifera* colonies due to this phenomenon (Rittschof and Nieh, 2021). Although some studies have questioned the "mite bomb" hypothesis, which refers to the massive transfer of mites from collapsing, heavily infested colonies, field experiments consistently demonstrate that increasing the distance between hives reduces the intensity of reinvasion (Kulhanek *et al*., 2021). Studies in both laboratories and fields have shown that increasing the distance between hives can reduce mite infestation levels by lowering the frequency of robbing and drifting events (Dynes *et al*., 2019). Distances of 0-10 m between colonies result in significantly higher parasite loads compared to colonies separated by 100 m (Nolan and Delaplane, 2017). Comparative studies conducted across different landscapes further indicate that *V. destructor* populations grow more rapidly in high-density apiary regions, with reinfestation rates during autumn being several times higher than those observed in low-density regions (Frey and Rosenkranz, 2014). In contrast, apiaries characterised by lower colony density and greater visual separation exhibit persistently lower parasite loads due to reduced drifting and resulting in higher overwintering success (Dynes *et al*., 2019).

After an initial infestation, *V. destructor* can establish a large population that grows rapidly within a relatively short period of time (three to four months). This population can affect more than just individual bees; it can also compromise the overall viability of the colony (van Dooremalen *et al*., 2013; Smith and Peck, 2023; Warner *et al*., 2024). Based on several studies, economic threshold levels for phoretic mites are estimated at approximately 2 mites per 100 adult bees during spring and around 4 mites per 100 adult bees prior to overwintering (Jack and Ellis, 2021; Kulhanek *et al*., 2021). Population growth of *V. destructor* varies considerably among colonies and depends on multiple behavioural and environmental factors, including hygienic behaviour, queen performance, swarming frequency, robbing tendency, foraging intensity, and ambient temperature (Fries *et al*., 1994; Rosenkranz *et al*., 2010; Smoliński *et al*., 2021). Numerous studies have demonstrated that, in temperate regions, most *A. mellifera* colonies collapse within 1-4 years as a consequence of varroosis if left unmanaged (van Dooremalen and van Lengaverde, 2021; Morfin *et al*., 2023). In contrast, population-dynamic relationships involving brood infestation rates, proportions of phoretic mites, and natural mite mortality remain less well understood (Smith and Peck, 2023). Seasonal differences in mortality between summer and winter mite populations are also insufficiently characterised. The dynamics of brood parasitism, phoretic mite proportions, and seasonal mortality patterns remain incompletely resolved, highlighting the need for further research to achieve a more precise understanding of *V. destructor* population biology (Rosenkranz *et al*., 2010; Kulhanek *et al*., 2021; Warner *et al*., 2024).

Overall, the host depending phenology of *V. destructor* is shaped by the combined effects of host density, apiary structure, seasonal behavioural patterns, and the biological characteristics of the parasite itself. This complexity substantially complicates the prediction of infestation processes and the development of effective control strategies.

2.3.6. Individual and colony level damage caused by *Varroa destructor*

Colonies affected by *V. destructor* pass through several stages before the level of damage reaches the economic threshold and subsequently escalate to a level that threatens colony survival (Morfin *et al*., 2023). In social insect colonies, the symptoms of varroosis become detectable at a later stage, as the proportion of damaged individuals increases in parallel with mite population size (Rosenkranz *et al*., 2010). Clinical manifestations of varroosis initially appear at the level of directly parasitised individuals; however, as the number of infested bees increases, the viability and organizational integrity of the entire colony become compromised (Rosenkranz, 2010; Corby-

Harris *et al*., 2019; Traynor *et al*., 2020). Consequently, it is essential to examine and understand both the social- and individual-level symptoms and damage associated with infestation (Ramsey *et al*., 2021; Morfin *et al*., 2023).

For nearly five decades, researchers and practitioners considered hemolymph to be the primary nutritional source for *V. destructor* (Amdam *et al*., 2004). This long-standing assumption was refined by Ramsey *et al*. (2019), who demonstrated that the mite's primary food source is not hemolymph but the host's fat body tissue (Ramsey *et al*., 2019). These findings were further refined by Han *et al*. (2024), who showed that mites preferentially exploit different tissue types at distinct stages of their life cycle. According to their results, mites in the phoretic phase predominantly damage and consume the fat body of adult bees, whereas during pupal development hemolymph represents the primary nutritional source for developing mites (Han *et al*., 2024; Piou *et al*., 2024). Damage to developing pupae disrupts multiple metabolic pathways. The loss of energetic resources impairs protein synthesis (Amdam *et al*., 2004). Reduced lipid and protein synthesis results in compromised metabolic turnover and, consequently, impaired immune function (Ramsey *et al*., 2019). Additionally, the tolerance of adult bees to pesticides is reduced because fat body cells play a central role in detoxification processes (van Dooremalen *et al*., 2013; Ramsey *et al*., 2019). Decreases in body mass and abdominal underdevelopment can be measured in all developing individuals infected with parasites, although the extent of these effects depends greatly on the number of mites present and the viruses they transmit (Amdam *et al*., 2003; Morfin *et al*., 2020). On average, worker bees have a body mass that is approximately 7% less than the emergence weight of intact adults (De Jong *et al*., 1982). This reduction is more pronounced in drones, ranging from 11 to 19%, depending on the intensity of the infestation (Duay *et al*., 2003).

The age structure of the colony shifts as a function of damage severity, with worker bees initiating foraging activities earlier in life. This precocious foraging significantly reduces the lifespan of individuals and further disrupts the demography of colonies (De Jong *et al*., 1982; Amdam *et al*., 2004). Of the described effects, fat body parasitism by phoretic mites is particularly harmful because it disrupts metabolic homeostasis in adult bees and suppresses the immune system (Morfin *et al*., 2023). Consequently, individuals that are parasitised during development or the phoretic phase exhibit impaired navigation and orientation abilities. This leads to increased drifting and reduced foraging performance. These factors ultimately result in a decline in colony population size and diminished nutritional resources (Muijres *et al*., 2020). At the colony level, parasitism weakens individual bees to such an extent that viable populations cannot be sustained, and tolerance to additional biotic and abiotic stressors is substantially reduced (Fries *et al*., 2003; Villa *et al*., 2008). At low infestation levels, clinical symptoms of mite infestation are often absent, and parasitism may remain largely concealed, manifesting primarily at the individual level (Morfin *et al.*, 2023). As mite populations increase, however, colony population size and food reserves gradually decline, a process that already exerts a substantial negative impact on honey yield (Le Conte *et al.*, 2007; Emsen *et al.*, 2014; Morfin *et al.*, 2023).

In temperate regions, the most pronounced damage associated with varroosis typically appears during autumn, when colonies are preparing for winter and reducing population size. During this period, shifts in the ratio between overwintering bees and mite populations result in an increasing proportion of damaged individuals within the colony (Fries *et al.*, 2003). In addition, the number of phoretic mites that parasitize the fat bodies of adult bees increases, further reducing the viability of overwintering bees (Warner *et al.*, 2024; Jeyapriya *et al.*, 2025). Once clinical symptoms of infestation become apparent, colony survival prospects are poor. These symptoms include deformed wings resulting from virus-mite interactions, trembling and crippled bees, and scattered, patchy capped brood (van Dooremalen *et al.*, 2012; Jack and Ellis, 2021). Studies conducted in Germany indicate that if the proportion of infected overwintering bees exceeds 7%, colony collapse is likely to occur within a short time frame (Genersch *et al.*, 2010; Frey and Rosenkranz, 2014). Similarly, if infestation levels reach approximately 30% during summer, colonies have a low probability of surviving the winter. North American studies suggest that the presence of approximately 3,000-4,000 mites is sufficient to induce colony collapse (Rosenkranz *et al.*, 2010). Overall, the damage caused by *V. destructor* cannot be attributed to a single factor but rather arises from the combined effects of individual metabolic impairment, immune suppression, behavioural alterations, and virus-mediated co-infections, ultimately leading to colony failure.

2.3.7. Viruses transmitted by *Varroa destructor*

V. destructor is considered the primary vector of viral diseases affecting *A. mellifera* (Traynor *et al.*, 2020). A strong association has been documented between severe mite infestation and high colony losses, including colony collapse disorder (CCD). Mite-virus interactions cause the most severe damage to *A. mellifera* colonies (Rosenkranz *et al.*, 2010; Francis *et al.*, 2013). Current research has identified more than 25 different honey bee viruses. Of these, approximately eight are currently confirmed to be vectored by *V. destructor*. However, vector competence for additional viruses is still being investigated (Traynor *et al.*, 2020; Eliash *et al.*, 2022). The viruses known to be transmitted by the mite include acute bee paralysis virus (ABPV), black queen cell virus (BQCV), chronic bee paralysis virus (CBPV), deformed wing virus (DWV), Kashmir bee virus (KBV), sacbrood virus (SBV), slow bee paralysis virus (SBPV), and Israeli acute paralysis virus (IAPV) (Berényi *et al.*, 2006; Damayo *et al.*, 2023; Doublet *et al.*, 2024). Most of the viruses possess a positive-sense, single-stranded RNA genome. Virion diameters typically range between 17 and 40 nm (Remnant *et al.*, 2017). These viruses exhibit icosahedral symmetry and are non-enveloped, with a capsid structure following T=3 symmetry. The capsid is composed of 60 protomers consisting of three major structural proteins (VP1, VP2, VP3), while in some viruses - such as BQCV and ABPV - an additional VP4 subunit can be distinguished (Ribière *et al.*, 2008). Currently, virus detection relies primarily on electron microscopy and, with advances in molecular genetics, real-time PCR (RT-PCR) techniques (Traynor *et al.*, 2020). Earlier diagnostic approaches included ELISA, agar gel immunodiffusion (AGID), and direct antigen-detection serological methods (Allen and Ball, 1995).

Within the colonies, multiple transmission pathways for viruses have been identified, of which two major routes are distinguished: vertical and horizontal transmission (Yañez *et al.*, 2020). Most of the viruses are capable of spreading via both pathways (Chen *et al.,* 2006a,b; Yañez *et al.*, 2020). Several studies have demonstrated that during vertical transmission, multiple viruses can already be detected simultaneously within eggs, including DWV, SBV, and BQCV (Shen *et al.*, 2005; Chen *et al.*, 2006b). Consequently, if a fertilised egg carrying viral infection develops into a queen, her offspring generation is also highly likely to be virus-infected (Chen *et al.*, 2006b). Horizontal transmission can occur as early as the larval feeding stage, as numerous viruses have been isolated from the hypopharyngeal glands of worker bees, allowing larvae to become infected during feeding (McMenamin and Genersch, 2015). Virus transmission is further facilitated by nutrient exchange among workers through trophallaxis (Geffre *et al.*, 2020). Even if a developing queen is initially virus-free, this does not guarantee long-term protection, as infection may occur during mating through virus-contaminated sperm, potentially infecting both the queen and the subsequent offspring generation (Amiri *et al.*, 2020). The presence of DWV, ABPV, BQCV, and SBV has been detected in semen collected from drones (Yue *et al.*, 2006). The probability of drone-mediated transmission is particularly high due to the mite's preference for drone brood cells (Chen *et al.*, 2006a). Physical transmission via body contact also plays a significant role in virus spread among workers and queens, as documented for IAPV and CBPV (Yañez *et al.*, 2020).

The most recognizable, widespread, and economically damaging virus is deformed wing virus (DWV), which is primarily identified by malformed, non-functional wings and reduced abdominal size in worker bees (Boecking and Genersch, 2008). DWV is the virus most strongly associated with CCD worldwide (Rosenkranz *et al.*, 2010). The emergence of DWV-related pathology in *A. mellifera* closely followed the spread of the *V. destructor,* with the earliest records dating back to the 1980s. Since then, DWV has remained the most prevalent and arguably the most influential honey bee virus of modern times (Ribière *et al*., 2008). Currently, three main DWV variants A, B (also referred to as VDV-1), and C are recognised, each capable of producing distinct symptoms depending on viral load and the timing of infection (Kevill *et al*., 2020). All variants are capable of replication in both bees and mites. DWV-A is most frequently associated with CCD due to its higher virulence and mortality rates. In contrast, DWV-B is more widespread, as colonies infected with this variant exhibit higher overwintering success compared to those infected with DWV-A (Mordecai *et al*., 2016; Kevill *et al*., 2020). The lower virulence and higher replication efficiency of DWV-B may confer a relative advantage through viral competition, as the presence of one variant can inhibit the replication of another via superinfection exclusion (SIE) (Mordecai *et al*., 2016). Because individual bees can typically sustain infection by only one dominant virus variant, DWV-B may effectively function as a "protective virus" at the colony level (Mordecai *et al*., 2016; Kevill *et al*., 2020). The most severe manifestation of DWV-A infection is the emergence of wingless or severely deformed-wing adults, which account for approximately 1% of virus-infected individuals (Lanzi *et al*., 2006). This is accompanied by reduced body size, often expressed as abdominal underdevelopment, as well as cuticular discoloration (Tentcheva *et al*., 2006; Anguiano-Baez *et al*., 2016). Ultimately, the disease process leads to the rapid mortality of newly emerged adult bees.

Naturally, both abiotic and biotic factors, as well as colony-level genetic tolerance and immune status, contribute to viral transmission dynamics and disease severity (Neov *et al*., 2019; Locke *et al*., 2021). Viral infection alone is generally insufficient to cause complete colony collapse. Consequently, from the current scientific perspective, viruses and the mite cannot be considered independently; rather, the *V. destructor*–virus complex must be examined as an integrated system. Understanding virus-mite-host interactions is fundamental to understanding the processes that lead to colony collapse, as well as to developing sustainable management and control strategies (Warner *et al*., 2024).

2.3.8. Tolerance phenomenon and mechanisms of *Apis* genus to *Varroa destructor*

When examining the evolutionary relationship between *V. jacobsoni* / *V. destructor* and *A. cerana*, several traits and behavioural patterns can be identified that effectively reduce the parasite's reproductive rate and, consequently, the overall level of damage inflicted on the host colony (Fries *et al*., 1996; Grindrod and Martin, 2023). The tolerance of *A. cerana* cannot be attributed to a single mechanism; rather, it emerges from the combined effects of multiple, interrelated behavioural and physiological adaptations (Grindrod and Martin, 2023). These include efficient grooming behaviour, which enables the direct removal of mites, as well as hygienic behaviour, during which infested brood is detected and removed from the colony (Rosenkranz, 1993). Together, these active defence mechanisms allow *A. cerana* colonies to eliminate a substantial proportion of mites according to some studies, exceeding 90% of the parasite population (Rosenkranz, 1993). In drone brood, the presence of a rigid pupal cap prevents heavily parasitised individuals from successfully emerging, causing both the developing drone and the associated mites to remain trapped within the cell (Boecking *et al.*, 1999). This phenomenon, referred to in the literature as entombing, can result in the sequestration of up to one quarter of developing mites within brood cells (Rath, 1999).

Naturally selected tolerance to *V. destructor* has also been documented in certain *A. mellifera* populations (De Guzman *et al.*, 2008; Guzman-Novoa *et al.*, 2024). The most resistant populations have emerged among so-called Africanised *A. mellifera* colonies in tropical regions (Bianchi *et al.*, 2023). These colonies exhibit both active grooming behaviour and a high level of hygienic behaviour, similar to those observed in *A. cerana* (Bianchi *et al.*, 2023). One of the earliest reports describing a high degree of tolerance under tropical conditions originated from an isolated *A. mellifera* population on Fernando de Noronha Island in northeastern Brazil, where colonies had not received Varroa treatments since 1977 (Castilhos *et al.*, 2024). The emergence of natural tolerance in these populations cannot be attributed solely to the genotype of Africanised bees but rather reflects the long-term interaction of multiple favourable ecological and population-dynamic factors over nearly five decades. Since then, numerous studies from both Europe and the Americas have reported tolerant populations and explored the underlying mechanisms of Varroa tolerance (Mondet *et al.*, 2020).

Considerable efforts have been made to selectively breed *A. mellifera* lines with increased tolerance to *V. destructor*. One prominent example is the American-Russian breeding program, often referred to as the “Primorsky” bees, which resulted in the development of 18 lines exhibiting enhanced tolerance (De Guzman *et al.*, 2007). German beekeepers later adopted these selected lines, however, under Central European climatic conditions, the colonies failed to maintain the same level of mite tolerance (Rosenkranz *et al.*, 2010). Varroa tolerance depends on a suite of traits whose genetic selection is complicated by their polygenic nature (Sprau *et al.*, 2024a). Advances in next-generation sequencing (NGS) and SNP-based genotyping platforms represent major milestones in both Varroa research and selective breeding efforts (Kolics *et al.*, 2020; Spötter *et al.*, 2014; Gabel *et al.*, 2023). Key traits associated with Varroa tolerance include hygienic behaviour, Varroa-sensitive hygiene (VSH), suppressed mite reproduction (SMR), and grooming behaviour, all of which exhibit moderate to high heritability estimates (h^2=0.2-0.9) (Harbo and Harris, 1999 a,b; Gabel *et al.*, 2023). A further challenge arises from the mating biology of honey bees, which under natural conditions allows controlled selection primarily on the maternal side (Paxton, 2005). Artificial insemination and isolated mating stations, while effective, remain logistically demanding and often inaccessible for routine beekeeping practice (Büchler *et al.*, 2025). Overall, Varroa tolerance is not the result of a single adaptive trait but rather emerges from a complex network of behavioural, physiological, and genetic mechanisms. Understanding this multifaceted system is essential for the development of sustainable beekeeping practices and future breeding strategies aimed at mitigating the impact of *V. destructor*.

2.4. Non-destructive imaging techniques in apicultural research

The application of imaging techniques has become increasingly important in apicultural research, as these methods provide non-invasive, high-resolution investigative opportunities that were previously unavailable or only partially accessible. Technological advances particularly in high-resolution computed tomography (CT), micro-computed tomography (micro-CT), infrared thermography, and deep learning-based image analysis have continuously expanded the applicability and relevance of these approaches over the past decade (Jonsson, 2023; Urban and Chlebo, 2024). At the same time, the rapid adoption of imaging-based methodologies has highlighted one of the most critical methodological limitations in apicultural research: the substantial time and labor demands associated with manual image evaluation (Batz *et al.*, 2022; Toulkeridou *et al.*, 2023).

Classical ethological observations, such as the assessment of hygienic behaviour (including Varroa-sensitive hygiene, VSH) or the analysis of hive entrance traffic, traditionally rely on manual video analysis that can require days or even weeks of work. This approach drastically limits the number of colonies that can be examined simultaneously and reduces both the reproducibility and statistical power of such studies (Batz *et al.*, 2022; Urban and Chlebo, 2024). Batz *et al.* (2022) demonstrated that the manual video analysis of hygienic behaviour is “very time-consuming” and represents one of the primary bottlenecks of the apicultural ethological research. In contrast, the implementation of machine learning based image processing in their study reduced analysis time by approximately 70%, while simultaneously increasing the number of detected behavioural events, thereby effectively enlarging the sample size and accuracy of the measurements (Batz *et al.*, 2022). Similar conclusions were drawn by Alves *et al.* (2020), who described the visual evaluation of comb frames as a “labour-intensive, tedious and error-prone” procedure, which was substantially accelerated and improved in accuracy through deep learning-based comb cell characterization (Alves *et al*., 2020). Together, these findings clearly indicate that AI-driven image analysis does not merely represent a technical innovation but rather constitutes a methodological breakthrough capable of overcoming long-standing limitations related to time, labor, and sample size in apicultural research (Batz *et al*., 2022; Astuti *et al*., 2024; Copeland *et al*., 2025).

As a result of these technological developments, imaging techniques have now been incorporated into several areas of apicultural research, including X-ray-based micro-CT and human diagnostic CT approaches (Alba-Tercedor and Alba-Alejandre, 2017; Facchini *et al*., 2019; Bader *et al*., 2022). Also, infrared thermography offers a novel perspective for investigating the thermal dynamics of the superorganism during summer and winter time, and to understand ore the social fever responses and overall, the colony thermoregulation (Stabentheiner *et al*., 2010; Goblirsch *et al*., 2020). In parallel, rapid advances in computer vision have enabled automated ethological and ecological studies that were previously impractical due to the constraints of manual data processing (Berkaya *et al*., 2021; Astuti *et al*., 2024). Overall, the integration of imaging technologies has opened a new methodological era in apicultural science, in which large-scale, reproducible, objective, and non-invasive investigations have become increasingly feasible.

2.4.1. Applications of human diagnostic computed tomography

Computed tomography (CT) is a widely used imaging technique in human and veterinary diagnostics, as well as in numerous physiological and anatomical studies (Easton, 2012; Csóka *et al*., 2022; Petneházy *et al*., 2023). In entomological research, however, its application has remained relatively rare to date, even though the method offers several advantages that are particularly valuable for the investigation of small-sized, sensitive, or cryptically developing organisms. CT enables non-destructive, X-ray-based three-dimensional reconstruction of morphological and certain physiological characteristics, allowing for precise quantitative and qualitative measurements of internal structures (Easton, 2012; Mazonakis and Damilakis, 2016).

X-ray radiation belongs to the category of ionizing radiation and has historically been applied in entomological research primarily for pest sterilization within sterile insect technique (SIT) programs (Buscarlet, 1982; Hallman, 2013). However, the radiation doses used in modern CT systems are several orders of magnitude lower than those applied for sterilization purposes. Consequently, multiple studies have clearly demonstrated that CT examination conditions do not induce measurable physiological or behavioural impairments in insects (Wipfler *et al.*, 2016; Hall and Martín-Vega, 2019). This was further confirmed by Keszthelyi *et al.* (2015), who reported significant mortality or developmental damage in granary weevils (*Sitophilus granaries* L 1758) (Coleoptera: Curculionidae) only when exposed to radiation doses several orders of magnitude higher than those used in CT imaging. The first documented entomological application of CT was reported by Fuchs *et al.* (2004), who investigated the nest architecture, tunnel systems, and spatial distribution of individuals in termite colonies (*Cryptotermes secundus* Hill 1925) (Blattodea: Cryptotermitinae). Their work demonstrated that CT provides a unique opportunity to study enclosed, hidden, or otherwise inaccessible structures without disrupting colony organization. Since then, CT has proven particularly valuable in insect research where cryptic developmental stages, wood-boring pests, or the dynamics of developmental impairments can only be examined using non-invasive approaches (Keszthelyi *et al.*, 2020; Donkó *et al.*, 2022).

In apicultural research, the application of human diagnostic CT is still considered novel, and the number of available studies remains limited. Nevertheless, existing research indicates that CT can be applied with high precision across various areas of bee-related studies, including the investigation of honey ripening dynamics, colony wax architecture, and the morphological analysis of pupae (Eyer *et al.*, 2016; Facchini *et al.*, 2019; Bader *et al.*, 2022). Facchini *et al.* (2019) performed large-sample three-dimensional reconstructions of *A. mellifera* pupae using human diagnostic CT and demonstrated that pupae developing in Varroa-infested cells exhibit significant differences in body length and developmental progression compared to those from intact brood cells (Facchini *et al.*, 2019). In the field of honey bee health, Facchini *et al.* can be considered pioneers, as they were the first to apply human diagnostic CT as a measurement methodology within this research context. One of the principal advantages of this approach lies in its ability to visualize the interior of capped brood cells, a feature of particular importance for research targeting the cryptic developmental stages of *V. destructor* (Facchini *et al.*, 2019).

Overall, human diagnostic CT provides novel, high-resolution, non-destructive investigative opportunities in apicultural research. It may be regarded as a relatively rapid imaging modality, enabling the examination of capped brood, Varroa-induced developmental alterations, and factors influencing colony health with a level of detail and sample size that was previously unattainable.

2.4.2. Applications of micro-computed tomography

Micro-computed tomography (micro-CT) is a miniaturised, high-resolution variant of conventional human diagnostic CT that can achieve micrometer-scale spatial resolution (1-50 μm) (Clark and Badea, 2014, 2021). This technique is particularly well suited for the non-destructive, three-dimensional examination of small organisms, including insects, pupae, and even cellular-level structures (Clark and Badea, 2021; Jonsson, 2023). The fundamental difference between micro-CT and human diagnostic CT lies in the size of the investigated objects and the achievable image resolution: while the latter provides sub-millimeter-scale diagnostic resolution, micro-CT enables the visualization of anatomical, histological, and fine morphological details in the micrometer range. Consequently, micro-CT has become one of the most important modern tools in insect anatomy research (Smith *et al.*, 2016; Alba-Tercedor and Alba-Alejandre, 2017; Castejón *et al.*, 2018). A major advantage of micro-CT is its ability to generate three-dimensional reconstructions of internal anatomical structures in a non-destructive manner, making it applicable to both living and preserved insect specimens (Smith *et al.*, 2016; Poinapen *et al.*, 2017). The technique allows detailed examination of the head, thorax, and abdomen cavities, tracheal systems, musculature, the central nervous system, and even one of the most difficult soft tissue types to detect the fat body (Smith *et al.*, 2016; Bell *et al.*, 2023a; Bell *et al.*, 2023b). However, the method also has limitations, including relatively long scanning times that depend on the desired resolution and the size of the investigated object. In addition, image processing is often performed manually, which represents a major bottleneck for studies involving large sample sizes (Jonsson, 2023; Toulkeridou *et al.*, 2023).

In apicultural research, the use of micro-CT has expanded rapidly in recent years and has been applied primarily to anatomical investigations. Alba-Tercedor and Alba-Alejandre (2017) produced a detailed anatomical atlas of the thoracic and respiratory systems of *A. mellifera* using micro-CT (Alba-Tercedor and Alba-Alejandre, 2017). De Paula *et al.* (2022) combined micro-CT with various histological staining techniques to integrate two-dimensional and three-dimensional imaging, thereby describing the functional organization of the *A. mellifera* digestive system and providing a more detailed anatomical characterization of the peritrophic matrix (De Paula *et al.*, 2022). Micro-CT-based anatomical mapping is particularly valuable in developmental biology studies, where the growth, reorganization, or impairment of internal organs can be effectively tracked; however, such applications remain relatively underexplored (Castejón *et al.*, 2018; Sharma *et al.*, 2025). Recent technological advances have further expanded the applicability of micro-CT. The use of contrast-enhancing staining protocols (e.g., ethanol, iodine, methanol) has improved soft tissue differentiation, while advanced reconstruction algorithms have enabled more accurate volume and surface area calculations (Metscher, 2009; Swart *et al.*, 2016; Jonsson, 2023). As a result, micro-CT has evolved beyond the creation of anatomical atlases and is now suitable for quantitative tissue analyses, such as monitoring pupal development dynamics, assessing parasite-induced internal structural changes, and investigating the hidden biology of parasites (O’Sullivan *et al.*, 2018; Toulkeridou *et al.*, 2023).

Overall, micro-CT has become a key methodological tool in entomological research by providing non-destructive, high-resolution, three-dimensional insights. Within apicultural science, it holds considerable potential for elucidating the anatomical organization and developmental processes of the *A. mellifera* and its parasites. By complementing human diagnostic CT through its superior level of detail, micro-CT enables the detection and quantification of fine structural alterations, thereby delivering novel information for both fundamental research and applied bee health studies.

2.4.3. Applications of infrared thermography

Infrared thermography is a non-invasive imaging technique that enables two-dimensional spatial mapping of surface temperature based on the infrared radiation emitted by objects. The method is particularly well suited for the investigation of living systems, as it provides contact-free information on metabolic processes, heat production, and the dynamics of heat distribution (Kastberger *et al.*, 2003; Keszthelyi *et al.*, 2020). In apicultural research, thermography has gained particular importance in colony-level investigations, where thermoregulation, behaviour, and health status are closely connected (Kovac *et al.*, 2007; Stabentheiner *et al.*, 2010).

One of the most important advantages of thermographic applications in apicultural research is the possibility of performing continuous and repeatable measurements without substantially disturbing colony behaviour or internal structure (Klein *et al.*, 2014; Stabentheiner *et al.*, 2021). Consequently, the method is well suited for tracking temporal changes in colony-associated thermal patterns and for comparative analyses of the effects of treatments, environmental stressors, or shifts in health status (Kovac *et al.*, 2007; Goblirsch *et al.*, 2020; Stabentheiner *et al.*, 2022).

Infrared thermography is primarily applied as an indicator-based imaging approach. Numerous studies have demonstrated that the stability and spatial homogeneity of colony heat distribution are highly sensitive to colony condition, parasite load, and overall vitality (Starks *et al.*, 2000; Bauer *et al.*, 2018). Changes in thermal patterns may therefore serve as early, non-specific indicators of colony stress or dysfunction, often preceding the appearance of overt clinical symptoms (Goblirsch *et al.*, 2020). Thermography has also played an important role in the investigation of heat-related social behaviours, particularly in cases where the observed phenomena are temporally rapid, spatially heterogeneous, and difficult to capture using conventional sensors. One such example is social fever, a complex process that requires further investigation and for which infrared thermography is particularly suitable under field conditions (Bauer *et al*., 2018; Goblirsch *et al*., 2020). The technique enables spatial visualization and quantitative analysis of these thermal changes, thereby opening new perspectives for interpreting colony-level response mechanisms. The significance of infrared thermography is further enhanced by recent technological advances, as modern handheld thermal cameras now allow high-resolution and even continuous data acquisition. In parallel, artificial intelligence-based image analysis facilitates objective and reproducible evaluation of thermal patterns, which is especially important in large-scale and long-term apicultural studies where manual assessment represents a major methodological constraint due to its substantial time and labour requirements (Astuti *et al*., 2024; Rathore and Agrawal, 2024).

Overall, infrared thermography in apicultural research is not primarily aimed at describing fundamental thermoregulatory mechanisms, but rather at investigating their dynamics, stability, and deviations. The method effectively complements human diagnostic CT and micro-CT-based anatomical and developmental approaches by providing functional information at both the individual and colony levels regarding the current physiological state of colonies and its temporal variation.

3. MATERIALS AND METHODS

Detailed descriptions of the materials and methods applied in the individual studies are provided in the respective articles presented in Chapter 4. To avoid redundancy, the present chapter does not repeat the experimental procedures. Instead, Table 2 provides an overview of the main objectives of each study, together with the corresponding measurements and analytical approaches.

Table 2. Overview of different investigations and experimental settings, listing the applied diagnostic techniques, and the measured parameters of *A. mellifera* specimens

	Diagnostic techniques	**Measured effect**	**Measured parameters**
Study 1	Diagnostic CT	*V. destructor*	- Pupae surface - Pupae volume - Hounsfield value of pupae - Pupae weight - *V. destructor* numbers
Study 2	Diagnostic CT RT-PCR	*V. destructor* DWV virus	- Pupae body length - Head length - Thorax length - Abdomen length - DWV presence by RT-PCR
Study 3	Diagnostic CT Micro-CT	Cell structure	- Head length - Thorax length - Abdomen length - Pupae volume - Cell volume - Hounsfield values of brood cell
Study 4	Diagnostic CT Light microscope	X-ray irradiation	- Mortality of *A. mellifera* - Mortality of *V. destructor* - Hemolymph composition of *A. mellifera*
Study 5	Infrared camera	*V. destructor*	- Infestation rate of brood - Capping temperature of different *A.mellifera* developmental stages

4. PUBLICATIONS INCLUDED IN THE THESIS

4.1. CT-supported analysis of the destructive effects of *Varroa destructor* on the pre-imaginal development of honey bee, *Apis mellifera*

Title	CT-supported analysis of the destructive effects of *Varroa destructor* on the pre-imaginal development of honey bee, *Apis mellifera*
Authors	Sándor Keszthelyi, Tamás Sipos, Ádám Csóka, Tamás Donkó
Journal	Apidologie
Year	2021
Volume	52
Issue	1
Pages	155-162
Quartile	Q1
Impact factor	2.722
DOI	10.1007/s13592-020-00805-x

Apidologie (2021) 52:155 162

DOI: 10.1007/s13592-020-00805-x

Original article

CT-supported analysis of the destructive effects of *Varroa destructor* on the pre-imaginal development of honey bee, *Apis mellifera*

Sándor KESZTHELYI[1], Tamás SIPOS[1], Ádám CSÓKA[2], Tamás DONKÓ[2]

[1]Department of Plant Production and Protection, Kaposvár University, S. Guba str. 40, Kaposvar H-7400, Hungary
[2]Medicopus Nonprofit Ltd., S. Guba str 40, Kaposvar H-7400, Hungary

Received 22 October 2019 – Revised 26 July 2020 – Accepted 19 August 2020

Abstract – The ectoparasitic mite, *Varroa destructor*, is a most important health risk for European honey bee subspecies (*Apis mellifera*) globally. There is a scarcity in experimental approaches addressing this issue by using computed tomography. Our purpose was to determine the decrease in the volume, surface, density and weight alteration triggered by *V. destructor* in pre-imaginal stages of *A. mellifera* using computer-based 3-D reconstruction technology. Computer tomography used in the current study proved to be sufficiently sensitive for the detection of *V. destructor* in comb cells. This non-invasive experimental setup revealed that the developing worker pupae have retained their volume and surface values, whereas the weight loss triggered by *V. destructor* was statistically confirmed. In addition, the disappearance of lower radiodensity tissues is shown to be due to mite parasitism, which can be primarily explained by haemolymph losses.

computer tomography / pre-imaginal development / honey bee / impairment / *Varroa destructor*

1. INTRODUCTION

The honey bee mite *Varroa destructor* (Acari: Varroidae) is one of the most destructive natural enemy of the western honey bee, *Apis mellifera* (Anderson and Trueman 2000). Its original host is the eastern honey bee, *Apis cerana*; however, it attacks only its drone broods. It became a parasite for *Apis mellifera* subsequently, in areas in which both bee species coexist. Other host of this parasite mite is not known (Rosenkranz et al. 2010). It is native in Southeastern Asia, from where it started spreading worldwide. It has been present in Holarctic, Neotropical and Indo-Australian regions for over 40 years (Sammataro et al. 2000).

There are several biological consequences in honey bee caused by *V. destructor*. Colony losses caused by *V. destructor* in the western honey bee are mainly due to worker bee injury caused by this parasite mite during pre-imaginal development (Duay et al. 2003). The most plausible side effect is the weight loss during the post-embryonic infestation. Body weight loss right after the onset of adult stage can reach 10% in infested populations (De Jong et al. 1982). The parasitised adult bee emerges injured with a reduced life expectancy and impaired orientation ability (De Jong and De Jong 1983).

Previous research results have been reported as to V. destructor being a typically haemolymph parasite of immature and adult honey bees (Shaw and Stobbart 1963). The latest results (Ramsey et al. 2019), however,

---

Corresponding author: S. Keszthelyi,
ostrinia@gmail.com
Manuscript editor: Yves Le Conte

showed that the parasite adheres to the body of the bee and weakens it by sucking its fat. It is a vector for at least 5 debilitating bee viruses including RNA viruses such as the virus inducing deformed wing development (Genersch and Aubert 2010; Anguiano-Baez et al. 2016). Through weakening the immune system, it facilitates the occurrence of other pathogens, which can cause the overall extinction of the infested bee family (Yang and Cox-Foster 2005).

Although a detailed, non-invasive study from Facchini et al.'s (2019) experiment on *V. destructor* infecting honey bees at different developmental stages has recently been published, experimental studies performed on honey bee hives mainly omitted the use of computed tomography hitherto, even though computed tomography offers a non-invasive approach.

The goal of this study was to analyse the effect brought about by *V. destructor* on the pre-imaginal stage of *A. mellifera* in a non-invasive manner. Our purpose was to assess the putative change in the volume, density and weight in post-embryonic stages of *A. mellifera* caused by this important mite parasite using computer-based three-dimensional reconstruction technology.

2. MATERIAL AND METHODS

2.1. Sampling

A "warm way"-built hive (with the frames perpendicular to the entrance) was placed next to Kaposi Somogy County Teaching Hospital, Dr. Baka Jozsef Diagnostic, Radiation Oncology, Research and Teaching Centre (GPS coordinates: WGS: X:46.381079 Y:17,826915), in which computer tomography (CT) was conducted at the commencement of August 2019. One colony of *Apis mellifera carnica* kept on 10 frames was the subject of our investigation. Copious honey and pollen were available to feed the colony, and in addition bees were fed with 50% sugar drops during the survey. The young honey bee queen providing the progeny emerged on 15 May 2019. The colony infested with *V. destructor* was kept under natural conditions throughout the study. The average abundance calculated right before the implementation of the non-invasive analysis was 108.6 adult mites/frame. The last acaricide treatment of this colony was effectuated on 08 September 2018, after which other pesticides were not administered.

2.2. Description of the examination setup

In the course of the experiment, the colony was observed daily and the batches of the eggs laid simultaneously were analysed by CT (18 August 2019.). The broods were uniformly closed on the 9th day following egg-laying. After the brood coverage, a brood comb of 8 × 10 cm of the workers was cut from the centre of the frame, which was subsequently assigned to CT examination at equal intervals, four times during the post-embryonic development: on the 14th, 16th, 18th, and 20th day from the onset of egg-laying. One hundred fifty pupae were assayed, from which 10 intact and 10 infested pre-imaginal specimens were randomly selected for comparison. The sensitivity of the CT-method was visually examined by detecting *V. destructor* in the brood's cells, which was tested by extracting unexamined brood's cells in 10 replications. This comparison method was always carried out by two persons. Volume and tissue density data of pupae were gathered by means of computed tomography, from which the change in physiological characteristics of the honey bee pupae could be concluded. Between each recording, the comb sample was placed back to its original position in the frame. At the end of the survey, these examined worker pupae were removed from their brood cells and the number of adult female mites per cell was determined by their distinct, darker cuticle and signs of wear; subsequently the host bees were weighed on a micro-scale (Sartorius A120S) with the accuracy of 1 mg.

2.3. Computed tomography-assisted imaging analysis

The CT measurements were performed using a Siemens Somatom AS + CT scanner (Siemens Ltd., Erlangen, Germany). The following scanning parameters were used for data collection: 140 kV, 200 mAs and spiral data collection with pitch 0.7, UHR (Ultra High Resolution) mode. Axial scans were reconstructed at every 0.1 mm increment with 0.6-mm slice thickness and 60-mm field of view using V80 u convolution kernel. The images were archived in DICOM (Digital Imaging and Communications in Medicine) format and each of the series was subsequently converted to NIFTI (Neuroimaging Informatics Technology Initiative) metafiles. The resolution of the meta-images was nearly isotropic: $0.117 \times 0.117 \times 0.1$ mm^3.

The first step during the implementation of the analysis was the separation and identification of the individuals. The pupae were segmented manually using the segment editor module of the 3D Slicer program (Fedorov et al. 2012). The average radiodensities and volumes of the pupae were calculated using the voxels belonging to the pupae. Subsequently, the coordinates of those pupae voxels were considered to be the coordinates of the surface points of the pupae. Based on these 3-D point clouds, the surfaces of individual seeds were reconstructed through triangularisation. The 3-D models of seeds were created for measuring the surface size and visualisation of the pupae, in order to test the volume, surface and tissue density [(Hounsfield Unit (HU) is a quantitative value for describing radiodensity. It is frequently used in CT scans, where its value is also termed CT number].

2.4. Statistical analysis

For Hounsfield Unit and the weight values of the examined honey bee pupae, the Shapiro–Wilk test was used. For the survey of the normal distribution of data ($P < 0.05$), the Ghasemi- and Zahediasl-type methods were employed. The effects of *V. destructor* (post-embryonic development and health condition were the independent variables) on the volume (mm^3), the surface (mm^2) and the tissue density (HU) of infested pupae (as dependent variables) and its interaction with pre-imaginal development were statistically analysed by two-way ANOVA. The impact of mite parasitism on the weight of honey bee pupae measured at the end of the survey was evaluated by one-way ANOVA via using the SPSS for Windows 11.5 software package. Mean values were separated by using the Tukey test, at $P \leq 0.05$.

3. RESULTS

3.1. Sensitivity of CT for mite detection and infestation rate

The detection rate of *V. destructor* present in the analysed comb by CT has continuously increased during the progress of post-embryonic development of honey bee pupae. The early developing stage of parasite can be seen in the lateral side of pre-imaginal honey bee pupae in Figure 1. The perception rates of the parasite in the four non-invasive recordings were the following: 1st recording, 43.33%; 2nd, 76.66%; 3rd, 90%; 4th, 100%.

The infestation in the experimental comb was 21.31% (Figure 2). Additionally, the average number of mites per one infested cell was 4.68, which has been determined after the opening of cells at the end of the experiment.

3.2. Volume, surface and tissue density data of pupae

The Shapiro–Wilk normality test showed that our CT-measured data are of normal distribution, $P > 0.05$. Uniform significant differences in the tissue density of pupae between intact and infested samples were revealed by statistical analysis.

The effect of post-embryonic development on the change in volume ($P = 2.47 \times 10^{-19}$), surface ($P = 4.91 \times 10^{-18}$) and tissue density ($P = 1.73 \times$

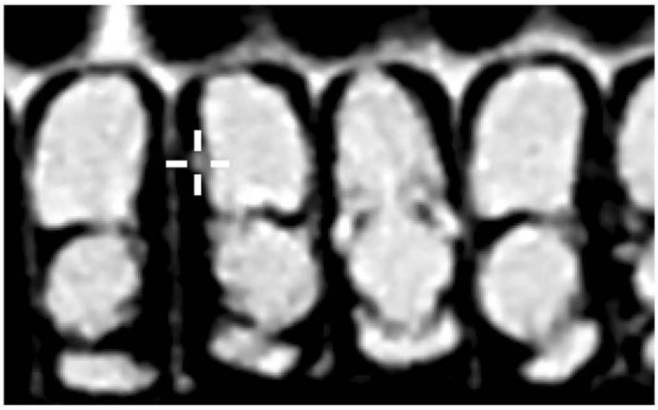

Figure 1. Axial CT recordings of honey bee pupae with feeding *V. destructor* (marked by white cross).

10^{-8}) data of pupae was confirmed by two-way ANOVA.

Volume reduction in pupae triggered by *V. destructor* could be detected in this experiment (Figure 3a, b, c, d, e, f, g, and h). The volumes of the parasite-infected pupae and intact pupae as well decreased in each observation record with the exception of the 2nd recording. We showed a remarkable difference on the 1st recording as well (2.898 mm^3), but the most spectacular difference (3.435 mm^3) between the volumes of the infested samples and those of the intact ones was measured on the 3rd recording. Nonetheless, the effect of mite parasitism on volume decrease in bee pupae could not be proven statistically ($P = 0.271$) by two-way ANOVA. The combined effect of pre-imaginal development and parasitism on the volume change in the bee pupae showed a not statistically proven relationship ($P = 0.692$).

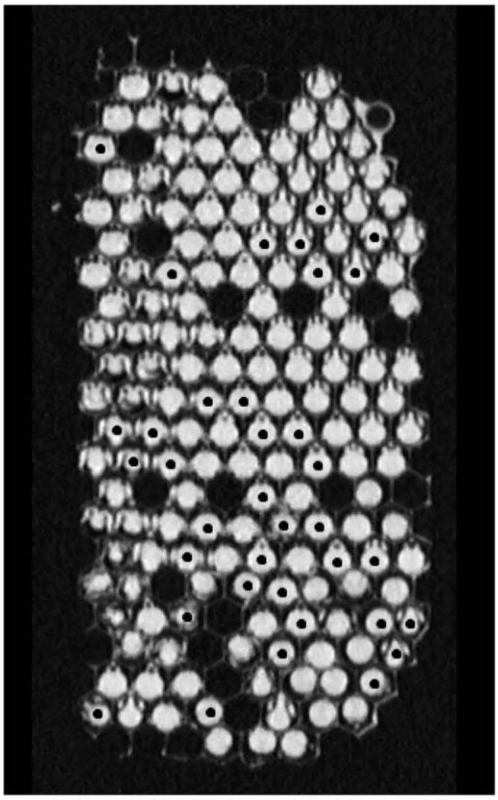

Figure 2. Experimental sample of honey bee comb with black spot marking of infested cells by *V. destructor*.

The surface of intact and infested samples within the same recording was examined in conjunction with the volume. The surface of the examined intact samples was 136.711 ± 1.276 mm^2 at the end of the examination. The surface loss in the infested pupae was 0.667 mm^2 on average on the 4th recording, but this decrease ($P = 0.842$) and the interaction with pre-imaginal development ($P = 0.085$) were not statistically confirmed.

The pupae tissue densities expressed by Hounsfield Unit (HU) of intact and infested honey bees are shown in Figure 4a, b, c, d, e, f, g, h, and i. The samples infested by *V. destructor* have lower radiodensity values than those of the intact samples, which has

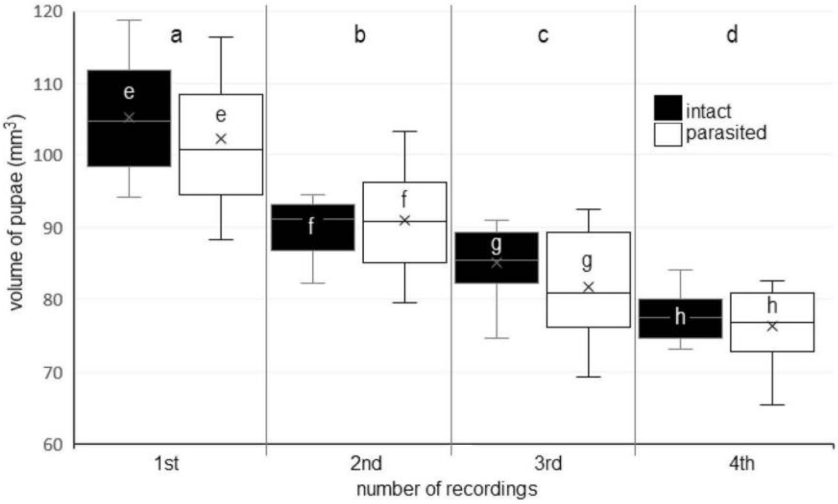

Figure 3. The volume (mm^3) changing of honey bee pupae during the examination as a function of *V. destructor* parasitism ($n = 20$). (a, b, c, d) Small letters indicate significant difference ($p \leq 0.05$) between means of different recording times; (e, f, g, h) small letters indicate significant difference ($p \leq 0.05$) between intact and parasite samples.

been confirmed by two-way analysis of variance ($P = 8.64 \times 10^{-6}$). The mean changing density of the infested pupae was 1.657 HU (1.481%). Eventually, the dense tissue formation has disappeared from the pupae of honey bee, which may be due to sucking by *V. destructor*. Nonetheless, the interaction of the parasitism and the development could not be statistically confirmed ($P = 0.084$).

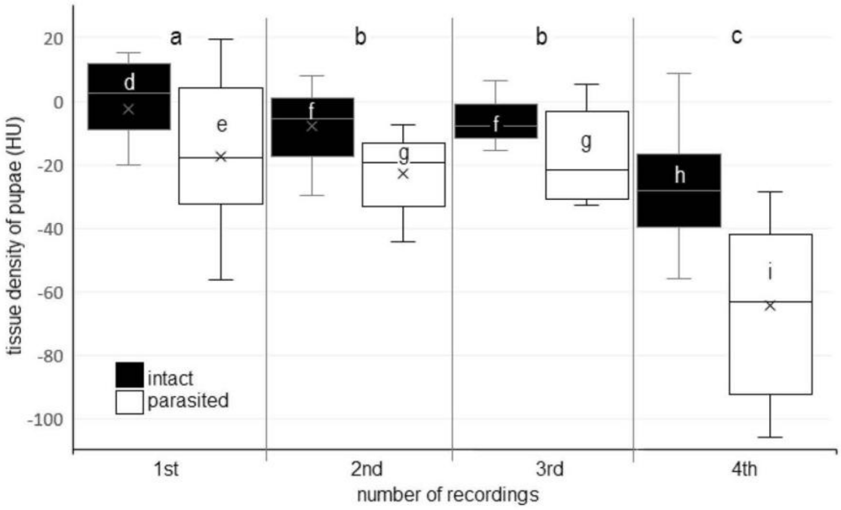

Figure 4. The tissue density (HU) changing of honey bee pupae during the examination as a function of *V. destructor* parasitism ($n = 20$). (a, b, c) Small letters indicate significant difference ($p \leq 0.05$) between means of different recording times; (d, e, f, g, h, i) small letters indicate significant difference ($p \leq 0.05$) between intact and parasite samples.

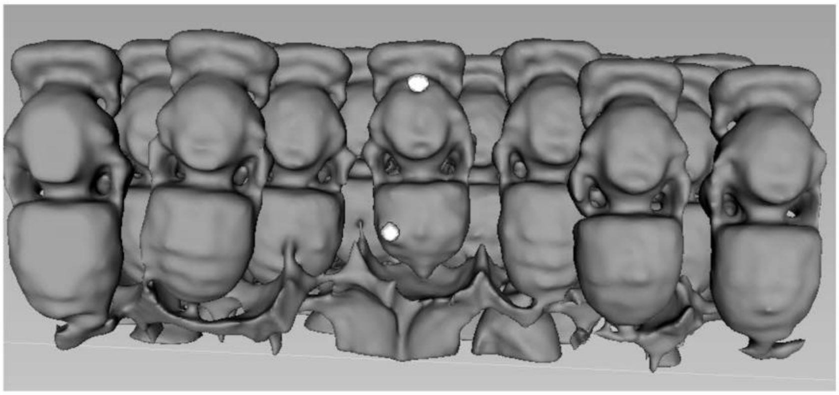

Figure 5. Computer-based three-dimensional reconstructions of honey bee pupae infested by *V. destructor* in the comb. *V. destructor* are marked by white spots.

3.3. Weight of pupae

The weight loss of honey bee pupae attacked by *V. destructor* (Figure 5) was evinced. The mean of calculated weight of the infested pupae was 105.2 ± 0.001 mg, while the same developing stage (healthy stage) was 121.9 ± 0.001 mg, which represents 16.6 mg (13.665%) weight loss in the case of the damaged honey bee pupae. The effect of parasitism on the weight of this pre-imaginal stadium of honey bee was statistically demonstrable ($P = 8.41 \times 10^{-7}$) by one-way ANOVA.

4. DISCUSSION

It is claimed that computer tomography as a new, non-invasive method in apiary researches is suitable for the detection of *V. destructor* in comb cells. Naturally, the detection rate depends on the operator's aptitude, but generally, the later the scan, the easier it is to spot a mite in a cell. However, it proved most suitable in observations at more advanced developing stages of mite, at which the deutochrysalis has already exhibited the final body shape. At the deutochrysalis stage, the coloration starts on the periphery of the opisthosoma and shifts to a reddish-brown colour after the moult of the female (Rosenkranz et al. 2010). Further, the better detection of parasites by CT at late developmental stages can be partly explained by the hidden lifestyle of both the founder mite and the larvae at earlier developing stages. The nymphs are generally located on the 5th segment on the bee pupa and near the so-called faecal accumulation site at the bottom of the cell (Kanbar and Engels 2003).

The infestation rate of *V. destructor* reported in this study can be considered to be the average infestation rate on the basis of the relevant data, which substantially vary between 7% (De Guzman et al. 2007) and 30% (Rosenkrantz et al. 2006). Besides, it cannot be excluded that the infestation rate can reach higher value in a comb as *V. destructor* might not infest cells in a uniform way within a comb (Facchini et al. 2019). The recorded number of parasite mites in one cell coincided with the normal progeny rate of *V. destructor* reported in previously published works. It is normal for a fertile mite to lay five eggs (one male and four females) in worker cells, which can be located close to each other (Martin 1995; Rosenkranz et al. 2010).

The anatomical features measured by CT in developing honey bee pupae were unequivocally influenced by parasitism. According to our CT-assisted observation, the developing honey bee pupae have retained their volume and surface values (which can be partially explained by the normal post-embryonic development too), while the weight loss triggered by *V. destructor* was observable. These results are in line with the data presented previously in the relevant literature (Colin et al. 1999; van Engelsdorp et al. 2007;

Facchini et al. 2019). Duay et al. (2003) have presented the first reliable data on individual drone weight loss, especially from the red-eyed pupal stage onwards. The resulting reduction in the weight of adult drones was related to the number of female mites (up to 20) that had invaded a brood cell.

The diminished radiodensity in animal tissues (e.g. fat) in infested pupae can be explained by the disappearance of high-density organic (e.g. proteins, carbohydrates) and inorganic (e.g. water) materials (Romvari et al. 1996; McEvoy et al. 2008). In this context, it is worth mentioning that water (as an essential component) can be found in the largest quantities in insect haemolymph (Shaw and Stobbart 1963).

Albeit direct tissue analysis was not carried out in this study, based on our results, it can be inferred that the content of haemolymph could be decreased primarily by *V. destructor* parasitism due to water being the densest and the highest proportion component of this insect tissue. The results of former experiments are confirmed by our findings. Ramsey et al. (2019) showed that this parasite does not only consume body fat but also damages host bees by haemolymph sucking, a phenomenon which could not be verified by our study. *Varroa* parasitism is associated with impaired development of immature bees, decreased lipid synthesis, reduced protein titers, desiccation, impaired metabolic function, inability to replace lost protein, precocious foraging, heightened winter mortality, impaired immune function, decreased longevity and reduced pesticide tolerance (Bowen-Walker and Gunn 2001; van Dooremalen et al. 2013).

In summary, our results can shed light on the consequences of the damage brought about by *V. destructor* during the pre-imaginal stages of honey bee development in a non-invasive way. Our reconnaissance study in the detailed biology of this important ectoparasite can play an important role in the understanding of some viral disorders transferred by mite (e.g. CCD) as well as the elaboration of strategies aimed at successful protection method against it. These novel data originating from CT imaging can contribute to the understanding of the complex phenomenon of colony collapse disorder.

AUTHORS' CONTRIBUTIONS

Sandor Keszthelyi and Tamas Donko conceived and designed the research project. Tamas Sipos provided the experimental bee colony. Tamas Donko and Tamas Sipos conducted the experiments. Adam Csoka and Tamas Sipos did the CT image post-processing and connected data analysis. All authors analysed the data. Sandor Keszthelyi wrote the manuscript. All authors read and approved the manuscript.

FUNDING INFORMATION

Open access funding provided by Kaposvár University. The work was supported by the GINOP-2.2.1-15-2016-00021 and the EFOP-3.6.3-VEKOP-16-2017-00008 projects. The project is co-financed by the European Union, the European Regional Development Fund and the European Social Fund.

COMPLIANCE WITH ETHICAL STANDARDS

Conflict of interest The authors declare that they have no potential conflict of interest in relation to the study presented in this paper.

OPEN ACCESS

Analyse par tomographie assistée par ordinateur des effets destructeurs de *Varroa destructor* sur le développement préimaginal de l'abeille, *Apis mellifera*.

tomographie par ordinateur / développement préimaginal / abeille domestique

Eine CT-Analyse der negativen Auswirkungen von *Varroa destructor* auf die on the preimaginal development of honey bee, *Apis mellifera.*

Computertomograph / präimaginale Entwicklung / Honigbiene

REFERENCES

Anderson, D.L., Trueman, J.W.H. (2000) *Varroa jacobsoni* (Acari: Varroidae) is more than one species. Exp. Appl. Acarol. **24** (3), 165–189

Anguiano-Baez, R., Guzman-Novoa, E., Hamiduzzaman, M.M., Espinosa-Montaño, L.G., Correa-Benítez, A. (2016) *Varroa destructor* (Mesostigmata: Varroidae) parasitism and climate differentially influence the prevalence, levels and overt infections of deformed wing virus in honey bees (Hymenoptera: Apidae). J. Insect Sci. **16** (1), 44.

Bowen-Walker, P.L., Gunn A. (2001) The effect of the ectoparasitic mite, *Varroa destructor* on adult worker honeybee (*Apis mellifera*) emergence weights, water, protein, carbohydrate, and lipid levels. Entomol. Exp. Appl. **101** : 207–217.

Colin, M.E., Fernandez, P.G., Ben Hamida, T. (1999) Varoosis, bee disease diagnosis. Opt. Méditerr. **25**, 121–142.

De Jong, D., De Jong, P.H. (1983) Longevity of Africanized honeybees (Hymenoptera: Apidae) infested by *Varroa jacobsoni* (Parasitiformes: Varroidae). J. Econ. Entomol. **76** (4), 766–768.

De Jong, D., De Jong, P.H., Gonçalves, L. (1982) Weight loss and other damage to developing worker honeybees from infestation with *Varroa jacobsoni* . J. Apic. Res. **21** (3), 165–167.

Duay, P., De Jong, D., Engels, W. (2003) Weight loss in drone pupae (*Apis mellifera*) multiply infested by *Varroa destructor* mites. Apidologie **34** (1), 61-65.

Facchini, E., Nalon, L., Andreis, M.E., Di Giancamillo, M., Rizzi, R., Mortarino, M. (2019) Honeybee pupal length assessed by CT-scan technique: effects of *Varroa* infestation, developmental stage and spatial position within brood comb. Sci. Rep. **9,** 10614

Fedorov, A., Beichel, R., Kalpathy-Cramer, J., Finet, J., Fillion-Robin, J.C., Pujol, S., Bauer, C., Jennings, D., Fennessy, F.M., Sonka, M., Buatti, J., Aylward, S.R., Miller, J.V., Pieper, S., Kikinis, R. (2012) 3D Slicer as an image computing platform for the quantitative imaging network. Magn. Reson. Imaging. **30**, 1323-1341.

Genersch, E., Aubert, M. (2010) Emerging and re-emerging viruses of the honey bee (*Apis mellifera* L.). Vet. Res. **41** (6), 54.

Guzman, L., Rinderer, T.E., Frake, A. (2007) Growth of *Varroa destructor* (Acari: Varroidae) populations in Russian honey bee (Hymenoptera: Apidae) colonies. Ann. Entomol. Soc. Am. **100** (2), 187-195.

Kanbar, G., Engels, W. (2003) Ultrastructure and bacterial infection of wounds in honey bee (Apis mellifera) pupae punctured by *Varroa* mites. Parasitol. Res. **90** (5), 349–354.

Martin, S.J. (1995) Ontogenesis of the mite *Varroa jacobsoni* Oud. In the drone brood of the honeybee *Apis mellifera* L. under natural conditions. Exp. Appl. Acarol. **19** , 199-210.

McEvoy, F.J., Madsen, M.T., Strathe, A.B., Svalastoga. E. (2008) Hounsfield Unit dynamics of adipose tissue and non-adipose soft tissues in growing pigs. Res. Vet. Sci. **84** , 300-304.

Ramsey, S.D., Ochoa, R., Bauchan, G., Gulbronson, C., Mowery, J.D., Cohen, A., Lima, D., Joklik, J., Cicero, J.M., Ellis, J.D., Hawthorne, D., van Engelsdorp D. (2019) *Varroa destructor* feeds primarily on honey bee fat body tissue and not hemolymph, Proc. Natl. Acad. Sci. **116** (5), 1792-1801.

Romvari, R., Milisits, G., Szendro, Z., Sorensen, P. (1996) Non-invasive method to study the body composition of rabbits by X-ray computerised tomography. World Rabbit Sci., *4* (4), 219-224.

Rosenkrantz, P., Fries, I., Imdorf, A. (2006) Survival of mite infested (*Varroa destructor*) honey bee (*Apis mellifera*) colonies in Nordic climate. Apidologie, **37** (5), 564-570.

Rosenkranz, P., Aumeier P., Ziegelmann, B. (2010) Biology and control of *Varroa destructor* . J. Invertebr. Pathol. **103** (1), 96–119.

Sammataro, D., Gerson, U., Needham, G. (2000) Parasitic mites of honey bees: life history, implications and impact. Ann. Rev. Entomol. **45,** 519-548.

Shaw, J., Stobbart, R.H. (1963) Osmotic and ionic regulation in insects. Adv. Ins. Physiol. **1** , 315-319.

van Dooremalen C, Stam, E., Gerritsen, L., Cornelissen, B., van der Steen, J., van Langevelde, F., Blacquière, T. (2013) Interactive effect of reduced pollen availability and *Varroa destructor* infestation limits growth and protein content of young honey bees. J. Insect Physiol. **59** : 487–493.

van Engelsdorp, D., Underwood, R., Caron, D., Hayes, J. (2007) An estimate of managed colony losses in the winter of 2006–2007: a report commissioned by the apiary inspectors of America. Am. Bee J. **147** , 599–603.

Yang, X., Cox-Foster, D.L. (2005) Impact of an ectoparasite on the immunity and pathology of an invertebrate: evidence for host immunosuppression and viral amplification, Proc. Natl. Acad. Sci. **102** (21), 7470–7475.

4.2. Study of Morphological Features in Pre-Imaginal Honey Bee Impaired by *Varroa destructor* by Means of Computer Tomography

Title	Study of Morphological Features in Pre-Imaginal Honey Bee Impaired by *Varroa destructor* by Means of Computer Tomography
Authors	Tamás Sipos, Tamás Donkó, Ildikó Jócsák, Sándor Keszthelyi
Journal	Insects
Year	2021
Volume	12
Issue	8
Pages	717
Quartile	Q1
Impact factor	3.141
DOI	10.3390/insects12080717

insects

MDPI

Article

Study of Morphological Features in Pre-Imaginal Honey Bee Impaired by *Varroa destructor* by Means of Computer Tomography

Tamás Sipos [1,†], Tamás Donkó [2,†], Ildikó Jócsák [1] and Sándor Keszthelyi [1,*]

[1] Department of Agronomy, Kaposvár Campus, Hungarian University of Agriculture and Life Sciences, S. Guba Str. 40, H-7400 Kaposvár, Hungary; sipostomi97@gmail.com (T.S.); jocsak.ildiko@uni-mate.hu (I.J.)
[2] Medicopus Nonprofit Ltd., S. Guba Str. 40, H-7400 Kaposvár, Hungary; donko.tamas@sic.medicopus.hu
* Correspondence: ostrinia@gmail.com
† These authors contributed equally to this work.

Simple Summary: The *Varroa* mite (*Varroa destructor*) is the most important natural pest of the honey bee, *Apis mellifera*, worldwide. The extent to which impairments in honey bees occur concomitantly upon infestation by this parasite greatly varies. Inter alia, the *Varroa* mite causes developmental disorders mediated by deformed wing virus in this host. Although there is a plethora of information regarding the consequences of this parasitism in the fully developed stage, data concerning the pre-imaginal honey bee stage inside the comb are rather scarce. In this study, morphological differences in the main body parts of the honey bee during the development stages of both intact and parasitized larvae were measured inside the comb by means of computed tomography. The images obtained reveal a visualization of the harmful effects of the *Varroa* mite on the pre-imaginal host. Our results demonstrate that the deformation of certain body parts was due to the presence of the parasite. Deformity, as the most conspicuous sign of infestation, is coupled with a decrease in the total-body size and abdomen size together with a disproportionate ratio of different body parts. In summary, information on the impairment of honey bee development triggered by the *Varroa* mite gives the opportunity to assess the damage caused by this serious pest, which occurs latently in honey bees.

Abstract: The honey bee (*Apis mellifera* L. 1778) is an essential element in maintaining the diversity of the biosphere and food production. One of its most important parasites is *Varroa destructor*, Anderson and Trueman, 2000, which plays a role in the vectoring of deformed wing virus (DWV) in honey bee colonies. Our aim was to measure the potential morphometric changes in the pre-imaginal stage of *A. mellifera* caused by varroosis by means of computed tomography, hence supplying evidence for the presumable role that *V. destructor* plays as a virus vector. Based on our results, the developmental disorders in honey bees that ensued during the pre-imaginal stages were evident. The total-body length and abdomen length of parasitized specimens were shorter than those of their intact companions. In addition, the calculated quotients of the total-body/abdomen, head/thorax, and head/abdomen in parasitized samples were significantly altered upon infestation. In our view, these phenotypical disorders can also be traced to viral infection mediated by parasitism, which was confirmed by reverse transcriptase polymerase chain reaction (RT-PCR) analysis. Capitalizing on a non-destructive method, our study reveals the deformation of the honey bee due to mite parasitism and the intermediary role this pest plays in viral infection, inside the brood cell.

Keywords: body part deformation; computed tomography; honey bee; non-destructive analysis; non-invasive method; varroosis; deformed wing virus; RT-PCR; virus impact

Citation: Sipos, T.; Donkó, T.; Jócsák, I.; Keszthelyi, S. Study of Morphological Features in Pre-Imaginal Honey Bee Impaired by *Varroa destructor* by Means of Computer Tomography. *Insects* **2021**, *12*, 717. https://doi.org/10.3390/insects12080717

Academic Editors: Alberto Satta and Panagiotis Theodorou

Received: 17 June 2021
Accepted: 4 August 2021
Published: 11 August 2021

1. Introduction

The role of the honey bee (*Apis mellifera* L. 1778) is essential in maintaining the diversity of the biosphere and food production. Approximately 35 percent of the world's agricultural production depends on these pollinators [1]. Pollination of numerous plant species carried out by bees in industrial agricultural environments is more effective and precise than other modern techniques, as has been pointed out by several researchers [2,3]. Therefore, it is essential to gain accurate and detailed information about abiotic and biotic factors that can endanger these pollinators.

Several organisms, e.g., viruses, bacteria, fungi, and arthropods, are known to have an adverse effect on the health conditions of bees. One of the most important factors among these is the *Varroa* mite (*Varroa destructor*, Anderson and Trueman, 2000), whose significance has increased worldwide over the past 25 years [4]. The beginning of its global spread can be dated back to the 1970s, and its role has become more substantial in apiary ever since [5]. This devastating parasite plays an important part in colony collapse disorder (CCD) syndrome, which has been detected worldwide [6–8]. Specimens impaired by varroosis are characterized by altered body size and weight, weakened immune system, and severe morphological and behavioral disorders [7,9–11]. The triggering factors of these impairments are the sucking of the hemolymph by the mites and parasitism of the fat cells of hosts as well as the vectoring of 20 different virus types [12–14].

The A, B, and C variants of deformed wing virus (DWV) are the most damaging factors to honey bees among all viruses vectored by the *Varroa* mite [15,16]. The *Varroa* mite plays an unequivocally important part in the spreading of several viruses in honey bee colonies, and its harmful activity is paralleled by the phenomenon of colony collapse disorder (CCD) and the virus titer degree, which has been characterized as a marker by Dainat et al. [17]. The morphological and other physiological consequences of this viral infection for the host are well-defined, such as underdeveloped wing initiatives, distortion and shortening of the abdomen, decrease in body weight, and decolorization of cuticles, as well as decreased carbohydrate content, behavioral abnormalities, and reduced lifespan [18,19].

The serious health-deteriorating role of DWV has already been proven. Moreover, the harmful insect-pathological consequences of *V. destructor* have significantly increased due to DWV, as was pointed out Roberts et al. [20]. These authors concluded that populations of *A. mellifera* in Papua New Guinea can tolerate *V. jacobsoni* because the damage from parasitism is significantly reduced without DWV. This study also provides further evidence that DWV does not exist as a covert infection in all honey bee populations.

In general, data gained by computed tomography are sporadic concerning the hidden developing stages of insects [21]. Nevertheless, the method can be applied with high efficiency for the assessment of pest morphology and the observation of arthropod development [22], which has been confirmed by several studies [23,24]. High-resolution computed tomography provides a new approach for more details on the metamorphosis of several insects, and it allows the measurement of the volumes of internal tissues and organs [24]. This approach allows the observation of the analyzed subject in its natural environment, without disturbing it. Laboratory circumstances can create an opportunity for the observation of the finest biological details, the gathering of which is not permitted by conventional diagnostic methods [21,22,25,26]. The results acquired by applying this non-invasive method can provide additional information about biological and ecological processes as to the hidden lifestyles of covertly developing arthropods. The thorough investigation of morphological structures, related environmental conditions, and hidden biological characteristics associated with the pest is a prerequisite for understanding the functions of ecological relationships [24,25]. Regarding the honey bee, the various behaviors inside the colony, especially within the cells, are mostly hidden. Siefert et al. [27] were the first to provide a comprehensive source of online video material that offers a view on honey bee behavior within comb cells, thereby providing a new mode of observation for the scientific community.

There are some studies [11,28] in connection with experimental investigations assisted by CT; nevertheless, the initial developing features of *V. destructor* are mainly unexplored. The explanation for this is to be mostly found in the hidden development of this species, whose harmful activities and consequences for the host are demanding to detect and measure within the comb. The objectives of our experimental work were to measure the potential morphometric changes during the pre-imaginal stage of *A. mellifera* caused by *V. destructor* in a non-invasive way and to detect the presence of DWV as the most common deformity-causing virus by using molecular biology tools. In addition, we intended to obtain information about the side effects of varroosis by means of computer-based three-dimensional reconstruction technology, which can be manifested in measurable size distortion of the host. This approach can assist in elucidating the role played by the virus vector *V. destructor* in honey bee biology.

2. Materials and Methods

2.1. Sampling and Origin of Honey Bees

The experimental comb originated from a honey bee colony located in Kaposvár (Somogy county, Hungary; GPS coordinates: WGS:X:46.381079 Y:17.826915). One colony of *Apis mellifera carnica* dwelling in a "warm way"-built hive (with the frames perpendicular to the entrance) was the subject of our investigation, which was settled in the previous year (September 2018). The colony was isolated in order to avoid infection from other bee pathogens and parasites.

The main expectation was a high infestation rate of the *Varroa* mite during the selection of the experimental colony. The degree of parasitism was assessed based on our previous, systematic observations [11], which were continuously monitored during the experimentation. Powdered sugar was used for the evaluation of the mite infestation rate. In the course of this evaluation, a nurse frame containing brood combs was shaken off in a bucket containing 200 g powdered sugar. Subsequently, the bees were separated by means of a sieve, prior to dissolving the sugar in filtered water. Mites remaining on the filter were counted in order to establish the mite infestation rate. The number of mites shaken off the frame was 100. The overall number of mites per hive was acquired by multiplying by the number of brood comb frames in the hive [29,30].

During the implementation of this part of the experiment, one frame was chosen, in which egg laying happened at the same time. Times of sampling were on 5, 7, and 9 September 2019, which coincided with the flowering of the giant goldenrod (*Solidago gigantea*, Aiton). A brood comb of 8 × 10 cm of workers was isolated from the comb, which was the subject of our examination. The excision of comb samples was done with a scalpel, after which the damaged honeycombs were immediately removed from the edge of this piece of comb. This comb piece was "returned" to the original frame in its original place until the beginning of the laboratory studies (5 September 2019) throughout the periods between the recordings. Thus, it was ensured that the colony had appropriate temperature and humidity for the optimal development of the investigated pre-imaginal stages. At the end of performing the non-invasive assay, the broods were opened, the weight of analyzed pre-imaginal stages was measured with an Ohaus Explorer Pro EP214CE device.9, and the mite numbers of the brood noted.

2.2. Description of the Examination Set-Up

As a first step, we determined the infestation rate of the *Varroa* mite using CT recordings based on the work of Keszthelyi et al. [11]. Based on this preparatory work, 15-15 parasitized and intact pieces of brood comb adjacent to each other (in an effort to exclude different developmental conditions such as temperature, relative humidity, etc.) were selected, which were computed tomography-measured three times during the post-embryonic development: on the 14th, 16th, and 18th days.

Transversal measurements (mm) were performed on the cross-section recordings in the following areas of the pre-imaginal stages (Figure 1): head (a); thorax (b); abdomen (c); total-body (A) (16 days old, red-eyed pupa (Pr); dark brown-eyed pupae with light pigmented thorax (Pdl); 20 days old, dark brown-eyed pupae with dark thorax (Pdd); following [31]). Slicer 4.11 software [32] was used for this survey. Additional proportion values were calculated in order to assess body distortion caused by parasitism and its virus impact:

quotients of the total-body and head (A/a), total-body and thorax (A/b), total-body and abdomen (A/c), head and thorax (a/b), and head and abdomen (a/c).

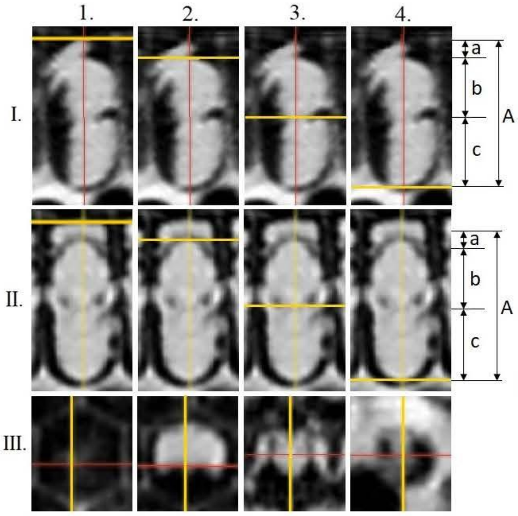

Figure 1. Different image reconstruction planes of examined brood cells as well as different measurement points at the 18th day of development of the pre-imaginal stage of the honey bee. I.: sagittal, II.: coronal, III.: transversal; 1, 2, 3, 4: the distances of measurements; a: head length, b: thorax length, c: abdomen length, A: total-body length.

2.3. Computed Tomography-Assisted Image Analysis

The separated brood comb pieces were scanned using a Siemens Somatom Definition AS+ CT (Siemens Ltd., Erlangen, Germany) cross-sectional digital imaging equipment. The acquisitions were performed in Ultra High Resolution (UHR) mode using the following parameters: tube voltage 140 kV, tube current 200 mAs, spiral data collection with pitch factor of 0.7. The transversal images were reconstructed by Somaris/7 Syngo CT (VA48A) software (Siemens Health Care, Erlangen, Germany) with the following settings: Field of View 60 mm, slice thickness 0.6 mm, increment 0.1 mm, convolution kernel V80u. The scans were archived in DICOM (Digital Imaging and Communications in Medicine) format, and then the data collection ranges were subsequently converted to NIFTI (Neuroimaging Informatics Technology Initiative) metafiles with almost isotropic resolution: $0.117 \times 0.117 \times 0.1\ \mathrm{mm}^3$. The image post-processing and visualization was carried out by 3D-Slicer software (www.slicer.org) (accessed on 24 February 2021). The fiducial module was used to settle the marker points. Python 3.6 programming language was used for the calculations of the distances between the marker points.

2.4. Detection of DWV with PCR Assay

The abdomens of five healthy and five parasitized specimens (developmental stage: Pdd) were homogenized immediately after death in the lysis buffer of the RNeasy Fibrous Tissue Mini Kit (Qiagen, 19300 Germantown Road, Germantown, MD, USA) in a Tissuelyser II high-throughput sample disruptor (Qiagen, 19300 Germantown Road, Germantown, MD, USA). In order to avoid RNA degradation, the adapter of the homogenizer was cooled down to −20 °C. RNA extraction was carried out according to the instructions of the manufacturer. Our choice of body part to be sampled was made based on preliminary studies in which the abdomen contained the highest concentration of DWV [33]. Furthermore, Ramsey et al. [12] found that *V. destructor* feeds primarily on honey bee body fat tissue. These results encouraged us to conduct the sampling on the abdomen, where most of the DWV is expected to be found. These molecular studies were conducted on 10 September 2019.

The quantity and quality of RNA were measured using a Thermo Scientific™ NanoDrop™ OneC Microvolume UV-Vis Spectrophotometer (Thermo Scientific™ 840274200, 168 3rd Ave, Waltham, MA, USA). cDNA synthesis was carried out with a QuantiTect Reverse Transcription Kit, for 15 min at 42 °C (Qiagen, 19300 Germantown Road, Germantown, MD, USA) according to the manufacturer's instructions, after the usage of DNA wipeout procedure for 2 min at 42 °C.

After cDNA synthesis, a PCR reaction was carried out with DWV primers F: ATT GTG CCA GAT TGG ACT AC; R: AGA TGC AAT GGA GGA TAC AG [34], under the conditions: initial denaturation at 95 °C for 15 min; 40 cycles of PCR, each consisting of 30 s at 94 °C, 50 s at 58 °C, and 1 min at 72 °C. The primers target the sequence of DWWqp1 polyprotein (NCBI accession number: AJ489744). Reactions were completed by a final elongation step for 7 min at 72 °C. The PCR products were electrophoresed in a 2% Tris-acetate-EDTA–agarose gel and stained with SYBR™ Gold Nucleic Acid Gel Stain (Thermo Scientific™ 840274200, 168 3rd Ave, Waltham, MA, USA). Bands were visualized under UV light. Fragment sizes were determined with reference to a 1 kb DNA ladder: GeneRuler™ 1 kb Plus DNA Ladder, ready-to-use (Thermo Scientific™ 840274200, 168 3rd Ave, Waltham, MA, USA).

2.5. Statistical Analysis

In order to determine whether the morphological data of the pre-imaginal stadium of honey bees came from a population with a specific distribution, the Kolmogorov–Smirnov test ($n < 50$) was used. For the survey of the normal distribution of data ($p < 0.05$), Ghasemi- and Zahediasl-type methods were employed. The effect of parasitism on the analyzed morphological parameters of this pre-imaginal stadium of honey bees was statistically demonstrable by one-way ANOVA with the help of SPSS 11.5 software. Means were separated by using the Tukey (HSD) test, at $p \leq 0.05$. The data of body sizes as a function of developmental time in different time points within groups were statistically examined by Pearson correlation and regression analysis.

3. Results

3.1. Comparison of the Weight and CT-Supported Evaluation of the Longitudinal Parameters

The mean mite number per cell of the examined brood was 4.58 ± 0.30. There were no statistically significant relationships between the number of mites and the weight, similarly to the observed morphometric values of the pre-imaginal developmental stage of the honey bees examined.

In contrast, the examination based on the non-invasive CT survey proved that the total-body (A: 11.025 ± 0.065 mm) and abdomen lengths (c: 5.21 ± 0.062 mm) of parasitized specimens were shorter than those (A: 11.37 ± 0.062 mm; c: 5.57 ± 0.056 mm) of their intact companions (Figure 2). The changes in the examined longitudinal parameters caused by parasitism were statistically significant in the case of all examined parameters (df:1; $p < 0.001$).

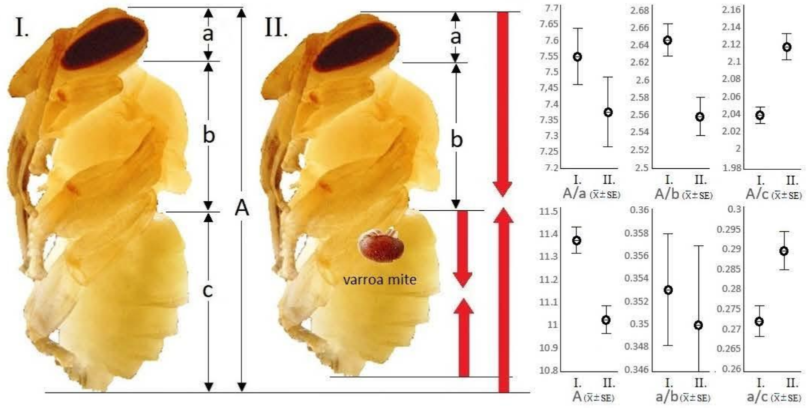

Figure 2. Morphological and size differences between intact and parasite workers at the 18th day of development of the pre-imaginal stage of the honey bee ($n = 35$; $p \leq 0.05$). I.: intact, II.: parasitized; a: head length, b: thorax length, c: abdomen length, A: total-body length. Red arrows show the direction of change.

3.2. Assay of Body Parts and Body Ratios Assisted by CT

The calculated quotients of the total-body and abdomen (A/c), head and thorax (a/b), and head and abdomen (a/c) in parasitized samples were significantly different from the values of the intact specimens ($n = 35$) (df:1; $p < 0.001$).

In damaged individuals, it was confirmed that the quotient of the total-body and abdomen is smaller by 3.77%, the quotient of the head and abdomen is 6.86% smaller, and finally the quotient of the total-body and thorax is 3.33% larger than the same parameters in intact individuals. Differentiation between the parasitized and the intact samples was not proven by the statistical comparison of the thorax length (b) and the quotients of the total-body and head (A/a) and head and thorax (a/b). That is, the size of the abdomen relative to the total body as well as to the head becomes smaller, while the size of the thorax relative to the total body was larger in parasitized specimens.

The morphological distinctions between the intact and parasite specimens originating from the adjacent brood cells could be visualized by computer-based 3D reconstructions (Figure 3). The phenotypical disorders caused by varroosis could also be seen by simple visual inspection.

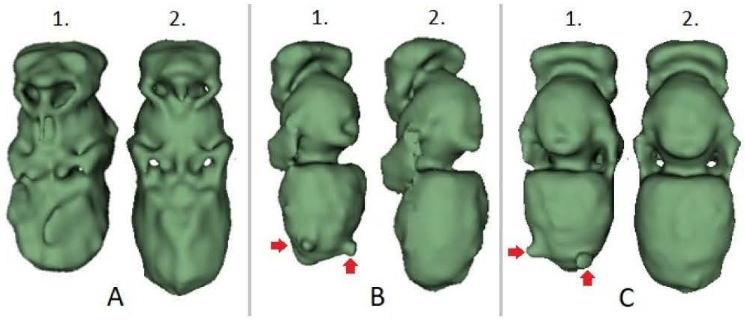

Figure 3. Computer-based three-dimensional reconstructions of honey bee pupae located beside each other in the comb. 1: parasitized by *V. destructor*, 2: intact; (**A**): ventral, (**B**): lateral, (**C**): dorsal views. Mites are marked by red arrows.

Values of the total-body and abdomen lengths measured at different times of the pre-imaginal stage are shown in Figure 4.

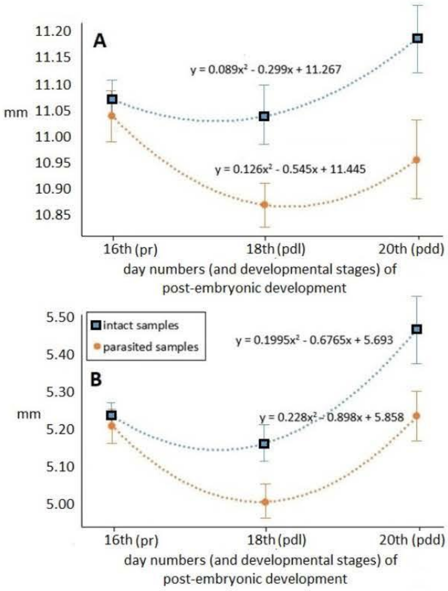

Figure 4. Tendency of the measured longitudinal parameters (mean ± SE) as a function of the different times of post-embryonic honey bee development. (**A**): total-body length; (**B**): abdomen length; pr, pdl, pdd: ontogenetic stages of worker bee development, following [26,31]; R^2 = uniformly 1.

Time-dependent hyperbolical changes at the different time points within groups were detected in both examined longitudinal parameters, which were statistically confirmed by regression analysis (df = 1; $p < 0.001$). The registered values were the lowest in the middle of pre-imaginal development (on the 18th day), and then immediately before becoming an adult, these hidden developmental forms reached their final, imago lengths both in the case of total-body and abdomen lengths. The parasitized specimens have apparently shorter length values during the pre-imaginal developmental stadium. The total-body and abdomen length values of parasitized specimens differed progressively from those of the intact samples—at similar standard deviation values—as development progressed. At the end of pre-imaginal development, the total-body length of the parasitized stage was 2.54 percent, while the abdomen length was 4.86 percent shorter than that of the intact samples.

The change in the proportions of different body parts during the pre-imaginal development can be seen in Figure 5. It was ascertained that the tendencies of the three parameters dependent on time followed different trends. The changes in the total-body–abdomen ratio are characterized by a parabolic curve, confirmed by the regression analysis. The higher values were always registered in parasitized specimens; this difference reached its maximum on the 20th day of development. However, both total-body and abdomen lengths were reduced by varroosis, while the decrease in the abdomen length was more determinative. These changes were also statistically confirmed (df = 1; $p < 0.001$). The change in the head–abdomen ratio as a function of time also had a parabolic feature, but this change was more characteristic in the case of the intact samples. The dependence of the head–abdomen ratio on time showed less difference in parasitized specimens. The values of the total-body–thorax ratio measured in the case of intact and parasitized individuals testify to an intriguing change. This tendency of thorax size relative to total body length in intact samples was an increasing logarithmic type. In contrast, the change in the parasitized samples revealed an exactly inverse tendency as compared to that of the intact samples, confirmed by the regression analysis. The thorax reached its final size continuously in intact individuals, while in parasitized individuals the final size of the thorax developed at a rapid rate in the last period of the development.

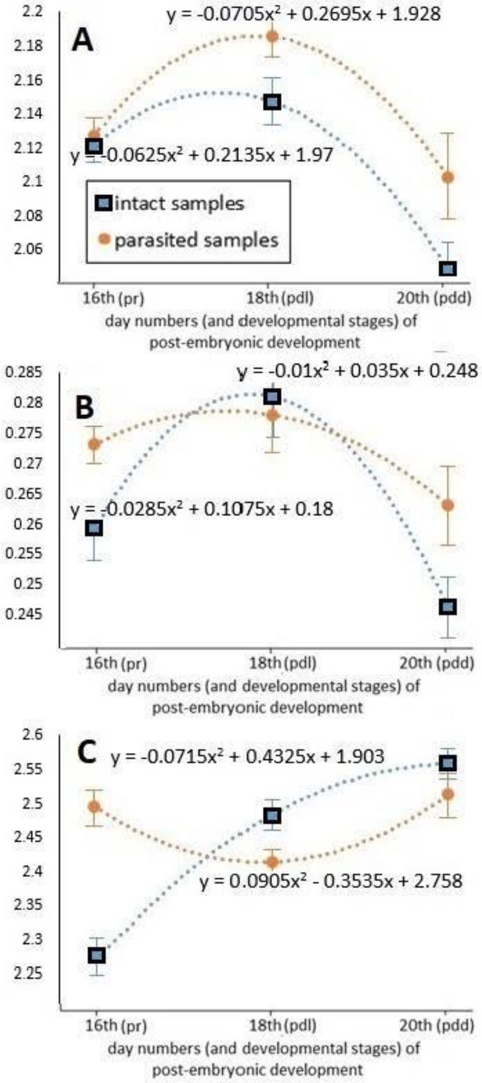

Figure 5. Tendency of the calculated body part ratios (mean ± SE) as a function of the different times in post-embryonic honey bee development. (**A**): total-body–abdomen ratio; (**B**): head–abdomen ratio; (**C**): total-body–thorax ratio. pr, pdl, pdd: ontogenetic stages of worker bee development, following [26,31]; R^2 = uniformly 1.

3.3. Detection of DWV with PCR Assay

In order to test for the presence of DWV, five samples of healthy parasitized specimens were selected, and an RT-PCR test was conducted. The results of the PCR investigation (Figure 6A,B) show that the distorted samples were positive for DWV virus infection. The run of the samples was in the 435 bp range, similar to the positive viral sample. In the case of non-template control, the PCR amplification did not result in detectable amplicon compared with the positive control.

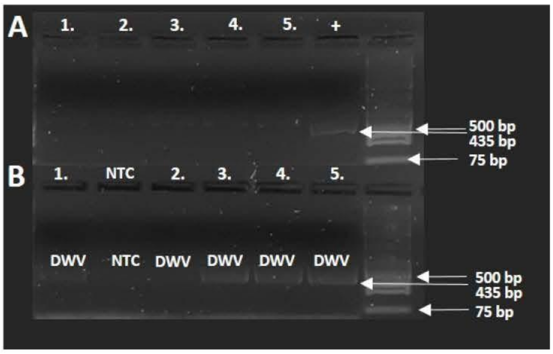

Figure 6. Results of the gel electrophoresis of RT-PCR honey bee samples. (**A**): Healthy specimens; (**B**): distorted specimens; +: positive control; NTC: non-template control.

4. Discussion

V. destructor is considered a major pest of honey bees worldwide. Mites suck the hemolymph from adults and developing pupae of honey bees, while vectoring several viruses, thereby shortening the lifespan of bees. Although the role that mites play in spreading DWV is evident, we have little information on wider DWV epidemiology, as well as their simultaneous roles in triggering pre-imaginal disorders [19,20].

In this study, morphological differences in the main body parts of honey bees in the development stages of both intact and parasitized larvae were measured inside the comb by means of computed tomography. Based on our investigation, it can be ascertained that the main morphological attributes and sizes of different body parts inside the brood cells can be well-studied by means of computed tomography. These benefits make this method suitable for further evaluation of clinical, toxicological, and parasitological consequences in the developmental stages of insects with hidden lifestyles. The CT-based measurement of smaller insect structures, such as wings, limb initials, or other segmentations, has been more cumbersome, as investigating these minor details requires higher-resolution techniques, for instance μ-CT, photomicrography, CLSM, or NMRI [35].

The developmental disorders of honey bees in the pre-imaginal stages were unequivocally confirmed by our results, which were mostly expressed by the deformation of the abdomen. Our data confirm the findings of Facchini et al. [28], who examined the *Varroa* infestation status, developmental stage, spatial position, and length of the pupa within the brood comb using CT. According to their results, pupae in infected cells were significantly shorter than those in *Varroa*-free cells, and this effect was linked to both mite number and stage and to their position in the comb. Based on related works [18,19], these symptoms suggest infection by deformed wing virus (DWV). The fact that the viral infection is vectored by the *Varroa* mite has been confirmed by earlier experimental studies [35–38]. Obviously, hemolymph sucking and body fat consumption of *V. destructor* can directly contribute to the size decrease in the parasitized honey bee pupae [12]. The life conditions of the attacked pupae are also significantly deteriorated because of their more intense metabolic process [27,39].

In addition, changes in the phenotypical ratios in these pre-imaginal stages were also detected, which in our view can also be traced to viral infection mediated by parasitism. An unexpected observation was an increased thorax size in the infected specimens. An explanation for this may be the constriction of other body parts (head and abdomen) as well as the deformation effects of the virus on the muscles involved in wing movement [18,19,34]. The parabolic development proven by regression analysis in the last stage of development can be explained by the temporal exposure of parasitism, which caused tissue degradation and energy exhaustion [12,17,25]. These verified physiological changes, such as the more intensive moving and also the increased metabolic processes in attacked specimens, can unequivocally be an additional triggering factor in several phenological and vitality impairments in attacked honey bee pupae.

Varroa infestation and DWV infection were at very high levels in our measurement. Nonetheless, these values fit the interval of the documented mite infestation rate, which can fluctuate between 2% and 74% [40].

Berényi et al. [34] identified six honey bee viruses, of which DWV was found to be the most common virus, that may have the most profound effect among honey bee viral infections [6,9,14,41]. Morphological DWV symptoms typically occur at high infection levels (>10^{10} genome copies/bee), which are almost exclusively coupled with acquiring the virus during the pupal stage via the feeding behavior of the ectoparasitic mite [42]. Presumably, the DWV infection in honey bees, which occurs in direct deformation of the wing, also has a distortion effect on the muscle moving the thorax. This hypothesis was fortified by the detection of the presence of DWV virus in RT-PCR investigations. Nonetheless, the RT-PCR method used during this investigation also provides a good future opportunity to identify all six major honey bee viruses and their connection to distortions revealed by the CT method. Limitations of our study were the low number of samples in the genetic examination, whose results could be reinforced by a traditional assay based on cell exploration in the future. In addition, in terms of practical use, the technique is rather expensive, expertise-demanding, and does not permit the obtainment of a dynamic view. The morphological disorders as a function of time have been confirmed during the hidden pre-imaginal development of honey bees in the comb. Our experimentation demonstrates that the parasite specimens follow a different morpho-phenological developmental pathway, which can probably be traced back to the *Varroa* parasitism and the viral infection vectored by it.

5. Conclusions

While observations of *V. destructor* are well-documented, the majority of these studies are limited to the exploration of its biological and ecological characteristics outside of brood cells. In this study, we highlight the host deformation and virus intermediary role of mite parasitism inside the brood cell using a non-invasive method.

The size of different body parts and other measurable consequences of the parasitism inside the brood comb can be monitored well by employing computed tomography. In addition to the deformation in examined stages caused by the *Varroa* mite, our findings also indicate infection by deformed wing virus.

The advantages offered by CT make the method suitable for the further evaluation of the other clinical, toxicological, and parasitological effects in the hidden development stages. Furthermore, molecular analysis enables the confirmation of CT investigations and may help in the future elaboration of CT-based parasite identification. Furthermore, the combination and sequential usage of these methods will provide an insight into detailed and specific knowledge on the major parasites of honey bees, which will aid in the development of possible prevention of these parasites.

Starting from our experimental data, a goal of further research in this field could be to verify the distortion effects caused by DWV using direct pupae extraction. In this future research, the assortment of viruses causing body deformation and the proportion of DWV within the exact population could become identifiable by examining a larger number of samples, whereby the correlation degree between the morphometric changes and viral presence would become detectable.

Author Contributions: Conceptualization, S.K.; Methodology, S.K., T.D., T.S. and I.J.; Software, T.S. and T.D.; Validation and Investigation, T.S., T.D., S.K. and I.J.; Data Curation, T.S. and T.D.; Writing—Original Draft Preparation, S.K.; Writing—Review and Editing, T.S., S.K., I.J. and T.D.; Visualization, S.K.; Supervision, T.S., S.K. and T.D.; Funding Acquisition, S.K. All authors have read and agreed to the published version of the manuscript.

Funding: This research was funded by projects of the European Union, the European Social Fund: EFOP-3.6.3.-VEKOP-16-2017-00008.

Institutional Review Board Statement: Not applicable.

Data Availability Statement: The data presented in this study are available on request from T.S., T.D. and S.K.

Acknowledgments: This publication was supported by the János Bolyai Research Scholarship of the Hungarian Academy of Sciences (BO/00871/19).

Conflicts of Interest: The authors declare no conflict of interest.

References

1. U.S. Department of Agriculture, Natural Resources Conservation Service (USDA-NRCS). Insects and Pollinators: Pollinators by the Numbers. 2016. Available online: www.nrcs.usda.gov/wps/portal/nrcs/main/national/plantsanimals/pollinate (accessed on 5 July 2021).
2. Sáez, A.; Negri, P.; Viel, M.; Aizen, A.M. Pollination efficiency of artificial and bee pollination practices in kiwifruit. *Sci. Hortic.* **2019**, *246*, 1017–1021. [CrossRef]
3. Sáez, A.; Aizen, M.A.; Medici, S.; Viel, M.; Villalobos, E.; Negri, E. Bees increase crop yield in an alleged pollinator-independent almond variety. *Sci. Rep.* **2020**, *10*, 3177. [CrossRef]
4. Potts, G.S.; Roberts, M.P.S.; Dean, R.; Marris, G.; Brown, A.M.; Jones, R.; Neumann, P.; Settele, J. Declines of managed honey bees and beekeepers in Europe. *J. Apic. Res.* **2010**, *49*, 15–22. [CrossRef]
5. Anderson, D.; Trueman, J. *Varroa jacobsoni* (Acari: Varroidae) is more than one species. *Exp. Appl. Acarol.* **2000**, *24*, 165–189. [CrossRef] [PubMed]
6. Williams, G.R.; van Engelsdorp, D.; Chauzat, M.P.; Cox-Foster, D.L.; Delaplane, K.S.; Neumann, P.; Pettis, J.S.; Rogers, R.E.L.; Shutler, D. Colony collapse disorder in context. *BioEssays* **2010**, *32*, 845–846. [CrossRef] [PubMed]
7. Rosenkranz, P.; Aumeier, P.; Ziegelmann, B. Biology and control of *Varroa destructor*. *J. Invertebr. Pathol.* **2010**, *103*, 96–119. [CrossRef]
8. Dainat, B.; Evans, J.D.; Chen, Y.P.; Gauthier, L.; Neumann, P. Predictive markers of honey bee colony collapse. *PLoS ONE* **2012**, *7*, e32151. [CrossRef] [PubMed]
9. De Jong, D.; De Jong, P.H.; Gonçalves, L. Weight loss and other damage to developing worker honeybees from infestation with *Varroa jacobsoni*. *J. Apic. Res.* **1982**, *21*, 165–167. [CrossRef]
10. Navajas, M.; Migeon, A.; Alaux, C.; Martin-Magniette, M.L.; Robinson, G.E.; Evans, J.D.; Cros-Arteil, S.; Crauser, D.; Le Conte, Y. Differential gene expression of the honey bee *Apis mellifera* associated with *Varroa destructor* infection. *BMC Genomics* **2008**, *9*, 301. [CrossRef] [PubMed]
11. Keszthelyi, S.; Sipos, T.; Csóka, Á.; Donkó, T. CT-supported analysis of the destructive effects of *Varroa destructor* on the pre-imaginal development of honey bee, *Apis mellifera*. *Apidologie* **2021**, *52*, 155–162. [CrossRef]
12. Ramsey, S.D.; Ochoa, R.; Bauchan, G.; Gulbronson, C.; Mowery, J.D.; Cohen, A.; Lima, D.; Joklik, J.; Cicero, J.M.; Ellis, J.D.; et al. *Varroa destructor* feeds primarily on honey bee fat body tissue and not hemolymph. *Proc. Natl. Acad. Sci. USA* **2019**, *116*, 1792–1801. [CrossRef] [PubMed]
13. Bakonyi, T.; Farkas, R.; Szendröi, A.; Dobos-Kovács, M.; Rusvai, M. Detection of acute bee paralysis virus by RT-PCR in honey bee and *Varroa destructor* field samples: Rapid screening of representative Hungarian apiaries. *Apidologie* **2002**, *33*, 63–74. [CrossRef]
14. Ullah, A.; Gajger, I.T.; Majoros, A.; Dar, S.A.; Khan, S.; Kalimullah; Haleem Shah, A.; Nasir Khabir, M.; Hussain, R.; Khan, H.U.; et al. Viral impacts on honey bee populations: A review. *Saudi J. Biol. Sci.* **2021**, *28*, 523–530. [CrossRef] [PubMed]
15. Ryabov, E.V.; Childers, A.K.; Chen, Y.; Madella, S.; Nessa, A.; van Engelsdorp, D.; Evans, J.D. Recent spread of *Varroa destructor* virus-1, a honey bee pathogen, in the United States. *Sci. Rep.* **2017**, *7*, 17447. [CrossRef] [PubMed]
16. Posada-Florez, F.; Ryabov, E.V.; Heerman, M.C.; Chen, Y.; Evans, J.D.; Sonenshine, D.E.; Cook, S.C. *Varroa destructor* mites vector and transmit pathogenic honey bee viruses acquired from an artificial diet. *PLoS ONE* **2020**, *15*, e0242688. [CrossRef] [PubMed]
17. Dainat, B.; van Engelsdorp, D.; Neumann, P. Colony collapse disorder in Europe. *Environ. Microbiol. Rep.* **2012**, *4*, 123–125. [CrossRef] [PubMed]

18. Tentcheva, D.; Gauthier, L.; Bagny, L.; Fievet, J.; Dainat, B.; Cousserans, F.; Colin, M.E.; Bergoin, M. Comparative analysis of deformed wing virus (DWV) RNA in *Apis mellifera* and *Varroa destructor*. *Apidologie* **2006**, *37*, 41–50. [CrossRef]
19. Anguiano-Baez, R.; Guzman-Novoa, E.; Hamiduzzaman, M.M.; Espinosa-Montaño, L.G.; Correa-Benítez, A. *Varroa destructor* (Mesostigmata: Varroidae) parasitism and climate differentially influence the prevalence, levels and overt infections of deformed wing virus in honey bees (Hymenoptera: Apidae). *J. Insect Sci.* **2016**, *16*, 44. [CrossRef] [PubMed]
20. Roberts, J.M.K.; Simbiken, N.; Dale, C.; Armstrong, J.; Anderson, D.L. Tolerance of Honey Bees to *Varroa* Mite in the Absence of Deformed Wing Virus. *Viruses* **2020**, *12*, 575. [CrossRef]
21. Himmi, S.K.; Yoshimura, T.; Yanase, Y.; Torigoe, T.; Akada, M.; Ikeda, M.; Imazu, S. Volume visualization of hidden gallery system of drywood termite using computed tomography. In *A New Approach on Monitoring of Termite Infestation. Sustainable Future for Human Security*; McLellan, B., Ed.; Springer: Singapore, 2018; pp. 61–68. ISBN 978-981-10-5429-7. [CrossRef]
22. Socha, J.J.; Westneat, M.W.; Harrison, J.; Waters, J.S.; Lee, W. Real-time phase-contrast x-ray imaging: A new technique for the study of animal form and function. *BMC Biol.* **2007**, *5*, 6. [CrossRef] [PubMed]
23. Richards, C.S.; Simonsen, T.J.; Abel, L.R.; Hall, M.J.; Schwyn, D.A.; Wicklei, M. Virtual forensic entomology: Improving estimates of minimum post-mortem interval with 3D micro-computed tomography. *Forensic Sci. Int.* **2012**, *220*, 251–264. [CrossRef]
24. Lowe, T.; Garwood, R.J.; Simonsen, T.J.; Bradley, R.S.; Withers, P.J. Metamorphosis revealed: Time-lapse three-dimensional imaging inside a living chrysalis. *J. R. Soc. Interface* **2015**, *10*, 20130304. [CrossRef]
25. Keszthelyi, S.; Pónya, Z.; Csóka, Á.; Bázár, G.; Morschhauser, T.; Donkó, T. Non-destructive imaging and spectroscopic techniques to investigate the hidden-lifestyle arthropod pests: A review. *J. Plant Dis. Prot.* **2020**, *127*, 283–295. [CrossRef]
26. Adedeji, A.A.; Ekramirad, N.; Rady, A.; Hamidisepehr, A.; Donohue, K.D.; Villanueva, R.T.; Parris, C.A.; Li, M. Non-destructive technologies for detecting insect infestation in fruits and vegetables under postharvest conditions: A critical review. *Foods* **2020**, *9*, 927. [CrossRef] [PubMed]
27. Siefert, P.; Buling, N.; Grünewald, B. Honey bee behaviours within the hive: Insights from long-term video analysis. *PLoS ONE* **2021**, *16*, e0247323. [CrossRef] [PubMed]
28. Facchini, E.; Nalon, L.; Andreis, M.E.; Andreis, M.A.; Di Giancamillo, M.; Rizzi, R.; Mortarino, M. Honeybee pupal length assessed by CT-scan technique: Effects of *Varroa* infestation, developmental stage and spatial position within the brood comb. *Sci. Rep.* **2019**, *9*, 10614. [CrossRef] [PubMed]
29. Bak, B.; Wilde, J.; Siuda, M.; Kobilinska, M. Comparison of two methods of monitoring honeybee infestation with *Varroa* destructor mite. *Ann. Warsaw Univ. Life Sci. Anim. Sci.* **2009**, *46*, 33–38.
30. Gregorc, A.; Knight, P.R.; Adamczyk, J. Powdered sugar shake to monitor and oxalic acid treatments to control *Varroa* mites (*Varroa destructor* Anderson and Trueman) in honex bee (*Apis mellifera*) colonies. *J. Apic. Res.* **2017**, *56*, 1–5. [CrossRef]
31. Odemer, R. Reproductive capacity of *Varroa destructor* in four different honey bee subspecies. *Saudi J. Biol. Sci.* **2020**, *27*, 247–250. [CrossRef] [PubMed]
32. Fedorov, A.; Beichel, R.; Kalpathy-Cramer, J.; Finet, J.; Fillion-Robin, J.-C.; Pujol, S.; Bauer, C.; Jennings, D.; Fennessy, F.M.; Sonka, M.; et al. 3D slicer as an image computing platform for the quantitative imaging network. *Mag. Res. Imaging* **2012**, *30*, 1323–1341. [CrossRef] [PubMed]
33. Fievet, J.; Tentcheva, D.; Gauthier, L.; Cousserans, F.; Colin, M.E.; Bergoin, M. Localization of deformed wing virus infection in queen and drone *Apis mellifera* L. *Virol. J.* **2006**, *3*, 16. [CrossRef]
34. Berényi, O.; Bakonyi, T.; Derakhshifar, I.; Köglberger, H.; Nowotny, N. Occurrence of Six Honeybee Viruses in Diseased Austrian Apiaries. *Appl. Environ. Microbiol.* **2006**, *72*, 2414–2420. [CrossRef] [PubMed]
35. Wipfler, B.; Pohl, H.; Yavorskaya, M.I.; Beutel, R.G. A review of methods for analysing insect structures—The role of morphology in the age of phylogenomics. *Curr. Opin. Insect Sci.* **2016**, *18*, 60–68. [CrossRef] [PubMed]
36. Bowen-Walker, P.L.; Martin, S.J.; Gunn, A. The transmission of deformed wing virus between honey bees (*Apis mellifera* L.) by the ectoparasitic mite *Varroa jacobsoni*. *J. Invertebr. Pathol.* **1999**, *73*, 101–106. [CrossRef]
37. Nordström, S. Distribution of deformed wing virus within honey bee (*Apis mellifera*) brood cells infested with the ectoparasitic mite *Varroa destructor*. *Exp. Appl. Acarol.* **2003**, *29*, 293–302. [CrossRef] [PubMed]
38. McMenamin, A.J.; Genersch, E. Honey bee colony losses and associated viruses. *Curr. Opin. Insect Sci.* **2015**, *8*, 121–129. [CrossRef] [PubMed]
39. Bauer, D.; Wegener, J.; Bienerfeld, K. Recognition of mite-infested brood by honeybee (*Apis mellifera*) workers may involve thermal sensing. *J. Therm. Biol.* **2018**, *74*, 311–316. [CrossRef] [PubMed]
40. Gisder, S.; Aumeier, P.; Genersch, E. Deformed wing virus: Replication and viral load in mites (*Varroa destructor*). *J. Gen. Virol.* **2009**, *90*, 463–647. [CrossRef]
41. Floris, I.; Pusceddu, M.; Satta, A. How the Infestation Level of *Varroa destructor* Affects the Distribution Pattern of Multi-Infested Cells in Worker Brood of *Apis mellifera*. *Vet. Sci.* **2020**, *7*, 136. [CrossRef] [PubMed]
42. Locke, B.; Semberg, E.; Forsgren, E.; de Miranda, J.R. Persistence of subclinical deformed wing virus infections in honeybees following *Varroa* mite removal and a bee population turnover. *PLoS ONE* **2017**, *12*, e0180910. [CrossRef]

4.3. Comparative micro-computed tomographic analysis of the structure of brood cells and its effect on the development of the pupae of honey bee (*Apis mellifera*)

Title	Comparative micro-computed tomographic analysis of the structure of brood cells and its effect on the development of the pupae of honey bee (*Apis mellifera*).
Authors	Tamás Sipos, Tamás Donko, Ádam Csóka, Tamás Kiss, Sándor Keszthelyi
Journal	European Journal of Entomology
Year	2023
Volume	120
Issue	
Pages	9-14
Quartile	Q2
Impact factor	1.225
DOI	10.14411/eje.2023.002

EUROPEAN JOURNAL OF ENTOMOLOGY
ISSN (online): 1802-8829
http://www.eje.cz
Eur. J. Entomol. **120**: 9–14, 2023
doi: 10.14411/eje.2023.002
ORIGINAL ARTICLE

Comparative micro-computed tomographic analysis of the structure of brood cells and its effect on the development of the pupae of honey bee (*Apis mellifera*)

Tamás SIPOS[1,3], **Tamás DONKÓ**[1,2], **Ádám CSÓKA**[2,3], **Tamás KISS**[4] and **Sándor KESZTHELYI**[1]

[1] Hungarian University of Agriculture and Life Sciences, Institute of Agronomy, Kaposvár Campus, Sándor Guba str. 40, H-7400 Kaposvár, Hungary; e-mails: sipostomi97@gmail.com, ostrinia@gmail.com

[2] Medicopus Ltd., Sándor Guba str. 40, H-7400 Kaposvár, Hungary; e-mails: Donko.Tamas@sic.medicopus.hu, Adam.Csoka@sic.medicopus.hu

[3] Hungarian University of Agriculture and Life Sciences, Doctoral School in Animal Science, Kaposvár Campus, Sándor Guba str. 40, H-7400 Kaposvár, Hungary

[4] János Szentágothai Research Centre & Centre for Neuroscience, University of Pécs, Ifjúság str. 20, H-7624 Pécs, Hungary; e-mail: kiss891012@gmail.com

Key words. Hymenoptera, Apidae, comb cell volume and size, developmental disorders, computer tomography, wax structure

Abstract. Most beekeepers worldwide use the same combs in their hives for many years, which can result in alterations in the inner volume of the comb cells. The objective of this survey using microcomputed tomography was to reveal developmental disorders caused by this beekeeping practice. The extent of the thickening of the wall of brood cells that occurs as a result of the long-term use of the combs was determined. This alteration resulted in a reduction in the inner volume of the comb cells, which had a significant effect on the size of the pupae and possibly the health of the imagoes. The walls of the cells can be divided into two well-determined parts, which can be exactly visualized using micro-CT. In addition, the inner structure of the wall in the first part of the cell was altered by very radio dense remains of cocoons. The material in the other part of the cell is less radio dense and as previously suggested is mainly wax. The decrease in the length, surface and volume of these cells adversely affected the developing pupae, which according to previous studies results in a reduction in the production of workers, colony strength and honey yield. The extent of the reduction in the body regions of pupae was on average 4.98%. Overall, the volume of the pupae that developed in these narrow comb cells were smaller by an average of 12.22%.

1. INTRODUCTION

The majority of crops relies on animal pollination and the decline of wild insect pollinators in many agricultural landscapes has made the western honeybee (*Apis mellifera* L. 1758) one of the key elements of global food production and the only source of bee products like wax, royal jelly and bee venom (Winfree et al., 2011; Garibaldi et al., 2013; Ellis et al., 2020). The 21st century is one of the most difficult times for the beekeeping industry due to several abiotic (drought, heat, temperature fluctuations) and biotic (*Varroa* mites, viruses, *Nosema* spp., *Tropilaelaps* spp., etc.) factors that cause colony losses of 20% every year worldwide (Williams et al., 2010; Dainat et al., 2012; Neov et al., 2019).

Conventional imaging methods, such as light and confocal microscopy, provide detailed images of the internal anatomy of insects, but for this one has to kill or dissect live individuals (Friedrich et al., 2014). Other disadvantages of these techniques are the limitations of repeated scanning of individuals. X-ray imaging techniques are widely used in the field of entomological research because they are non-invasive (Smith et al., 2016; Alba et al., 2018). While μ-CT is mainly used for anatomical studies, due to its resolution being higher than human diagnostic CT, which is used in studies on crop protection for understanding insect biology and analysing the development of damage (Smith et al., 2016; Keszthelyi et al., 2020; Sonenshine et al., 2022). There is, however, only a few references on bee health using computed tomography and 3D imaging (Facchini et al., 2019; Keszthelyi et al., 2021; Sipos et al., 2021).

Most of the studies on bee health are concerned with the pathology of the imago, which provides little information on pathogenesis, especially during the larval and pupal stages. Beekeepers worldwide use their combs for many years, 50% of combs should be replaced annually, but there are cases of the utilization of combs for even up to 6 years (Taha & Al-Kahtani, 2020). This results in several disadvantages, with the reasons for them remaining unknown in

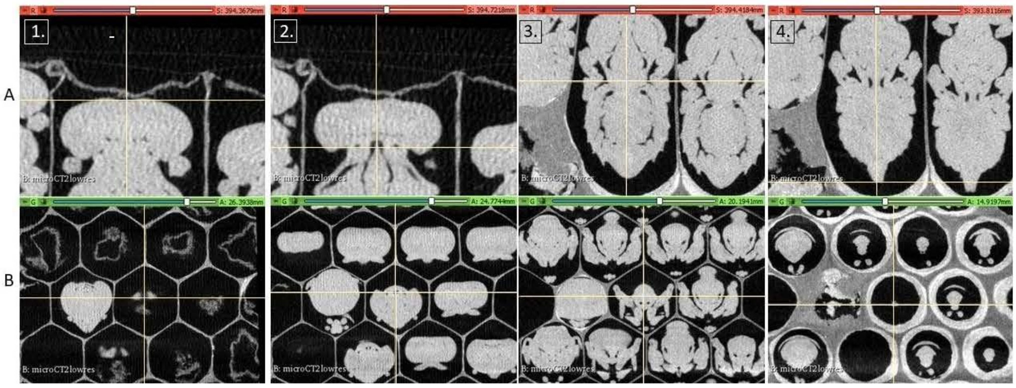

Fig. 1. Points used to measure the sizes of body parts of pupae on full layout cross-sectional images.

the majority of cases. Several of the disorders in bee development begin or even occur within the brood cells, which is attributable to improper beekeeping practise. Naturally, the features of these disorders are difficult to determine or are unknown in certain cases. Non-invasive imaging can be used to reveal the developmental processes and anatomical changes that occur due to improper beekeeping practise (Wipfler et al., 2016).

The objective of this study was to determine the reduction in the size of pupae caused by inappropriate beekeeping technology based on the previous results of Berry & Delaplane (2001). First, the extent of the thickening of the brood cell wall that occurs as a result of the use of old combs and its consequences for the size of bee pupae were determined. In addition, the potential significance of modern non-invasive imaging methods, especially computer tomography, in apicultural research is stressed.

2. MATERIALS AND METHODS

2.1. Origin of comb samples

The brood combs were collected from one *Apis mellifera carnica* colony located on Kaposvár Campus (Somogy county, Hungary; GPS coordinates: WGS: X:46.381079 Y:17.826915) during April. The uniformity of the age of the specimens was provided by the size of the Nagyboczonádi (NB) frame queen confinement cage. The combs contained 18-day-old worker pupae at the pre-imaginal developmental stage. The preparation was done using a scalpel to cut out four pieces of the comb (90 × 60 mm) containing brood from a 3-year-old frame for further selection using medical diagnostic CT. After the human diagnostic measurement, 10 normal and 10 narrow pupae were cut out and used for producing more detailed digital images using μ-CT, which was necessary because of the limitations of the μ-CT scanning of the length and diameter. The different experimental groups (normal and narrow) were separated visually based on the medical CT imaging. The samples were kept in an incubator under stable environmental conditions at 34° ± 0.5°C and 60% ± 10% relative humidity (RH), which are similar to the conditions inside a healthy colony until required for the CT scans.

After the preliminary medical CT visualization, one of the separated comb cells was selected for micro-CT. After this, the remaining pupae were removed and wax of one of the scanned combs was melted. The melting of the wax was done in order to visualize the different thicknesses of the bottoms of the cells (Fig. 2).

2.2. Descriptions of computed tomographic settings and instruments

The μ-CT image acquisition was carried out using a Bruker Biospin SkyScan 1176 at the University of Pécs Szentágothai Research Centre. The samples were examined using the following CT parameters: PANalytical's Microfocus Tube source type, 50 kV source voltage, 500 μA source current, 700 ms exposure time and 0.71 rotation step (deg). NRecon reconstruction program, version 1.7.4.2, was used to produce the final images from raw data. The program created 8bit BMP files with 3336 × 3336 pixels and the pixel size was 8.74355 μm. BMP images were converted to NIFTI (Neuroimaging Informatics Technology Initiative, 2005) files.

The same samples were examined using a Siemens SOMATOM Definition AS+ CT scanner a few hours after the μCT scans using the following parameters: 100 kV tube voltage, 140 mAs X-ray radiation dose, spiral data collection mode with 0.7 pitch, the field of view 50 mm. Standard DICOM (Digital Imaging and Communications in Medicine) images were reconstructed using Siemens Syngo CT VA48A program with convolution kernel V80u. The resolution of the images was 0.0977 mm × 0.0977 mm × 0.1 mm. Each series examined was converted from a DICOM to NIFTI (Neuroimaging Informatics Technology Initiative, 2005) file format. The human diagnostic CT was used for preliminary screening and Hounsfield Unit (HU) scaling.

The image post-processing and visualization were done using 3D-Slicer software (www.slicer.org) (accessed on 24 February 2021).

2.3. Description of the μ-CT-based measurements

To determine the density of the different structural parts of a cell, the values produced by μ-CT were converted to Hounsfield Units (HU) using the following equation:

$$HU = \mu\text{-CT voxel value} \times 20.78 - 1024$$

This equation compares the images measured using CT and μ-CT. 3D Slicer's Elastix module was used for the rigid registration of the images.

Five, randomly chosen segments represented each of the visually different parts of a cell (n = 5). The segment is a manually designated area from the visually distinguished parts of the cell, which contains a slightly different number of voxels due to their manual selection.

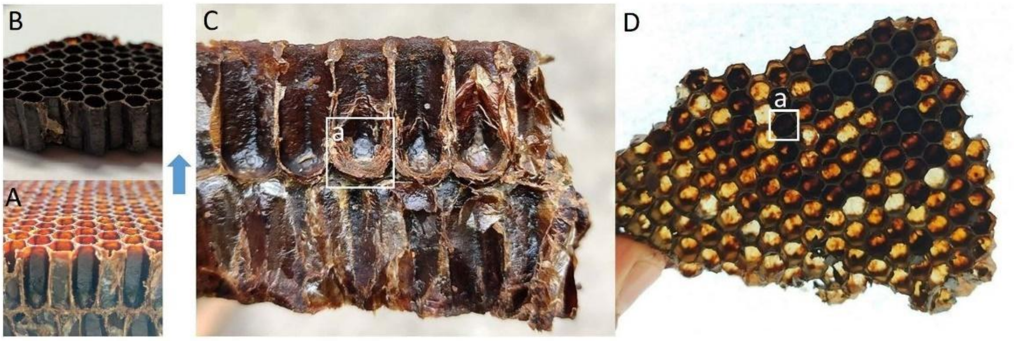

Fig. 2. Cells of different sizes in comb. The combs in the frames contain narrow cells (a). A – comb covered with wax; B – fibre-reinforced composite without wax; C – axial cross-section of comb, D – top view of comb.

To establish and compare the volume and surface parameters of different sized brood cells and developing pupae, they were measured using μ-CT. This study was based on 10 normal and 10 narrow brood cells determined by preliminary human diagnostic CT screening and then selected visually and marked.

In order to measure developing individuals in 10 normal and 10 narrow cells their lengths (Fig. 1) and volumes were based on μ-CT scans. The lengths of their whole body, head, thorax and abdomen were measured using mark-ups. Fiducial mark-ups were placed using 3D Slicer software and Python 3.6 programming language was used for calculating the distances between the marker points. In addition, the relative proportions of the whole body of each body part were measured for specimens from different brood cells.

The surface area and volume of the insects and the inner space of the cells were generated using the segment editor module in the 3D Slicer program. The pupae and the combs were manually segmented utilizing the measured density values of the structural parts of the comb (Fedorov et al., 2012). The information for the segments was generated individually by the segment statistics module.

2.5. Statistical analysis

The Kolmogorov-Smirnov test was used to test the morphological data for the pupal stage of honey bees ($n < 50$). For determining whether the data was normally distributed ($p < 0.05$), the Ghasemi- and Zahediasl-type methods were used. The effect of comb cell size on the morphological parameters of this pre-imaginal stage of honey bees was statistically analysed using one-way ANOVA with the help of SPSS 11.5 software. Means were separated using the Tukey (HSD) test, at ($p \leq 0.05$).

3. RESULTS

3.1. Structural analysis of comb cells of different sizes using μ-CT

The first picture shows a piece of used comb after brood was removed (Fig. 2A). The structure of the fibre-reinforced material remaining after the removal of wax clearly reveals the remains of the pellicle and cocoon of the previous generations reared in the cells (Fig. 2B). Most visible, however, is that the wall and especially the bottom of some cells are thicker and more enlarged than those of the cells that are even directly adjacent to them. Differences in the wall and bottom thickness of individual cells are seen in both cross-sections (Fig. 2C) and top-view (Fig. 2D) of light transmitted perspectives.

The μ-CT analysis of the comb still containing wax reveals structural differences between normal and narrow cells (Fig. 3). It is clear that the structural components differ in colour in the images, which is due to different radiodensity values. The walls of cells consist of two distinct parts, which can also be visualized using μ-CT. The first part surrounding the inner surface is brighter (Fig. 3b). This part is composed of a fibre-reinforced composite product (FRP), which originated from developing pupae, for instance the spinning of a silken cocoon, residues of stored pollen and remains of moulted pellicle. The second part is darker, due to the presence of wax (Fig. 3a), that is composed of a fibre-reinforced composite product with wax (FRPW).

The average volume of normal cells was 234.103 ± 4.105 mm^3. In contrast, that of the narrow cells with thick walls

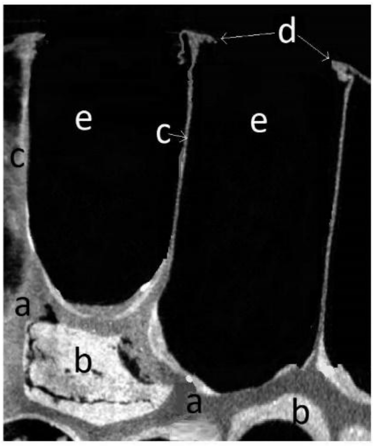

Fig. 3. Vertical section of narrow cells obtained using μ-CT. a – fibre-reinforced composite with wax (FRPW); b – fibre-reinforced composite without wax (FRP); c – wall of cell, d – remains of capping material of brood cell; e – interior space of cell.

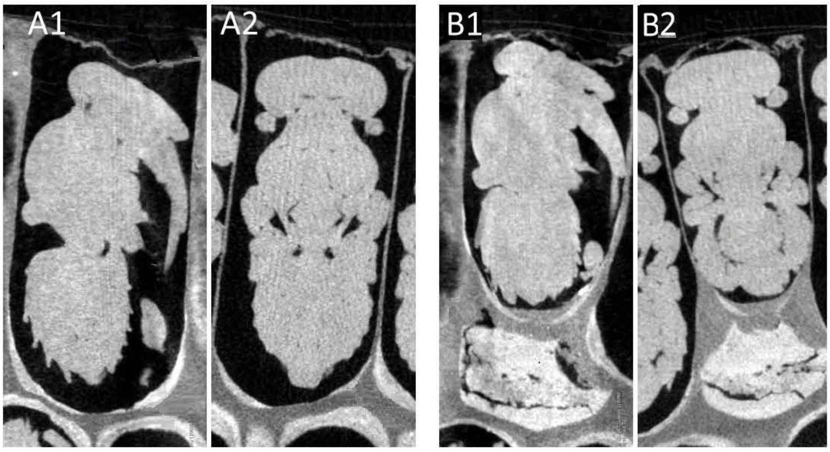

Fig. 4. Sections of honey bee pupae in cells obtained using µ-CT. A1 – saggital record of honey bee pupa in a normal cell; A2 – axial record of honey bee pupa in a normal cell; B1 – saggital record of honey bee pupa in narrow cell; B2 – axial record of honey bee pupa in narrow cell.

were 151.237 ± 4.957 mm^3, which is significantly different ($p \leq 0.05$). The volume of narrow brood cells was 35.41% lower than that of normal comb cells.

The thickened regions in the wall and bottom of cells mainly contain the so-called FRP fraction of the insect developmental origin. Density indices (HU) of the different structural components of the comb also indicate the different positions of each component in the structure of the cells (Table 1). The FRP is mainly included in the formation of the cell wall and build up at the bottom of the cells. This fraction is primarily responsible for the abnormal thickening of the cell, which causes a significant loss of brood cell volume. The primary role of the waxy FRPW fraction is in the capping of the brood cells.

The density of different parts of the comb is statistically different ($p < 0.05$). This is the case for both structurally different (FRP-FRPW) and spatially different components of comb cells. The density of the wax component (FRPW) is lower than that of the brood components attributable to the development of bees (FRP). This is supported by the density of the spatially different cell structures. The cell wall has a slightly denser composition than the higher wax content structures like the capping of the brood cells.

Table 1. Radio density values (HU) (mean ± SE) of the different parts of comb cells (n = 20).

Parts of cell	Radio density (HU) (mean ± SE)
FRPW (a)	–422.48 ± 13.91 ^{a}
FRP (b)	162.99 ± 4.03 ^{b}
Wall of comb cell (c)	–310.13 ± 10.85 ^{a}
Tapping remains of brood cell (d)	–342.51 ± 3.95 ^{b}
The air in the brood cell (e)	–991.19 ± 1.77 ^{c}

$^{a, b, c}$ – small letters indicate significant differences (p ≤ 0.05); FRPW – fibre-reinforced composite with wax; FRP – fibre-reinforced composite.

3.2. The effect of different sized comb cells on the development of honey bee pupae

Egg-laying and the development of honey bees occurs naturally in narrow comb cells with a small volume. This results, however, in developmental disorders at the pupal stage of workers (Fig. 4). Individuals developing in these cells are smaller than those developing in normal brood cells. The relative proportions of the body may even change (Table 2). The differences in the size of pupae is well illustrated in the 3 dimensional figure (Fig. 5).

The mean surface area of pupae developing in normal cells was 266.86 ± 2.23 mm^2, whereas that of the pupae developing in narrow cells with thick walls was 218.97 ± 1.94 mm^2. These values are statistically different ($p \leq 0.05$), which indicates that the average surface area of pupae developing in narrow cells, resulting from intensive use, was about 17.94% lower than that of pupae developing in normal brood cells.

The average volume of pupae developing in normal cells was 120.61 ± 1.43 mm^3 and of those eveloping in narrow cells was 105.87 ± 1.29 mm^3. These values are also statisti-

Table 2. Length (mean ± SE) of honey bee pupae in normal and narrow cells measured using micro CT on the 18th day of postembryonic development (n = 10).

		Length (mm)	Ratios		
				Length	dr (%)
Normal	head (a)	1.41 ± 0.05 ^{a}	a/b	0.29	
	thorax (b)	4.74 ± 0.05 ^{b}	d/a	7.84	
	abdomen (c)	5.03 ± 0.04 ^{c}	d/b	2.33	
	whole body (d)	11.06 ± 0.05 ^{d}	d/c	2.19	
Narrow	head (a)	1.16 ± 0.18 ^{e}	a/b	0.32	9.37
	thorax (b)	3.60 ± 0.09 ^{f}	d/a	7.64	2.55
	abdomen (c)	4.15 ± 0.07 ^{g}	d/b	2.46	5.28
	whole body (d)	8.87 ± 0.11 ^{h}	d/c	2.13	2.73

dr – degree of reduction; $^{a, b, c, d, e, f, g, h}$ – small letters indicate significant differences (p ≤ 0.05).

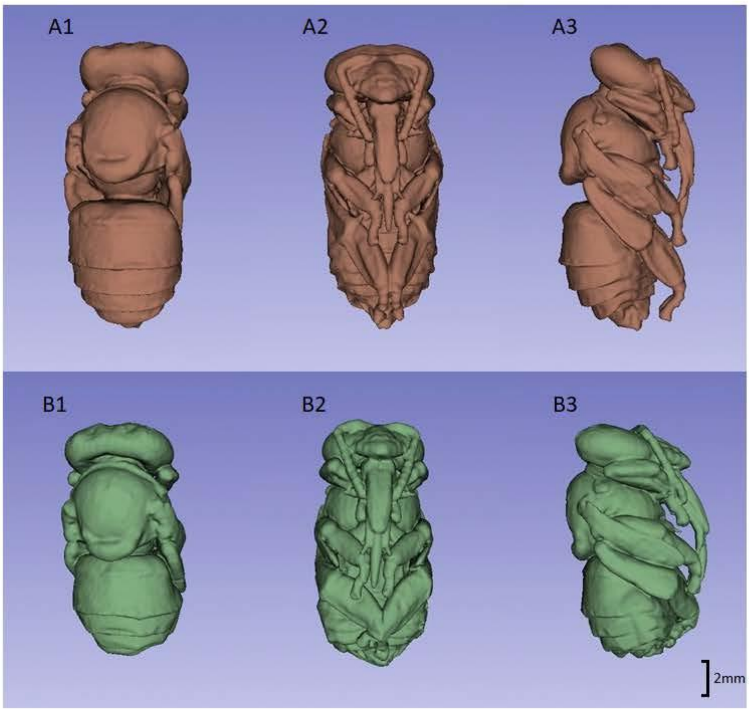

Fig. 5. 3D images of honey bee pupae that developed in different sized brood cells. A – pupa from a normal cell; B – pupa from a narrow cell; 1 – dorsal; 2 – ventral; 3 – lateral view.

cally different ($p \leq 0.05$), which indicates, as above, that pupae developing in narrow cells are in terms of volume 12.22% smaller.

Table 2 shows the length of 18-day-old pupae developing in normal and narrow cells. This reveals that in terms of the length of the body and main body parts the development of the bee in narrow cells is distorted. The degree of reduction in the different parts of the body ranges from 2.55 to 9.37%. In relation to the total body length, the greatest reduction was recorded for the thorax size of the developing pupae. This has consequences in terms of reductions in the length of the abdomen and head. The lengths of the pupae originating from the normal and narrow cells differed significantly for each of the body parts measured ($p \leq 0.05$).

4. DISCUSSION

The differences in the bottoms of comb cells was unequivocally confirmed using CT. It was further confirmed that the alterations in the inner volume of the cells resulting from rearing several generations in them had adverse effects on the preimaginal development of honey bees (Berry & Delaplane, 2001). As a result of this ontogenetic effect the cell walls gradually become darker and more brittle, which is also reported by Hepburn (1998). The cells with extremely thick bottoms are in those parts of the comb most intensively used for rearing brood or in which there are residues of pollen.

The decrease in transparency following the thickening of the walls of cells can be traced back to the sedimentation of several types of organic matter associated with the rearing of larvae (honey, pollen or propolis) (Taha et al., 2010) or the metabolism of the larvae, such as, faeces, silken cocoon and pellicle (Free & Williams, 1974). The accumulation of organic matter results in a decrease in the volume and diameter of the brood cells (Karihaloo et al., 2013; Shawer et al., 2021).

There are other studies on the effect of the age of the comb on honey bee colonies (Al-Kahtani, 2018; Shawer et al., 2021). According to Berry & Delaplane (2001), colonies with new combs produce a greater area of brood, a greater area of sealed brood and the young bees are heavier. Interestingly, they report that brood survival in old combs is the only variable that is significantly higher. Taha & Al-Kahtani (2020) report a strong relationship between the thickness of residues in the comb and the activity of the honey bee colonies in collecting pollen, worker brood production, colony strength and honey yield. In comparison with colonies with 4-year-old combs, the number of returning workers, number of returning workers with pollen loads, rate of storing pollen, rate of worker brood production and size of the colony were significantly greater for those with younger combs. Eventually, old combs result in a lower honey yield of poor quality (Taha & El-Sanat, 2007; Taha et al., 2010).

The aim of the present study was to illustrate how modern imaging methods can be used for improving beekeeping, especially by revealing the inner structure of the comb using new tools like medical CT and μ-CT. The necessity for regularly changing combs is unequivocally reinforced by our μ-CT survey. The combined use of these two diagnostic techniques is unique and has great potential for improving beekeeping.

ACKNOWLEDGMENTS. We are indebted for the financial support from projects of the European Union, the European Social Fund: EFOP-3.6.3-VEKOP-16-2017-00008 and EFOP-3.6.3-VEKOP-16-2017-00005. The publication is supported by the János Bolyai Research Scholarship of the Hungarian Academy of Sciences (BO/00871/19). This research was done in collaboration with the Animal imaging core facility at the Szentágothai Research Centre of the University of Pécs. We are grateful to Zs. Helyes for her help in the organizing this cooperation and for technical support.

AUTHOR CONTRIBUTIONS. T. Sipos and S. Keszthelyi designed the methodology and wrote the manuscript, T. Sipos and T. Donkó collected the research material and produced the samples, T. Donkó, T. Sipos and T. Kiss carried out the laboratory experiments; Á. Csóka, T. Donkó and S. Keszthelyi supported the research and evaluated the data. All authors read and approved the manuscript.

CONFLICT OF INTEREST. The authors declare that they have no conflict of interest.

REFERENCES

Alba-Alejandre I., Alba-Tercedor J. & Vega F.E. 2018: Micro-CT to document the coffee bean weevil, *Araecerus fasciculatus* (Coleoptera: Anthribidae), inside field-collected coffee berries (*Coffea canephora*). — *Insects* **9**: 100, 9 pp.

Al-Kahtani S.N. 2018: Morphometrical characteristics of Carniolan honeybee workers in relation to age of comb Sci. — *Sci. J. King Faisal Univ.* (*Basic Appl. Sci.*) **19**: 47–54.

Berry J.A. & Delaplane K.S. 2001: Effects of comb age on honey bee colony growth and brood survivorship. — *J. Apic. Res.* **40**: 3–8.

Dainat B., van Engelsdorp D. & Neumann P. 2012: Colony collapse disorder in Europe. — *Env. Microbiol. Rep.* **4**: 123–125.

Ellis R.A., Weis T., Suryanarayanan S. & Beilin K. 2020: From a free gift of nature to a precarious commodity: Bees, pollination services, and industrial agriculture. — *J. Agr. Chan.* **20**: 437–459.

Facchini E., Nalon L., Andreis M.E., Di Giancamillo M., Rizzi R. & Mortarino M. 2019: Honeybee pupal length assessed by CT-scan technique: effects of *Varroa* infestation, developmental stage and spatial position within the brood comb. — *Sci. Rep.* **9**: 10614, 6 pp.

Fedorov A., Beichel R., Kalpathy-Cramer J., Finet J., Fillion-Robin J.C., Pujol S., Bauer C., Jennings D., Fennessy F.M., Sonka M., Buatti J., Aylward S.R., Miller J.V., Pieper S. & Kikinis R. 2012: 3D Slicer as an image computing platform for the quantitative imaging network. — *Magn. Reson. Imag.* **30**: 1323–1341.

Free J.B. & Williams I.H. 1974: Factors determining food storage and brood rearing in honey bee (*Apis mellifera* L.) comb. — *J. Entomol. (A)* **49**: 47–63.

Friedrich F., Matsumura Y., Pohl H., Bai M., Hörnschemeyer T., & Beutel R.G. 2014: Insect morphology in the age of phylogenomics: innovative techniques and its future role in systematics. — *Entomol. Sci.* **17**: 1–24.

Garibaldi L.A., Steffan-Dewenter I., Winfree R., Aizen M.A., Bommarco R., Cunningham S.A. & Klein A.M. 2013: Wild pollinators enhance fruit set of crops regardless of honey bee abundance. — *Science* **339**: 1608–1611.

Hepburn H.R. 1998: Reciprocal interactions between honey bees and combs in the integration of some colony functions in *Apis mellifera* L. — *Apidologie* **29**: 47–66.

Karihaloo B.L., Zhang K. & Wang J. 2013: Honeybee combs: how the circular cells transform into rounded hexagons. — *J. R. Soc. Interf.* **10**: 20130299, 4 pp.

Keszthelyi S., Pónya Z., Csóka Á., Bázár G., Morschhauser T. & Donkó T. 2020: Non-destructive imaging and spectroscopic techniques to investigate the hidden-lifestyle arthropod pests: a review. — *J. Plant Dis. Prot.* **127**: 283–295.

Keszthelyi S., Sipos T., Csóka Á. & Donkó T. 2021: CT-supported analysis of the destructive effects of *Varroa destructor* on the pre-imaginal development of honey bee, *Apis mellifera*. — *Apidologie* **52**: 155–162.

Neov B., Georgieva A., Shumkova R., Radoslavov G. & Hristov P. 2019: Biotic and abiotic factors associated with colonies mortalities of managed honey bee (*Apis mellifera*). — *Diversity* **11**: 237, 16 pp.

Shawer D.M., Rakha O.M., Taha E.K.A., Al-Kahtani S.N. & Elnabawy E.M. 2021: The impact of caging the queens during the flow season on some biological activities of honeybee colonies. — *Saudi J. Biol. Sci.* **28**: 2975–2979.

Sipos T., Donkó T., Jócsák I. & Keszthelyi S. 2021: Study of morphological features in pre-imaginal honey bee impaired by *Varroa destructor* by means of computer tomography. — *Insects* **12**: 717, 12 pp.

Smith D.B., Bernhardt G., Raine N.E., Abel R.L., Sykes D., Ahmed F., Pedroso I. & Gill R.J. 2016: Exploring miniature insect brains using micro-CT scanning techniques. — *Sci. Rep.* **6**: 21768, 10 pp.

Sonenshine D.E., Posada-Florez F., Laudier D., Gulbronson C.J., Ramsey S. & Cook S.C. 2022: Histological atlas of the internal anatomy of female *Varroa destructor* (Mesostigmata: Varroidae) mites in relation to feeding and reproduction. — *Ann. Entomol. Soc. Am.* **115**: 163–193.

Taha E.K.A. & Al-Kahtani S.N. 2020: The relationship between comb age and performance of honey bee (*Apis mellifera*) colonies. — *Saudi J. Biol. Sci.* **27**: 30–34.

Taha E.K.A. & El-Sanat S.I. 2007: Effect of combs age on honey production and its physical and chemical properties. — *Bull. Entomol. Soc. Egypt* **2**: 9–18.

Taha E.K.A., Manosur H.M. & Shawer M.B. 2010: The relationship between comb age and the amounts of mineral elements in honey and wax. — *Bee World* **49**: 202–207.

Williams G.R., Tarpy D.R., van Engelsdorp D., Chauzat M.P., Cox-Foster D.L., Delaplane K.S., Neumann P., Pettis J.S., Rogers R.E. & Shutler D. 2010: Colony Collapse Disorder in context. — *BioEssays* **32**: 845–846.

Winfree R., Gross B.J. & Kremen C. 2011: Valuing pollination services to agriculture. — *Ecol. Econ.* **71**: 80–88.

Wipfler B., Pohl H., Yavorskaya M.I. & Beutel R.G. 2016: A review of methods for analysing insect structures – the role of morphology in the age of phylogenomics. — *Curr. Opin. Insect Sci.* **18**: 60–68.

Received July 18, 2022; revised and accepted November 21, 2022

4.4. Analysis of X-ray irradiation effects on the mortality values and hemolymph immune cell composition of *Apis mellifera* and its parasite, *Varroa destructor*

Title	Analysis of X-ray irradiation effects on the mortality values and hemolymph immune cell composition of *Apis mellifera* and its parasite, *Varroa destructor*
Authors	Tamás Sipos, Csaba Glavák, Janka Turbók, Katalin Somfalvi-Tóth, Tamás Donkó, Sándor Keszthelyi
Journal	Journal of Invertebrate Pathology
Year	2024
Volume	204
Issue	
Pages	108109
Quartile	Q1
Impact factor	3.6
DOI	10.1016/j.jip.2024.108109

Contents lists available at ScienceDirect

Journal of Invertebrate Pathology

journal homepage: www.elsevier.com/locate/jip

Analysis of X-ray irradiation effects on the mortality values and hemolymph immune cell composition of *Apis mellifera* and its parasite, *Varroa destructor*

Tamás Sipos [a,e,*], Csaba Glavák [b], Janka Turbók [c], Katalin Somfalvi-Tóth [a], Tamás Donkó [d], Sándor Keszthelyi [a]

[a] *Institute of Agronomy, Hungarian University of Agriculture and Life Sciences, Kaposvár Campus, Guba Sándor str. 40., H-7400 Kaposvár, Hungary*
[b] *Moritz Kaposi Teaching Hospital, Dr. József Baka Diagnostic, Radiation Oncology, Research and Teaching Center, Guba Sandor str. 40., H-7400 Kaposvár, Hungary*
[c] *Department of Physiology and Animal Health, Institute of Physiology and Nutrition, Hungarian University of Agriculture and Life Sciences, Kaposvár Campus, Guba Sándor str. 40., H-7400 Kaposvár, Hungary*
[d] *Medicopus Nonprofit Ltd., Guba Sándor str. 40., H-7400 Kaposvár, Hungary*
[e] *Institute for Farm Animal Gene Conservation, National Centre for Biodiversity and Gene Conservation, H-2100 Gödöllő, Hungary*

ARTICLE INFO

Keywords:
Alternative control strategy
Hemocytes
Honey bee
Mortality
varroosis
Ionizing irradiation

ABSTRACT

Varroa destructor is one of the most destructive enemies of the honey bee, *Apis mellifera* all around the world. Several control methods are known to control *V. destructor*, but the efficacy of several alternative control methods remains unexplored. Irradiation can be one of these unknown solutions but before practical application, the effectiveness, and the physiological effects of ionizing radiation on the host and the parasite are waiting to be tested. Therefore, the objective of our study was to investigate the effects of different doses (15, 50, 100, and 150 Gy) of high-energy X-ray irradiation through mortality rates and hemocyte composition changes in *A. mellifera* workers and record the mortality rates of the parasite. The mortality rate was recorded during short-term (12, 24, and 48 h) and long-term periods (3, 6, 12, 18, and 24d).

The sensitivity of the host and the parasite in case of the higher doses of radiation tested (50, 100, and 150 Gy) been demonstrated by total mortality of the host and 90 % of its parasite has been observed on the 18th day after the irradiation. *V. destructor* showed higher sensitivity (1.52-times higher than the adult honey bee workers) at the lowest dose (15 Gy). *A. mellifera* hemocytes were influenced significantly by radiation dosage and the elapsed time after treatment. The higher radiation doses increased plasmatocyte numbers in parallel with the decrease in prohemocyte numbers. On the contrary, the numbers of granulocytes and oencoytes increased in the treated samples, but the putative effects of the different dosages on the recorded number of these hemocyte types could not be statistically proven. In summary, based on the outcome of our study X-ray irradiation can be deemed an effective tool for controlling phoretic *V. destructor*. However, further research is needed to understand the physiological response of the affected organisms.

Introduction

The recent decline in managed honey bee (*Apis mellifera* L., 1758) populations has been attributed to the combination of multiple stressors such as parasites, pathogens, inappropriate usage of pesticides, and the consequences of global climate change (Peck and Seeley, 2019; Traynor et al., 2020; Breda et al., 2022). The worldwide spread of the *V. destructor* (*Varroa destructor* Anderson and Trueman, 2000) began in the second half of the 20th century and has led to the outbreak of several mite-transmitted viruses weakening the colonies and causing the declining health status of the managed and that also of the wild honey bee populations (Loftus et al., 2016; Traynor et al., 2020). Currently, the most stressful bee health problem is the mite-generated direct (fat body parasitism, hemocyte alteration, body weight loss) and indirect (virus vectorization, immunosuppression) damage observable at different developmental stages (pupa and imago) of *A. mellifera* (Garedew et al., 2004; Yang and Cox-Foster, 2007; Jefferson et al., 2013). In general, colonies suffering from high levels of parasitism collapse by the end of

---

* Corresponding author at: Hungarian University of Agriculture and Life Sciences, Kaposvár Campus, Institute of Agronomy – H-7400, Sándor Guba str. 40. Kaposvár, Hungary (Tamás Sipos).

E-mail addresses: sipos.tamas8@uni-mate.hu (T. Sipos), glavak.csaba@sic.medicopus.hu (C. Glavák), turbok.janka@uni-mate.hu (J. Turbók), somfalvi-toth.katalin@uni-mate.hu (K. Somfalvi-Tóth), donko.tamas@sic.medicopus.hu (T. Donkó), keszthelyi.sandor@uni-mate.hu (S. Keszthelyi).

https://doi.org/10.1016/j.jip.2024.108109
Received 9 February 2024; Received in revised form 28 March 2024; Accepted 11 April 2024

late autumn or during the winter depending on the occurrence of other stressors and their combination or synergic interaction (Guzmán-Novoa et al., 2010; Flores et al., 2021).

The main expectation of the beekeeping industry is to find new effective treatments for successful control of *Varroa* infestations due to the limited number of effective acaricides. (Guzmán-Novoa et al., 2012; Grozinger and Robinson, 2015; Gracia et al., 2017; Jack and Ellis, 2021; Kolics et al., 2021). Historically the usage of hard miticides lead to the development of resistant biotypes of *V. destructor* and residues buildup in beekeeping products. Integrated Pest Management (IPM) strategies are based on that certain levels of pests and damage caused are tolerable and do not require complete eradication of the latter (Roth et al., 2020; Jack and Ellis, 2021; Vilarem et al., 2021).In that manner IPM strategies were developed to prevent resistance, and chemical buildup with the rotation of soft and hard acaricides and mechanical treatments.

Fundamental research approaches for alternative pest management methods can be supplemented by ionizing radiations (UV, X-ray, γ-irradiation) that specificity could be guaranteed by applying at a dose of sufficient potency (Vreysen and Robinson, 2011; Arthur et al., 2015; Machi and Mastrangelo, 2015). These techniques can result in irreversible cytological and molecular level changes (DNA double-strand breaks, increased reactive oxygen species and apoptosis of damaged cells) (Newcombe, 1971; Cheng et al., 2009; Shim et al., 2009, Yamada et al.,2022). Arthropods are well-tolerant to ionizing exposures of different wavelengths and can survive several times the maximum levels of shortwave γ-irradiation and X-ray radiation that are lethal for mammals (Hofmeyr et al., 2016, Paithankar et al., 2017). These exposures can damage gametes as well as somatic cells, and the hemocyte formation processes of insects (Richardson and Myser, 1973; Moskalev et al., 2015; Giglio et al., 2018; Tilton and Brower, 2018).

The consequences of any physical and biological impact on the *A. mellifera* adult immune system can be assessed by total hemocyte count (THC) and differential hemocyte count (DHC) (Szymaś and Jędruszuk, 2003). The irradiation effect profoundly impacts the immune system, with the induced consequences reflected in the changes in total hemocyte numbers and the proportions of different cell types (Vogelweith et al., 2017; Gábor et al., 2020). The most common circulating hemocyte cells of *A. mellifera* such as plasmatocytes, prohemocytes, granulocytes and oenocytes can be visualised with staining by light microscopic analysis (Vilcinskas *et al*., 1997). Several studies are aimed at disentangling the consequences of the effects of biotic and abiotic factors on the immune cell composition and titer values of the circulating hemocytes of eusocial insects (Sallem *et al.*, 2006; Burritt et al., 2016, Brandt et al., 2017; Mohamed et al., 2023). Certain hemocyte types, such as plasmatocytes, demonstrate partial plasticity, contributing to the rapid and efficient immune response in phagocytosis. This plasticity appears to depend on the age, and developmental stage of the insect and on the vitality and health condition of the organism (Evans et al., 2006; Evans and Spivak, 2010; Negri et al., 2016).

A fundamental difficulty in controlling varroosis by irradiation is the different exposure of the parasite and the host to be protected. *Varroa* is an obligate ectoparasite of *A. mellifera* and thrives only in bee hives (Rosenkranz et al., 2010; Dietemann, et al., 2012; Egekwu et al., 2018). Thus, fulfilling biological requirements for maintaining *Varroa* in the laboratory on *A. mellifera* may represent further difficulty in estimating the effect against *V. destructor* (Jack et al., 2020). Therefore, this technique may be justified if the host-parasite is more susceptible than the organism to be protected and the effects do not impair the biological parameters of the latter (Gomes et al., 2002). Most research in insect science predominantly examines gamma irradiation, the effects of high-energy X-ray beams less well known (Mastrangelo et al., 2010; Kaboré et al., 2023). Moreover, from a practical standpoint, the utilization of gamma irradiation raises concerns because the radiation source is radioactive, and the prescribed dose distribution of modern linear X-ray accelerators is much more precise (Poirier et al., 2020; Wang et al., 2023). Studies about the effects of X-ray radiation on *A. mellifera* and *V. destructor* are scarce (Matthes et al., 1991; De Guzman et al. 2019 . A study reporting that *A. mellifera*has lowerresistance to γ-radiation compared to *V. destructor* was published more than 30 years by Matthes et al. (1991). The experiment showed that the *V. destructor* was only sensitive to gamma-radiation above 160 Gy, while the bees died at 15 Gy. This raises fundamental questions about the practical applicability thus for the justification of the technique further basic researches are required to validate the technique with the usage of high-energy X-ray beams irradiation.

The aim of our study was to investigate the effects of different doses of high-energy X-ray irradiation on the mortality rates of the host adult bee workers and the parasite phoretic *V. destructor*. Additionally, we conducted a cytological investigation of *A. mellifera* physiological response to irradiation, which is reflected in a measurable change in hemolymph composition.

Based on these facts, our aims were to objectively map the effects of X-rays, an ionizing radiation, on the mortality consequences of *V. destructor* and adult *A. mellifera* workers under laboratory conditions. The results obtained were intended to lay the foundations for a possible alternative strategy or to refute the practical application of this technique. We were further interested in exploring the impact of ionizing radiation on the hemocyte composition of workers. Overall, our results were intended to lay the foundations of a less known approach to the apicultural sciences.

2. Material and methods

2.1. Sampling

The living sample for the studies was provided by four newly established *A. mellifera* colonies maintained at the Hungarian University of Agriculture and Life Sciences, Kaposvár Campus (Somogy county, Hungary; GPS coordinates: WGS: X:46.381079 Y:17.826915). The hives were set up in the summer of 2022 (01. June. 2022) with a freshly mated queen and 1.5 kg of young worker bees and 5 frames of Hungarian standard NB (Nagyboczonádi) with pollen and honey storage. The artificial swarms were treated with 1.5 g × hive ^{1} of sublimated oxalic acid (99.5 % purity) to reduce the *Varroa* population in order to homogenize the parasite level of the experimental hives. The treatment was carried out four days after the colonies were established with no capped broods in the colony. An essential nutrient supply for the colonies was provided by supplementary pollen patties *ad libitum* and 1 l of 40 % sucrose solution per week until the end of August. At sampling (28. October. 2022), the colonies were free of capped brood. Therefore, the phoretic parasites in the colonies were present on all the workers. The worker bees from the wintering cluster were shaken into a plastic box to achieve a homogenous distribution of the parasite. A total of 20 experimental samples were taken from the colonies, five samples per colony from the shaken bees; a laboratory balance (A&D, EK-2000i) was used to prepare the samples to obtain a nearly equal number of individuals in each experimental box. The experimental samples containing 60 g of worker bees (n = 500) were placed in our design 380 ml polypropylene (PP) plastic cages until the irradiation treatments were implemented.

2.2. Description of the examination setup

The individuals of the experiment were placed in custom-made 380 ml cages in order to the realization of the X-ray irradiation (Fig. 1). Special radiation treatment cages were built, to diminish the air space between individuals and to achieve a homogenous dose distribution. To ensure the breathability and avoid overheating of the bees, 2 mm holes were made on the bottom and top and the side of the irradiation cages. The samples were kept at 25 °C during the radiation treatments. After the irradiation treatments, the bees were transported to the laboratory and placed in finishing custom-made cages with a hygienic bottom until the end of the experiment. The finishing cages had a volume of 1540 ml,

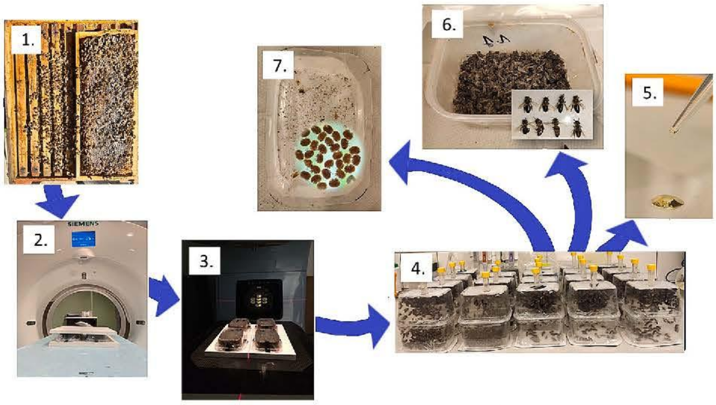

Fig. 1. Graphical illustration of the crucial steps of the experiment. (1) Preparation of the living samples for irradiation treatment, (2) CT-based radiotherapy treatment planning for *A.mellifera* experimental groups, (3) High energy X-ray irradiation of the experimental samples in special 380 ml irradiation cages, (4) the different experimental groups in 1540 ml custom-made *in-vitro* laboratory honey bee cages, (5) hemolymph collection process with micropipette, (6) the highest dose received cage at the 18th day of the experiment, dead *A. mellifera* were uniformly black without any hair on their body, (7) hygienic board of the *in-vitro* laboratory cages with fallen, dead *V. destructor*.

each with a hygienic bottom; the structure of the cages can be seen in Fig. 1. A plastic grid with a hole diameter of 3 mm was placed on the top and bottom to ensure air permeability. The diameter of the bottom grid allowed the dead mites to fall onto the hygienic board, but the dead bees were hung on the top of the grid. The bees were kept at 25 °C and 70 % RH during the laboratory experiment. To ensure the *ad libitum* feeding, three 15 ml centrifuge tubes were placed in the upper part of the cages with punching holes in the grid. Air-brake feeder tubes provided adequate water and sugar (40 % sucrose syrup) supply *ad libitum* during the experiment.

Mites and dead bees were counted at each exposure time. Studies on the short-term effect of the X-ray irradiation were performed at 12 h (here in after: h), 24 h, 48 h, and 72 h, whereas the long-term effect-studies were performed at 6 days (here in after: d), 12d, 18d, and 24d. In addition to the irradiated samples, untreated samples were also used as controls with the same experimental setup parameters. The number of *V. destructor* that fell on the hygienic board was used to determine the mortality rates of *V. destructor*. Only those mites that did not give any signs of life for physical stimulation, just continuously laid motionless on the hygienic board, were counted as positive dead mites. Dead bees that lay on the propolis grid were recorded for the calculation of the mortality rates of the host. After all exposure times, the bees and dead mites were removed from the experimental cages. The dead bees were continuously collected into a plastic box until the end of the experiment and placed into a freezer (−20 °C) for further *Varroa* washing procedure. On the 24th day of the experiment, the surviving *A. mellifera* were freeze-killed and were checked for *V. destructor* load. The mites that remained on dead bees were counted as survived. The surviving mites were washed off from the dead workers by the Varroa Shaking Device according to Posada-Flórez et al. (2022) technique.

2.3. Description of a high-energy X-ray irradiation set-up

The experimental cages were irradiated with high-energy X-ray photon beams generated by a Varian Clinac IX linear accelerator. Two opposing anteroposterior fields were used, the field size was 40 × 40 cm, and the dose rate was 600 MU × min^{-1}. Four samples were irradiated at the same time. The nominal energy of the photon beams was 6 MV. Solid water phantom slabs were placed under and above the samples to achieve good dose homogeneity in the samples (at least 1.5 cm was needed because of the build-up effect of 6 MV photons). To evaluate the effect of X-ray irradiation on the parasite and the host, 15, 50, 100, and 150 Gy mean doses were prescribed for the samples. The Varian Eclipse treatment planning system was used to calculate the absorbed dose based on computer tomograph (CT) images of the samples. The same samples were examined with Siemens SOMATOM Definition AS + CT scanner half hours before the irradiation scans with the following parameters: 100 kV tube voltage, 140 mAs X-ray radiation dose, spiral data collection mode with 0.7 pitch, the field of view 50 mm. Standard DICOM (Digital Imaging and Communications in Medicine) (The DICOM Standard) images were reconstructed by Siemens Syngo CT VA48A program with convolution kernel V80u. The resolution of the images was 0.0977 × 0.0977 × 0.1 mm. Each exam series was converted from DICOM to NIFTI (Neuroimaging Informatics Technology Initiative, 2005) file format. The experimental cages were contoured onto the CT slices as planning target volumes PTV1, PTV2, PTV3, and PTV4. The dose prescription of the irradiation plan was set to achieve 15, 50, 100, and 150 Gy mean doses to the sum of the PTVs. At least 92 % of the volume of the PTVs received 95 % of the prescribed dose, and the most significant dose was at 106 % of the prescribed dose. There were some lower dose (<95 % of the prescribed dose) regions at the outer edges of the cages. The homogeneity of the maximum dose (150 Gy) absorbed can be seen in Fig. 2. The continuously whirling movement of the bees could result in even better dose homogeneity than the calculated one.

2.4. Hemolymph collection, light microscopic analysis

Hemolymph was collected from four randomly selected workers of the untreated and treated group according to Borsuk et al. (2017) technique at the 6th and 12th day of the experiment. The individuals were placed on a styrofoam tray and fixed by gently pressing the thorax. The hemolymph was extracted from the antennal vesicles of the workers by removing their antennae with forceps and pressing the hemolymph contents of the abdomen and thorax towards the head with the fingertip. A 0.1–10 μL micropipette was used for the collection, and the tip was changed after every specimen. If the hemolymph deviated from the translucent light amber colour and was contaminated (e.g., faecal matter, gastric contents, or tissue components), the sample was considered invalid and discarded. The collected hemolymph was immediately dropped onto a microscope slide (HistoBond M+). and

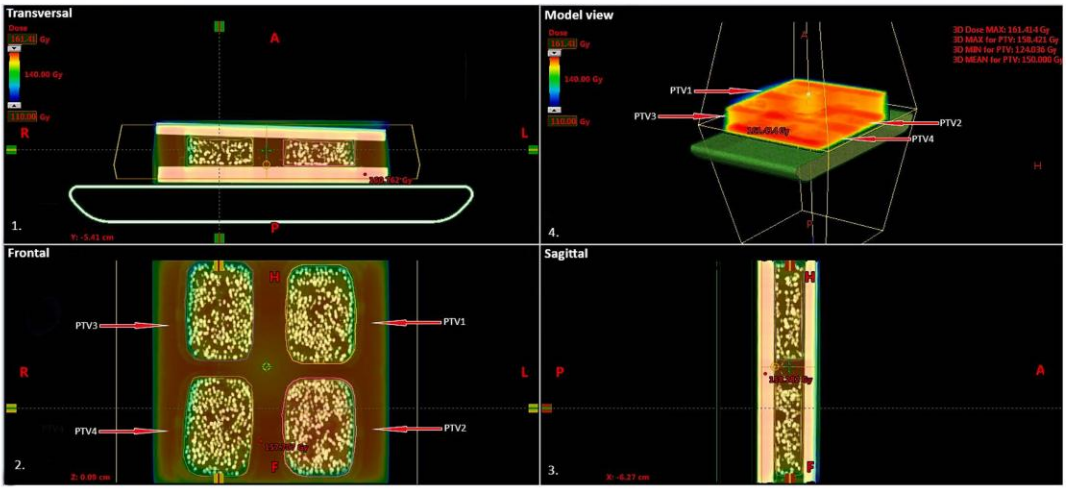

Fig. 2. The absorbed dose view of the highest dose (150 Gy) received experimental group based on the Varian Eclipse treatment planning system. The experimental cages were contoured on the CT slices as planning target volumes PTV1, PTV2, PTV3, and PTV4.

spread out with fine circular motion using the micropipette tip.

Smears were fixed using 100 % methanol applied to the samples by an atomizer glass bottle sprayer and dried overnight in the open air at room temperature. The slides were stained by RAL 555 Romanowsky type (RAL 555®, RAL Diagnostics, Martillac, France) rapid cytological staining kit after overnight drying. The components of the staining kit were applied similarly to the methanol by an atomizer sprayer creating a thin layer on the surface of the slides. The slides were dipped after each staining step according to the manufacturers protocol in clean distilled water five times for 1 s to wash off residual dye. After removing the finisher blue dye, the samples were placed on a paper completely dry towel in a diagonal standing position at room temperature. The smears were fixed with Entellan® rapid mounting medium (Merck KGaA, Darmstadt, Germany) for further light-microscopic analysis.

The differential hemocyte count (DHC) was performed by light microscope (OLYMPUS BX43, OLYMPUS Corporation, Tokyo, Japan) to study the changes in the immune cell composition of the hemolymph due to different irradiation dosages. The different cell types were separated on the stained smears and judged under 600 × magnification, and DHC values were recorded as a percentage distribution. The DHC numbers were created by counting 400 hemocytes on each smear to enhance the evaluation accuracy. The immune cells were classified into four categories depending on their morphological characteristics: prohemocytes, plasmatocytes, granulocytes, and oenocytes. The main

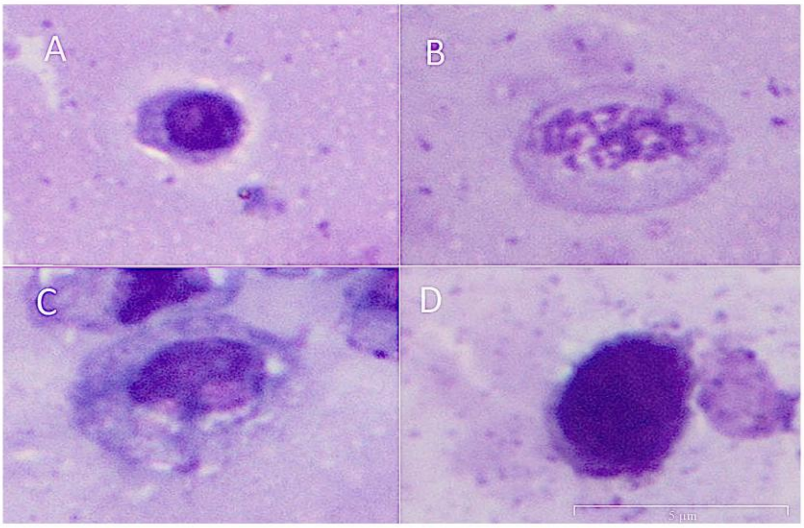

Fig. 3. The main circulating hemocytes of *A. mellifera* imaged at 1000X magnification photographed by Olympus DP21 digital camera (OLYMPUS Corporation, Tokyo, Japan). Representative images show (A) prohemocyte, (B) plasmatocyte, (C) granulocyte, (D) oenocyte.

circulating hemocytes of *A. mellifera* can be seen in Fig. 3.

2.5. Data evaluation and statistical analysis

Statistical analyses were performed using R statistics software version 4.2.1 and Microsoft Excel (Office version 2016). Figures visualizing data were created using Microsoft Excel (Office version 2016) except Duncan's test tables which were created by R statistics software version 4.2.1. The Abbott formula was used to correct the mortality rates of the parasite and the host. The mortality values of each examined species were calculated by Abbott's (1925) formula (M), where: $M = [(C - T)/C] \times 100$; where: C = number of survived individuals in control; T = number of survived individuals in treated (Abbott, 1925). To test the distribution of the hemocyte types the Kolmogorov-Smirnov normality test was used. The effect of different X-ray doses and elapsed time on the mortality rates of the host and the parasite were evaluated using two-way ANOVA coupled with Duncan multiple range *post hoc* test to prove the differences between treatment groups ($p < 0.05$). The two-way ANOVA and Duncan's *post hoc* test were applied to test the effect of different doses and elapsed time on the different hemocyte-type values.

3. Results

3.1. Mortality values of parasite and host

The different doses of X-ray irradiation-treated worker bees mortality values were recorded during the experiment and corrected by applying the Abbott correction formula. The effect of different doses on *A. mellifera* is shown in Fig. 4. The ionizing radiation- generated mortality values were independent of the doses at the short-term exposure time up to day 6. The higher mortality of the workers was recorded in the case of 50, 100, and 150 Gy from the 12th day. The experimental groups that received the 50,100,150 Gy doses mortality rates were 100 % in contrast to the 15 Gy with 27,3% on the 24th day of the experiment. The mortality rates of the lowest dosage at the end of the experiment only differed by 5 % compared to the untreated group. A two-way analysis of variance (ANOVA) showed a statistically validated correlation between the recorded mortality values of treated bees and the applied radiation doses (df = 3; F = 91.9110; $p < 0.001$) and the duration of treatment (df = 7; F = 247.9129; $p < 0.001$) also between their interaction (df = 21; F = 22.4863; $p < 0.001$).

The mortality rate of the phoretic *V. destructor* induced by 50, 100, and 150 Gy doses showed a similar pattern and a close correlation trend-like relationship (Fig. 5). All experimental groups mortality rates were zero at the short-term (12 h and 24 h inspection). However, dose-dependent trend of mortality of physically exposed parasites was recorded from day 3, the mortality numbers in the highest dose-receiving group were the highest from day 3 to day 12. Nearly three-fold *Varroa* fall was recorded from day 6 to day 12. The 50, 100, and 150 Gy had induced almost 90 % in average mortality of the experimental *V. destructor* populations, except for samples treated with the lowest dose (15 Gy) by day 18. The trends in mortality of the different doses are visible in the plotted values in Fig. 5. The 15 Gy irradiation induced 49 % eradication of the parasite population with the combination of the host which survived on the 24 d. The mortality in the lowest dose-treated group of *V. destructor* was 1.52-times higher as compared to the untreated group. The results of the two-way analysis of variance confirmed that both the time that elapsed after irradiation (df = 7; F = 43.4104; $p < 0.001$), the applied radiation dose (df = 3; F = 7.979; $p < 0.001$) and the interaction of these factors (df = 21; F = 2.072; $p = 0.009$) had a significant effect on the mortality values of the experimental *V. destructor* population.

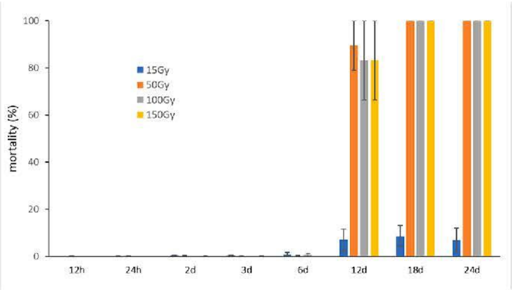

Fig. 4. Dose-dependent Abbott-corrected mortality rates of *A. mellifera* at different exposure times.

In all treated groups, the mortality values induced by each radiation dose as a function of time can be described along a polynomial curve with a close correlation, as was confirmed by the calculated coefficients of determination (Table 1). Fig. 5 can be divided into three distinct phases. After the treatments, the mortality rate in the *V. destructor* population slowly rises, followed by an exponentially increased mortality rate and mass mortality in the mite population from day 6. Before the average 90 % mortality rate in the treated *V. destructor* population, the mortality rate slows down again until the total mortality of the mite population rapidly starts. Differences in the mortality trends induced by different doses are reflected in the steeper slope of the curve and the nearly complete eradication ensuing after the treatment in a shorter time.

3.2. Hemolymph composition changes of the host

X-ray irradiation affected the composition of the circulating immune cells (DHC value) and the development of certain cellular elements (Fig. 6). The abundance of specific immune cells in the hemolymph was also significantly influenced by the time that elapsed after each treatment.

The quantitative changes in plasmatocytes and prohemocytes followed similar trends. Interestingly, low irradiation doses (15 Gy) induced opposite quantitative changes in the number of these cellular as compared to the higher irradiation doses. The 15 Gy group prohemocyte level was the highest (Fig. 7A) which resulted in the lowest plasmatocyte numbers (Fig. 7B). The highest plasmatocyte mean level was registered in the case of 100 Gy-receiving group, which co-occurred with the lowest percentage of prohemocyte content (Fig. 7A, B) The Dunan's test showed that the high mortality groups hemocyte profile changed, and the high dose-receiving groups prohemocyte and plasmatocyte mean values differed (Fig. 7 A, B). The effect on the changed hemocyte numbers was similar to the mortality values of the bees in case of the 50, 100 and 150 Gy dose-receiving groups (Fig. 4.). The prohemocyte and plasmatocyte ratio in the untreated group was similar to those of the 50 Gy and 15 Gy treated groups. Statistical analysis confirmed that the evolution of the recorded plasmatocyte (df = 4; F = 5.63442; $p < 0.001$) and prohemocyte count (df = 4; F = 5.5753; $p < 0.001$) were significantly affected by the dose of X-ray radiation applied, but the time that elapsed after the treatment did not affect the number of these cellular components recorded in the measured samples ($p > 0.05$).

On the contrary, the two-way analysis of variance coupled with the Duncan test showed that the abundance of granulocyte and oncocyte numbers was influenced by the time that elapsed after the treatment (granulocyte: df = 1; F = 15.2708; $p < 0.001$; oenocytes: df = 1; F = 4.7872; $p = 0.0302$) and the interaction of the elapsed time and the irradiation doses applied (granulocytes: df = 4; F = 4.633; $p = 0.00148$; oenocytes: df = 4; F = 2.4906; $p = 0.0456$) also had a statistically significant effect. Fig. 7 shows the changes in granulocytes (Fig, 7D) and oenocytes (Fig. 7C) percentages on the 6th and the 12th day of the experiment. For both cell types, their number in the plasma increases

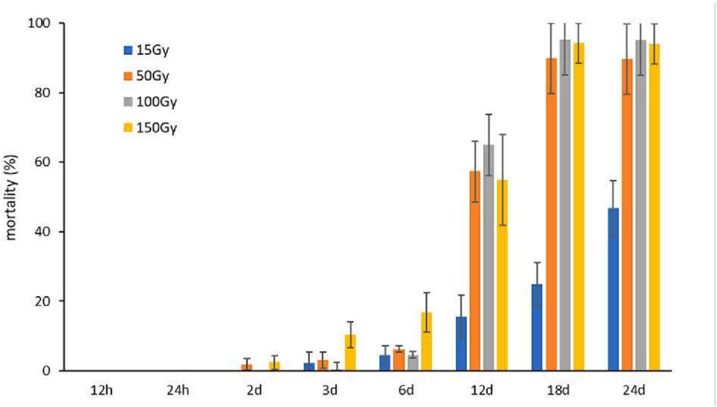

Fig. 5. Dose-dependent Abbott-corrected mortality rates of *V. destructor* at different exposure times.

Table 1
The mathematical quantities describing the nature and severity of Abbott-corrected mortality trends the applied different X-ray doses generated.

Doses	Polynomial equation	R^2
15 Gy	$y = 0.0625x^2 + 0.3065x - 0.9579$	0.9923
50 Gy	$y = -0.0158x^2 + 5.1648x - 13.012$	0.9594
100 Gy	$y = -0.0547x^2 + 6.3666x - 17.494$	0.9417
150 Gy	$y = -0.0443x^2 + 5.8355x - 12.425$	0.9753

with time of exposure, an observation that could be confirmed with the Duncan test. However, the different doses did not statistically influence the number of granulocytes and oenocytes.

4. Discussion

Successful control of *A. mellifera* most mortal parasite, the *V. destructor*, is essential to maintain the health of managed bee populations. Alternative solutions are crucial for bee health. due to the limited number of successful control methods and miticides. We investigated the response of *A. mellifera* and *V. destructor* to multiple doses of high-energy X-ray irradiation by measuring the mortality values of both and the immune cell composition of bees under *in vitro* conditions as an alternative anti-varroa treatment. It was confirmed that X-ray radiation affects the vitality of the host and its parasites, according to previous findings of Matthes et al. (1991).

Nevertheless, it has been challenging to establish the *V. destructor* mortality rates because the parasites life activities are significantly influenced by the optimal metabolic processes, vitality, and the behaviour of the host (Rosenkranz et al., 2010; Guzman *et al.*, 2012). If the host life activity and metabolic processes deteriorate, the vital rates of the parasite can be shown to decrease under the influence of any biotic and abiotic stressor (Rosenkranz et al., 2010; Egekwu et al., 2018; Traynor et al., 2020). Hence, understanding the effect of X-ray radiation on a specific parasite is difficult under *in vitro* conditions. This phenomenon is due to the obligate nature of the parasite, as it has been confirmed by several studies (Egekwu et al.,2018; Traynor et al., 2020).

For the higher doses of radiation tested (50, 100, 150 Gy), both parasite and host sensitivity have been demonstrated by our test results, and with increasing radiation doses, both experimental species mortality rates increased. All the treated groups of *A. mellifera* suffered 100 % mortality compared with the 90 % mortality rate of *V. destructor* at these higher doses on the 18th day after the irradiation treatment. Bees in all experimental groups died uniformly by day 18, which corroborates the observation of Matthes et al. (1991). *A. mellifera* resistance against ionizing radiation is much less than that of other insect species, the reason for which may be that the complexity of an organism increases the chance of irreversible, lethal changes in DNA and transcriptomic level occurring (Gomes et al., 2002; Cheng et al., 2009; Moskalev et al., 2015; Paithankar et al., 2017).

Compared with the previous dosages, a difference in induced mortality was found for the lowest dose used (15 Gy). According to these results, the phoretic stages of *V. destructor* showed higher sensitivity than those of the host. These findings contradict the results of Matthes et al. (1991). The mortality rates of the *Varroa* were higher in that dosage than that of the host. At the radiation dose of 15 Gy, it was noted

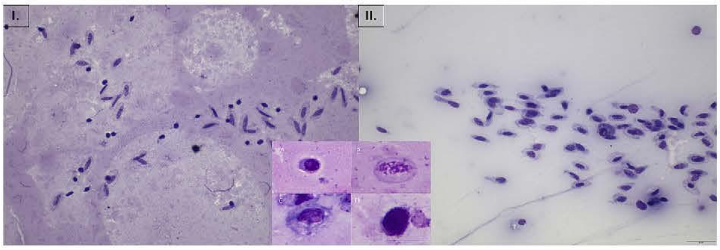

Fig. 6. Stained smears of *A. mellifera* hemolymph under 600 × magnification. (I.) Light microscopic field of view of the highest radiation dose (150 Gy) received worker *A. mellifera* stained hemolymph smear at the experiment 12th day, (II.) Light microscopic field of view of untreated worker *A. mellifera* hemolymph at the experiment 12th day. The representative four hemocyte classes of *A. mellifera* hemolymph: (A) prohemocyte, (B) plasmatocyte, (C) granulocyte, (D) oenocyte.

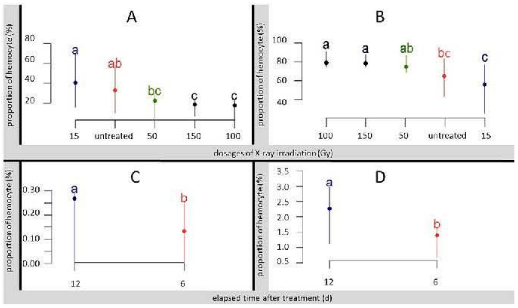

Fig. 7. Different doses of X-ray irradiation affect the circulating hemocytes of *A. mellifera*, proven by statistical analysis results of the Duncan test. (A) prohemocyte numbers, (B) plasmatocyte numbers, (C) oenocyte numbers, (D) granulocyte numbers, lowercase letters indicate the differences in mean values of the different experimental groups.

that neither the counts of hemocytes nor the mortality rates of bees exhibited the same level of aggressiveness as observed at other doses. The outcomes from the Duncan test align with the mortality curves, indicating that the hemocyte counts were profoundly altered even prior to significant mortality. The scales of the doses used did not allow us to determine the most effective dose for *Varroa* with minimal *A. mellifera* mortality. Although the low dose shown causes higher mortality to the parasite than to the host, it does not induce an expected efficacy (above 95 %). Moreover, the severe involvement of the host raises various questions in connection with the practical application of this method.

In order to develop a successful control method, understanding the physiological responses is of overriding importance. *A. mellifera* main circulating hemocytes were influenced significantly by the applied radiation dosages and the elapsed time in laboratory conditions (Giglio et al., 2018). The increased number of plasmatocytes by 6 days and 12 days after the irradiation can be expounded by the role of the triggered cellular responses. Plasmatocytes play a part in repair mechanisms by phagocytosis of microorganisms, encapsulation of larger invaders, clotting, and melanisation of the cuticle after physical injury (Evans et al., 2006; Evans *et al.*, 2010; Gábor et al.,2020).

Granulocytes carry out immune functions that strongly relate to plasmatocytes these cell types are two key factors of the cell-mediated immunity of *A. mellifera*. Granulocytes, by phagocyting the bacterial invaders of the hemocoel and following plaque formation play a role in plaque removal and breakdown encapsulation response, which can explain the increase in the percentage of granulocytes during the experiment (Evans et al., 2006; Honti et al., 2014; Negri et al., 2016).

The decrease in the percentage of prohemocytes results from the direct physical damage of the nucleus which the irradiation generated because of the more active cellular activity of this immune cell lineage. Similar to our result, decreased prohemocyte numbers were observed in different insecticide oral feeding experiments in *Apis* spp. due to the genotoxic DNA damaging effect of different herbicides (Perveen and Ahmad, 2017; Mohamed et al., 2023).

The number of oenocytes helps enhance the cellular immune response through phenoloxidase and nucleic acid release (Altincicek et al., 2008). The time-dependent changes in the percentage of oenocytes could be generated due to the tissue damage that the radiation affected (Evans et al., 2006; Altincicek et al., 2008; Negri et al., 2016.).

In conclusion, ionizing radiation strong physical effects were not only shown to induce mortality, but also have a demonstrable effect on the immune cell composition of the hemolymph. For the practical application of ionizing radiation to *V. destructor* control, it is essential to identify the exact dose of radiation that has a negligible destructive effect on the bees while reducing the *V. destructor* numbers. The physiological changes that the ionizing radiation generates must be considered, and further research is needed to understand the immunological, and transcriptomic changes which concomitantly occur upon the treatment. Our study will allow a better understanding of the effects of ionizing radiation types such as UV-A and UV-B, UV-C, or X-ray and Gamma-radiation on *Apis mellifera* hemocyte composition.

5. Conclusions

Our study demonstrated that *A. mellifera* workers and phoretic *V. destructor* exposed to X-rays has suffered increased mortality and changes the hemocyte composition of the host. Different doses of radiation applied and the elapsed time after treatments showed statistically verifiable changes in mortality and *A. mellifera* workers hemocyte composition. However, the practical applications of these methods because of the health-deteriorating effect caused to the protectable organism and the point of view from an efficacy are highly doubtful. X-ray doses higher than 50 Gy generate high mortality of *A. mellifera* workers 18 days after the irradiation.

The 15 Gy irradiation against *V. destructor* is the most promising of the treatments tested because of the least negative outcome in the case of hemocyte alteration and mortality of *A. mellifera*. Higher doses of radiation (50, 100, 150 Gy) have definite mortality on the organism to be protected as well as alter the immune cell composition. The increased plasmatocyte and granulocyte relative numbers signal an increased cellular immune response, while the decrease in prohemocytes and oenocytes reflects an alteration in homeostasis, which were confirmed by the mortality values and the results of the Duncan's test.

As a basic research, our work does not support a direct practical application but contains theoretically positive outcomes. The X-ray-induced mortality of *V. destructor* does not reach the expected efficiency, but our results may provide a basis for more advanced investigations related to the immune system and cellular immune response of *A. mellifera* to high-energy X-ray beams. Future research on the physiological changes caused by X-rays and other ionizing radiation in *A. mellifera* and *V. destructor* could further refine our results and provide a basis for the development of new approaches to the ecological relationships between bees and *V. destructor*.

CRediT authorship contribution statement

Tamás Sipos: Supervision, Resources, Data curation, Conceptualization. **Csaba Glavák:** Writing – original draft, Software, Resources, Methodology, Data curation. **Janka Turbók:** Writing – original draft, Resources, Methodology, Investigation, Data curation. **Katalin Somfalvi-Tóth:** Validation, Software, Formal analysis. **Tamás Donkó:** Supervision, Resources, Data curation, Conceptualization. **Sándor Keszthelyi:** Writing – review & editing, Writing – original draft, Visualization, Supervision, Resources, Project administration, Methodology, Investigation, Funding acquisition, Formal analysis, Conceptualization.

Declaration of competing interest

The authors declare that they have no known competing financial interests or personal relationships that could have appeared to influence the work reported in this paper.

Acknowledgment

We thank Zsolt Pónya for reading the manuscript and the insightful suggestions and language corrections.

Funding

This work was supported by the ÚNKP-22-3-1 New National Excellence Program of the Ministry for Culture and Innovation from the

source of The National Research, Development, and Innovation Fund.

References

Abbott, W.S., 1925. A method of computing the effectiveness of an insecticide. J. Econ. Entomol 18 (2), 265–267. https://doi.org/10.1093/jee/18.2.265a.

Altincicek, B., Stötzel, S., Wygrecka, M., Preissner, K.T., Vilcinskas, 2008. A., Host-derived extracellular nucleic acids enhance innate immune responses, induce coagulation, and prolong survival upon infection in insects. J. Immunol. 181(4), 2705-2712. DOI: 10.4049/jimmunol.181.4.2705.

Anderson, D.L., Trueman, J.W.H., 2000. *Varroa jacobsoni* (*Acari: Varroidae*) is more than one species. Exp. Appl. Acarol. 24, 165–189. https://doi.org/10.1023/A:1006456720416.

Arthur, V., Machi, Arthur, V., Machi, A., Mastrangelo, T., 2015. Ionizing radiations in entomology. Evol. Ioniz. Rad. Res. 213-34.

Borsuk, G., Ptaszyńska, A.A., Olszewski, K., Domaciuk, M., Krutmuang, P., Paleolog, J., 2017. A new method for quick and easy hemolymph collection from *Apidae* adults. PloS One 12 (1), e0170487.

Brandt, A., Grikscheit, K., Siede, R., Grosse, R., Meixner, M.D., Büchler, R., 2017. Immunosuppression in honeybee queens by the neonicotinoids thiacloprid and clothianidin. Sci. Rep. 7 (1), 4673. https://doi.org/10.1038/s41598-017-04734-1.

Breda, D., Frizzera, D., Giordano, G., Seffin, E., Zanni, V., Annoscia, D., Topping, C.J., Blanchini, F., Nazzi, F., 2022. A deeper understanding of system interactions can explain contradictory field results on pesticide impact on honey bees. Nat. Comm. 13 (1), 5720. https://doi.org/10.1038/s41467-022-33405-7.

Burritt, N.L., Foss, N.J., Neeno-Eckwall, E.C., Church, J.O., Hilger, A.M., Hildebrand, J. A., Warshauer, D.M., Perna, N.T., Burritt, J.B., 2016. Sepsis and hemocyte loss in honey bees (*Apis mellifera*) infected with Serratia marcescens strain sicaria. PloS One 11 (12), e0167752.

Cheng, I.C., Lee, H.J., Wang, T.C., 2009. Multiple factors conferring high radioresistance in insect Sf9 cells. Mutagen. 24 (3), 259–269. https://doi.org/10.1093/mutage/gep005.

De Guzman, Lilia I., Michael Simone-Finstrom, Amanda M. Frake, and Philip Tokarz. 2019. "Comb Irradiation Has Limited, Interactive Effects on Colony Performance or Pathogens in Bees, *Varroa destructor* and Wax Based on Two Honey Bee Stocks" Insects 10, no. 1: 15. https://doi.org/10.3390/insects10010015.

Dietemann, V., Pflugfelder, J., Anderson, D., Charrière, J.D., Chejanovsky, N., Dainat, B., de Miranda, J., Delaplane, K., Dillier, F.X., Fuch, S., Gallmann, P., 2012. *Varroa destructor*: research avenues towards sustainable control. J. Apic. Res. 51 (1), 125–132. https://doi.org/10.3896/IBRA.1.51.1.15.

Egekwu, N.I., Posada, F., Sonenshine, D.E., Cook, S., 2018. Using an in vitro system for maintaining *Varroa destructor* mites on *Apis mellifera* pupae as hosts: studies of mite longevity and feeding behavior. Exp. Appl. Acarol. 74, 301–315. https://doi.org/10.1007/s10493-018-0236-0.

Evans, J.D., Aronstein, K., Chen, Y.P., Hetru, C., Imler, J.L., Jiang, H., Kanost, M., Thompson, G.J., Zou, Z., Hultmark, D., 2006. Immune pathways and defence mechanisms in honey bees *Apis mellifera*. Ins. Mol. Biol. 15 (5), 645–656. https://doi.org/10.1111/j.1365-2583.2006.00682.x.

Evans, J.D., Spivak, M., 2010. Socialized medicine: individual and communal disease barriers in honey bees. J. Invertebr. Pathol. 103, S62–S72. https://doi.org/10.1016/j.jip.2009.06.019.

Flores, J.M., Gámiz, V., Jiménez-Marín, Á., Flores-Cortés, A., Gil-Lebrero, S., Garrido, J. J., Hernando, M.D., 2021. Impact of *Varroa destructor* and associated pathologies on the colony collapse disorder affecting honey bees. Res. Vet. Sci. 135, 85–95. https://doi.org/10.1016/j.rvsc.2021.01.001.

Gábor, E., Cinege, G., Csordás, G., Rusvai, M., Honti, V., Kolics, B., Török, T., Williams, M.J., Kurucz, É., Andó, I., 2020. Identification of reference markers for characterizing honey bee (*Apis mellifera*) hemocyte classes. Dev. Comp. Immunol. 109, 103701 https://doi.org/10.1016/j.dci.2020.103701.

Garedew, A., Schmolz, E., Lamprecht, I., 2004. The energy and nutritional demand of the parasitic life of the mite *Varroa destructor*. Apidologie 35 (4), 419–430. https://doi.org/10.1051/apido:2004032.

Giglio, A., Manfrin, C., Zanetti, M., Aquiloni, L., Simeon, E., Bravin, M.K., Battistella, S., Giulianini, P.G., 2018. Effects of X-ray irradiation on haemocytes of *Procambarus clarkii* (*Arthropoda: Decapoda*) males. Eur. Zool. J. 85 (1), 26–35. https://doi.org/10.1080/24750263.2017.1423119.

Gomes, S.A.O., Graciano, G.L., Nogueira, N.F.S., De Souza, W., Garcia, E.S., Azambuja, P., 2002. Effects of gamma irradiation on the development of *Trypanosoma rangeli* in the vector *Rhodnius prolixus*. J. Invertebr. Pathol. 79 (2), 86–92. https://doi.org/10.1016/S0022-2011(02)00011-3.

Gracia, M.J., Moreno, C., Ferrer, M., Sanz, A., Peribáñez, M.Á., Estrada, R., 2017. Field efficacy of acaricides against *Varroa destructor*. Plos One 12 (2), e0171633.

Grozinger, C.M., Robinson, G.E., 2015. The power and promise of applying genomics to honey bee health. Curr. Op. Ins. Sci. 10, 124–132. https://doi.org/10.1016/j.cois.2015.03.007.

Guzmán-Novoa, E., Eccles, L., Calvete, Y., Mcgowan, J., Kelly, P.G., Correa-Benítez, A., 2010. *Varroa destructor* is the main culprit for the death and reduced populations of overwintered honey bee (*Apis mellifera*) colonies in Ontario, Canada. Apidologie 41 (4), 443–450. https://doi.org/10.1051/apido/2009076.

Guzmán-Novoa, E., Emsen, B., Unger, P., Espinosa-Montaño, L.G., Petukhova, T., 2012. Genotypic variability and relationships between mite infestation levels, mite damage, grooming intensity, and removal of *Varroa destructor* mites in selected strains of worker honey bees (*Apis mellifera L.*). J. Invertebr. Pathol. 110 (3), 314–320. https://doi.org/10.1016/j.jip.2012.03.020.

Hofmeyr, H., Hofmeyr, M., Slabbert, K., 2016. Postharvest phytosanitary disinfestation of *Thaumatotibia leucotreta* (*Lepidoptera: Tortricidae*) in citrus fruit: tolerance of eggs and larvae to ionizing radiation. Flo. Entomol. 48–53.

Honti, V., Csordás, G., Kurucz, É., Márkus, R., Andó, I., 2014. The cell-mediated immunity of *Drosophila melanogaster*: hemocyte lineages, immune compartments, microanatomy and regulation. Dev. Comp. Immunol. 42 (1), 47–56. https://doi.org/10.1016/j.dci.2013.06.005.

Jack, C.J., Dai, P.L., van Santen, E., Ellis, J.D., 2020. Comparing four methods of rearing *Varroa destructor in vitro*. Exp. Appl. Acarol. 80, 463–476. https://doi.org/10.1007/s10493-020-00488-0.

Jack, C.J., Ellis, J.D., 2021. Integrated pest management control of Varroa destructor (Acari: Varroidae), the most damaging pest of (*Apis* mellifera L. (Hymenoptera: Apidae)) colonies. J. Ins. Sci. 21 (5), 6. https://doi.org/10.1093/jisesa/ieab058.

Jefferson, J.M., Dolstad, H.A., Sivalingam, M.D., Snow, J.W., 2013. Barrier immune effectors are maintained during transition from nurse to forager in the honey bee. Plos One 8 (1), e54097.

Kaboré, B. A., Nawaj, A., Maiga, H., Soukia, O., Pagabeleguem, S., Ouédraogo/Sanon, M. S. G., ... & De Beer, C. J., 2023. X-rays are as effective as gamma-rays for the sterilization of *Glossina palpalis gambiensis* Vanderplank, 1911 (Diptera: Glossinidae) for use in the sterile insect technique. Sci. Rep., 13(1), 17633. DOI: 10.1038/s41598-023-44479-88.

Kolics, É., Sajtos, Z., Mátyás, K., Szepesi, K., Solti, I., Németh, G., Taller, J., Baranyai, E., Specziár, A., Kolics, B., 2021. Changes in lithium levels in bees and their products following anti-varroa treatment. Ins. 12 (7), 579. https://doi.org/10.3390/insects12070579.

Loftus, J.C., Smith, M.L., Seeley, T.D., 2016. How honey bee colonies survive in the wild: testing the importance of small nests and frequent swarming. PloS One 11 (3), e0150362.

Mastrangelo, T., Parker, A.G., Jessup, A., Pereira, R., Orozco-Dávila, D., Islam, A., Walder, J.M.M., 2010. A new generation of X ray irradiators for insect sterilization. J. Econom. Entomol. 103 (1), 85–94. https://doi.org/10.1603/EC09139.

Matthes, H.F., Huebner, M., Hiepe, T., Boehme, R., Proesch, U., 1991. Ionising radiation for control of *Varroa jacobsoni* infestation. Tierärzt. Umsc. 46 (1), 20–23.

Mohamed, I.A., Omar, E.M., Tawfik, A.I., Amro, A., Al Naggar, Y., 2023. Sublethal effects of herbicides clethodim, haloxyfop-P-methyl, and their mixture on honey bee health. Apidologie 54 (1), 1–17. https://doi.org/10.1007/s13592-022-00982-x.

Moskalev, A., Zhikrivetskaya, S., Krasnov, G., Shaposhnikov, M., Proshkina, E., Borisoglebsky, D., Danilov, A., Peregudova, D., Sharapova, I., Dobrovolskaya, E., Solovev, I., 2015. A comparison of the transcriptome of *Drosophila melanogaster* in response to entomopathogenic fungus, ionizing radiation, starvation and cold shock. BMC Gen. 16, 1–18. https://doi.org/10.1186/1471-2164-16-S13-S8.

Negri, P., Maggi, M., Ramirez, L., Szawarski, N., De Feudis, L., Lamattina, L., Eguaras, M., 2016. Cellular immunity in *Apis mellifera*: studying hemocytes brings light about bees skills to confront threats. Apidologie 47, 379–388. https://doi.org/10.1007/s13592-015-0418-2.

Newcombe, H.B., 1971. The genetic effects of ionizing radiations. Adv. Gen. 16, 239–303. https://doi.org/10.1016/S0065-2660(08)60360-0.

Paithankar, J.G., Deeksha, K., Patil, R.K., 2017. Gamma radiation tolerance in different life stages of the fruit fly *Drosophila melanogaster*. Int. J. Rad. Biol. 93 (4), 440–448. https://doi.org/10.1080/09553002.2016.1266056.

Peck, D.T., Seeley, T.D., 2019. Mite bombs or robber lures? The roles of drifting and robbing in Varroa destructor transmission from collapsing honey bee colonies to their neighbors. PloS One 14 (6), e0218392.

Perveen, N., Ahmad, M., 2017. Toxicity of some insecticides to the haemocytes of giant honeybee, *Apis dorsata* F. under laboratory conditions. Saudi J. Biol. Sci. 24 (5), 1016–1022. https://doi.org/10.1016/j.sjbs.2016.12.011.

Poirier, Y., Belley, M.D., Dewhirst, M.W., Yoshizumic, T.T., Down, J.D., 2020. Transitioning from gamma rays to X rays for comparable biomedical research irradiations: Energy matters. Rad. Res. 193 (6), 506–511. https://doi.org/10.1667/RADE-20-00039.1.

Posada-Flórez, F.J., Abban, S.K., Smith Jr, I.B., Cook, S.C., 2022. Development and evaluation of a new effective tool and method for assessing *Varroa destructor* (*Acari: Varroidae*) mite populations in honey bee colonies. Insects 13 (5), 457. https://doi.org/10.3390/insects13050457.

Richardson, B.L., Myser, W.C., 1973. Radiation effects on the hemolymph free amino acid pool of the honeybee prepupa (*Apis mellifera*) and the waxmoth larva (*Galleria mellonella*). Rad. Res. 54 (2), 274–283. https://doi.org/10.2307/3573705.

Rosenkranz, P., Aumeier, P., Ziegelmann, B., 2010. Biology and control of *Varroa destructor*. J. Invertebr. Pathol. 103, S96–S119. https://doi.org/10.1016/j.jip.2009.07.016.

Roth, M.A., Wilson, J.M., Tignor, K.R., Gross, A.D., 2020. Biology and management of *Varroa destructor* (Mesostigmata: Varroidae) in Apis mellifera (Hymenoptera: Apidae) colonies. J. Integr. Pest Manag. 11 (1), 1. https://doi.org/10.1093/jipm/pmz036.

Shim, J.K., Aye, T.T., Kim, D.W., Kwon, Y.J., Kwon, J.H., Lee, K.Y., 2009. Gamma irradiation effects on the induction of three heat shock protein genes (piac25, hsc70 and hsp90) in the Indian meal moth, *Plodia Interpunctella*. J. Stored Prod. Res. 45 (2), 75–81. https://doi.org/10.1016/j.jspr.2008.09.005.

Szymaś, B., Jędruszuk, A., 2003. The influence of different diets on haemocytes of adult worker honey bees, *Apis Mellifera*. Apidologie 34 (2), 97–102. https://doi.org/10.1051/apido:2003012.

Tilton, E.W., Brower, J.H., 2018. Radiation effects on arthropods. Preservation of Food by Ionizing Radiation (269–316). CRC Press.

Traynor, K.S., Mondet, F., de Miranda, J.R., Techer, M., Kowallik, V., Oddie, M.A., Chantawannakul, P., McAfee, A., 2020. *Varroa destructor*: A complex parasite, crippling honey bees worldwide. Trends Parasitol. 36 (7), 592–606. https://doi.org/10.1016/j.pt.2020.04.004.

Vilarem, C., Piou, V., Vogelweith, F., Vétillard, A., 2021. *Varroa destructor* from the laboratory to the field: Control, biocontrole and ipm perspectives—A review. Insects 12 (9), 800. https://doi.org/10.3390/insects12090800.

Vogelweith, F., Körner, M., Foitzik, S., Meunier, J., 2017. Age, pathogen exposure, but not maternal care shape offspring immunity in an insect with facultative family life. BMC Evol. Biol. 17, 1–9. https://doi.org/10.1186/s12862-017-0926-y.

Vreysen, M.J., Robinson, A.S., 2011. Ionising radiation and area-wide management of insect pests to promote sustainable agriculture. Sustain. Agric. 2, 671–692. https://doi.org/10.1007/978-94-007-0394-0_29.

Wang, L.M., Li, N., Ren, C.P., Peng, Z.Y., Lu, H.Z., Li, D., Deng, S.Q., 2023. Sterility of *Aedes albopictus* by X-ray Irradiation as an Alternative to γ-ray Irradiation for the Sterile Insect Technique. Pathog. 12 (1), 102.

Yamada, H., Dias, V.S., Parker, A.G., Maiga, H., Kraupa, C., Vreysen, M.J., Mamai, W., Schetelig, M.F., Somda, N.S.B., Bouyer, J., 2022. Radiation dose-rate is a neglected critical parameter in dose–response of *insects*. Sci. Rep. 12 (1), 6242. https://doi.org/10.1038/s41598-022-10027-z.

Yang, X., Cox-Foster, D., 2007. Effects of parasitization by *Varroa destructor* on survivorship and physiological traits of *Apis mellifera* in correlation with viral incidence and microbial challenge. Parasitol. 134 (3), 405–412. https://doi.org/10.1017/S0031182006000710.

4.5. Tracking Varroa Parasitism Using Handheld Infrared Cameras: Is Eusocial Fever the Key?

Title	Tracking Varroa Parasitism Using Handheld Infrared Cameras: Is Eusocial Fever the Key?
Authors	Tamás Sipos, Szilvia Orsi-Gibicsár, Tamás Schieszl, Tamás Donkó, Zsombor Zakk, Sándor Farkas, Antal Binder, Sándor Keszthelyi
Journal	Insects
Year	2024
Volume	15
Issue	9
Pages	693
Quartile	Q1
Impact factor	2.9
DOI	10.3390/insects15090693

insects

MDPI

Article

Tracking Varroa Parasitism Using Handheld Infrared Cameras: Is Eusocial Fever the Key?

Tamás Sipos [1,*], Szilvia Orsi-Gibicsár [1], Tamás Schieszl [2], Tamás Donkó [3], Zsombor Zakk [1], Sándor Farkas [4], Antal Binder [1] and Sándor Keszthelyi [1]

[1] Department of Agronomy, Institute of Agronomy, Kaposvár Campus, Hungarian University of Agriculture and Life Sciences, S. Guba Str. 40, H-7400 Kaposvár, Hungary; ostrinia@gmail.com (S.K.)
[2] Department of Physiology and Animal Health, Institute of Physiology and Nutrition, Kaposvár Campus, Hungarian University of Agriculture and Life Sciences, Guba Sándor Str. 40, H-7400 Kaposvár, Hungary
[3] Medicopus Nonprofit Ltd., Guba Sándor Str. 40, H-7400 Kaposvár, Hungary; donko.tamas@sic.medicopus.hu
[4] Department of Nature Conservation Biology, Institute for Wildlife Management and Nature Conservation, Kaposvár Campus, Hungarian University of Agriculture and Life Sciences, Guba Sándor Str. 40, H-7400 Kaposvár, Hungary
* Correspondence: sipos.tamas8@uni-mate.hu

Simple Summary: *Varroa destructor* is a significant global honey bee parasite and the primary threat to bee health. Due to its latent lifestyle, detecting the mite in a brood requires invasive techniques. Enhancing detection methods is critical for advanced research on mite population dynamics, spread, selection efforts, and control methodologies. In this study, we employed infrared thermal imaging, a less-explored technique in apicultural studies, to detect parasitism in *Apis mellifera* broods. Our findings indicate that handheld infrared thermal cameras can generate adequately detailed heat maps of the hive. These maps distinctly separate cells containing honey, pollen, and brood, with stable, reproducible temperature measurements observable in late autumn. Notably, mite parasitism induces a sustained temperature increase in developing honey bee pupae, consistently detected regardless of mite numbers in the cell. This study reveals an advanced thermoregulatory behavior in the honey bee colony, manifesting as a social fever phenomenon. Further research is necessary to explore the health benefits of this behavior for bees and the negative effects on the mite. Our method, combined with the development of AI-based image evaluation software, could provide beekeepers and researchers with a valuable tool for *Varroa* research and bee biological studies.

Abstract: The *Varroa destructor* is the most significant bee parasite and the greatest threat to bee health all around the world. Due to its hidden lifestyle, detection within the brood cell is only possible through invasive techniques. Enhancing detection methods is essential for advancing research on population dynamics, spread, selection efforts, and control methodologies against the mite. In our study, we employed infrared imaging to measure the thermal differences in parasite and intact *Apis mellifera* worker broods. Experiments were conducted over two years at the MATE Kaposvár Campus in Hungary involving five beehives in 2022 and five beehives in 2023. A FLIR E5-XT WIFI handheld infrared camera was used to create a heat map of capped brood frames. Our results indicate that the resolution of these cameras is sufficient to provide detailed IR images of a bee colony, making them suitable to detect temperature differences in intact and *Varroa* parasitized capped brood cells. Mite parasitism causes a time-dependent and sustained temperature increase in developing bee pupae, observable regardless of mite number. Our work demonstrates two different heating patterns: hotspot heating and heating cells that are responsible for the elevated temperature of the Varroa-infested cells as a social fever response by the worker bees. Based on our results, future research combined with AI-based image evaluation software could offer beekeepers and researchers practical and valuable tools for high-throughput, non-invasive *Varroa* detection in the field.

Keywords: *Apis mellifera*; *Varroosis*; social immunity; infrared thermography

check for updates

Citation: Sipos, T.; Orsi-Gibicsár, S.; Schieszl, T.; Donkó, T.; Zakk, Z.; Farkas, S.; Binder, A.; Keszthelyi, S. Tracking Varroa Parasitism Using Handheld Infrared Cameras: Is Eusocial Fever the Key? *Insects* **2024**, *15*, 693. https://doi.org/10.3390/insects15090693

Academic Editor: Brian Johnson

Received: 19 July 2024
Revised: 21 August 2024
Accepted: 11 September 2024
Published: 13 September 2024

1. Introduction

As a prominent species among eusocial insects, the honey bee (*Apis mellifera*, L. 1758) exhibits highly developed climate regulation strategies in every season [1,2]. Maintaining homeostasis is crucial, especially because eggs, larvae, and pupae are highly sensitive to temperature fluctuations. The importance of thermoregulation is exemplified by the amount of energy expended: an average-sized colony consumes approximately 2,000,000 kJ of energy in a year for thermoregulation, representing 40% of the total energy expenditure [3]. We accept the correction. optimal ambient temperature for the colony's development ranges between 32 °C and 36 °C, ensuring healthy growth across different developmental stages [4,5]. Consequently, thermoregulation accuracy is high in the brood nest but becomes more variable and spans a wider range during periods without brood rearing in the wintertime [5,6]. Eggs and larvae tolerate lower temperatures better compared to pupae enclosed in brood cells [6,7]. Pupae exposed to prolonged temperatures below 32 °C are prone to developmental abnormalities, potentially leading to reduced memory and orientation abilities in worker bees [8]. Similarly, larvae exposed to temperatures below 32 °C for more than thirty minutes face significantly increased risks of pathogenic infections. Adult bees also exhibit behavioral and neurological issues due to substantial temperature fluctuations [8,9].

It is well known that insects with variable body temperatures are not able to heat their own environment and body independently, except during the process of chemoregulation, whereby some insects produce heat by burning chemical compounds through muscle work to increase locomotor and metabolic activity. In honey bee colonies, the preimaginal stages (larvae and free pupae) developing in the brood cells are unable to thermoregulate in the absence of active movement [5,6]. Larvae and preimaginal stages are considered poikilothermic, lacking inherent thermoregulation mechanisms and unable to generate sufficient heat independently for proper development; thus, imago worker bees must ensure thermal stability for them [10–12]. Honey bees maintain thermal homeostasis of the colony, and especially of the brood, by heating actively with their wing muscles, clustering for insulation when the external temperature is below 10 °C or cooling by vaporizing water and wing fanning when it is above 32 °C [13–15]. A colony, as a superorganism, must be understood as a homeothermic organism which tries to control its core temperature at a constant level [15–17]. Among eusocial insects, elevated body temperature or social fever is often considered a form of social immunity, closely intertwined with colony homeostasis and thermoregulation [18,19]. Social immunity encompasses diverse behavioral and organizational mechanisms that eusocial insects employ to defend against parasites and pathogens, thereby safeguarding colony health [19]. This collective effort among individuals possibly aims to constrain pathogen and parasite dissemination [20]. Brood temperatures elevated by approximately 0.03–0.19 °C have been observed in the developmental stages of honey bees parasitized by *Varroa destructor* (Anderson and Trueman 2000); however, the precise underlying mechanisms remain unclear [21].

Enhancing detection methods is critical for advanced research on mite population dynamics, spread, selection efforts, and control methodologies [22,23]. Indirect, non-invasive infrared thermal imaging is not unknown in entomological research. This methodology can provide insights into specific characteristics of poikilothermic organisms such as insects by measuring their surface temperature in a non-invasive manner [24,25]. For instance, it has been used to study chemoregulation-generated temperature changes in certain *Lepidopteran* spp. [26], to analyze the thermal characteristics of social insects like bees and wasps [27], and to investigate the specificity of parasitism phenomena in honey bee colonies [21,28]. Overall, the method is effective for indirectly mapping physiological changes in individual and social insects [21,29]. Consequently, the information obtained can be used to infer direct biological phenomena [21,30,31]. However, the number of research studies utilizing this methodology is limited, and its potential has thus far been only partially exploited.

The aim of our field and laboratory research was to map the temperature patterns observed on the capped brood using an infrared thermal camera (IR). Over the course of our two-year study, we investigated whether physiological changes due to varroosis are related to temperature variations in developing individuals. Ultimately, our work aims to increase understanding of the thermoregulation mechanism of honey bee colonies and explore the possibilities for indirect mapping of *Varroa* mite to lay the foundations for a potential new prodiagnostic method.

2. Materials and Methods

2.1. Colony Setup

The experiments were carried out in 2022 and 2023. In both years, the experiments were conducted at the same location and with the same settings. For the duration of the experiment, 5 hives were set up each year on the campus of the Hungarian University of Agricultural and Life Sciences in Kaposvár (WGS:X:46.381259, Y:17.82654). The experimental colonies were limited to 8 Nagyboczonádi (Nb)-size frames built to withstand cold in a standard Hungarian vertical-type hive; the same hives were used in each year. In order to avoid the results of the experiment being influenced by varroosis symptoms and, thus, the premature death of the colonies, artificial swarms were created. The colonies were established on 7 June 2022 for the 2022 year and on 7 June 2023 for the 2023 year; the experiments were carried out using the same technique. The artificial swarms contained 1.5 kg of worker bees and a one-year-old Carniolan (*Apis mellifera carnica*) queen. The bees were installed on 8 NB frames with 6 kg of honey in identical hives, and a pollen supply was added. The colonies received 0.5 L of 50% of sucrose solution for two weeks until the nucleus colonies were fully established. The queens of the colonies were from non-varroa-tolerant lines. Our objective was to mimic the natural mite infestation process by sublimating 2 g of oxalic acid (99.5% purity) twice, thus delaying the increase of phoretic *Varroa* mites by 5 and 8 days, respectively, after establishing the colonies. For the duration of the infrared thermography measurements, the colonies were nearly identically strong, and they were extended to 8 active frames, with an almost equal number of brood frames (2–3). To ensure that heat loss in the hives did not affect the results of the experiment, the top of the frames was fully covered with 400 µm thick polyethylene foil for agriculture and the top of the hives was insulated with a 4 cm thick expanded polystyrene thermal insulation board.

2.2. Brood Temperature-Monitoring Thermal Imaging Studies

Thermal imaging was conducted for five days constantly prior to dissection at consistent intervals in the afternoon between 12:00 and 16:00 for both years. The experiments were carried out from October 10 to 15 in 2022 and 2023 under similar weather conditions. The temperature was 18–23 °C in both years during the afternoons when the thermal imaging was carried out. The images were captured using a FLIR E5-XT WIFI handheld infrared thermal imager with a resolution of 160 × 120 pixels, a frame rate of 9 Hz, an accuracy of 0.1 °C, and a 0.95 emissivity rate. All images of the specimens were utilized as the basis for the experiment, with the thermal images taken from a uniform distance of 50 cm. To ensure that the brood surfaces did not cool within 30 s of removal, the imaging was performed in the back of a van: this was an enclosed space shielded from direct sunlight, maintained at a temperature of 23 °C. Prior to capturing the thermal images, the frames were shaken to remove imago worker bees, and the images were then captured.

The thermal images were analyzed using Teledyne FLIR Thermal Studio. In order to compare the infrared images of the same brood frame in the function of time, the color scale of the thermal images was converted to grayscale coloring by FLIR Thermal Studio. The converted grayscale images' pixel intensity histograms were analyzed with the help of GIMP 2.10.32 software. All five thermal images captured at different time points (from 10 to 15 October) were used to assess the thermal imaging patterns of the colonies.

To examine different developmental stages of brood and intact and infested cell temperatures, a polyline tool was employed to measure the exact hexagonal areas bounded by the brood cells, each containing an average of 38 ± 4 pixels. The average temperature values of the hexagon-shaped areas were recorded. Conversely, evaluation of the effect of mites on the temperature of the capped cells was based on thermal images captured on the 5th day (15 October) of each year. The 21 brood frames' thermal values were analyzed retrospectively after dissection, measuring the parasitized cells and adjacent intact brood cells at the same stage of development. Temperature values were determined for a total of 1005 parasitized and 1005 intact individuals of mixed age composition, selected according to specified criteria, over the two years. These individuals' data were also used to calculate the statistical differences in the developmental stages.

2.3. Dissection of the Capped Brood

After the five thermal images of each brood frame were captured over five days for each hive, the frames were removed from the hive to ensure that the location of the mites and the developmental state of the specimens remained similar compared to the thermal images. The frames were then stored at −20 °C until dissections were started. To allow for the dissection of the brood cells, the frames were placed in an incubator at 30 °C for 30 min to ensure proper thawing. During the dissections, the developmental status of the bees was determined based on the work of Rembold et al., 1980 [32], along with the presence of parasitization. All the capped broods from both sides of the frames were dissected. For the parasitized cells, the number of mites was recorded, and the location of the cell was documented on the pre-captured photographs to facilitate retrospective temperature determination. Dissections were conducted using a laboratory microchip under a stereomicroscope [33]. For each brood cell, the stage of development of the individuals was noted on the pre-captured photographs, and the number and the developmental stages of the parasites were recorded.

2.4. Data Analysis

To test the normal distribution of the data, a Shapiro–Wilk normality test was performed ($p \leq 0.05$). To establish the consistency of the heating pattern of the brood nest, the identity of the thermal images captured at five different time points prior to the experiment was tested, and the pixel intensity histograms were compared using Pearson correlation analysis. To evaluate the differences between developmental stages, paired *t*-test was used ($n = 100$) ($p \leq 0.05$). To calculate the thermal differences in various pupal stages ($n = 200$), one-way ANOVA was carried out. To determine the effect of the *Varroa* mite on temperature, a one-way ANOVA was performed for intact and parasitized individuals ($n = 1005$) ($p \leq 0.05$). The effect of the number of mites on temperature difference was tested using a one-way analysis of variance ($p \leq 0.05$). Temperature distribution on the surface of parasitized brood cells parasitized in the case of different numbers of *Varroa* mites was calculated by one-way ANOVA ($p \leq 0.05$) ($n = 508$). Statistical tests were conducted using the R-4.2.1 and Microsoft Excel software packages.

3. Results

3.1. Abundance of Varroa Destructor in the Brood

During the experiments in 2022, we dissected 10 NB-size frames containing 8887 capped worker broods; during the work in 2023, we dissected 9256 cells on 11 NB frames. The colonies' brood, on average, were 5.653% parasitized with Varroa mites in 2022 compared to 5.435% in 2023. The infestation level of the experimental colonies' brood varied, ranging from 3.117% to 12.936% in the two years. Dissection of 1.005 mixed-age worker cells infested by Varroa mites demonstrated that the number of mites in a brood cell can vary from 1 parasite to 13 parasites. If we examine the absolute prevalence of mite numbers in a cell, we find that the most common is a single parasite in the year 2022, while with an increasing number of mites in a cell, a power-type decreasing trend is demonstrated. An exponential decay curve describing the variation in the abundance of mite numbers in a cell shows a tight correlation, which is well represented by the value of the coefficient of determination ($R^2 = 0.98$). The population dynamics of the mite were considerably different in 2023: the most frequent prevalence was four mites in a cell, and the distribution of mites followed a parabolic curve, which is shown in Figure 1.

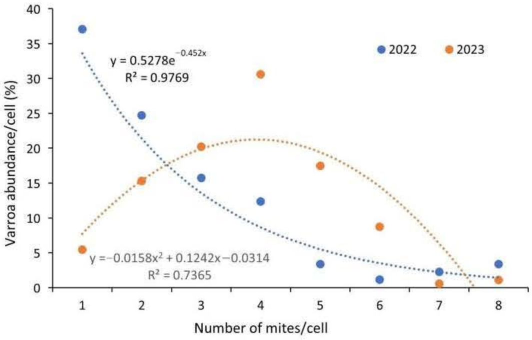

Figure 1. Plots of the relative abundance of mites in dissected brood cells over two years revealed differing trends.

In 2022, mite abundance followed an exponential trend line. In contrast, the evolution of mite abundance in the 2023 sampling was best described by a second-degree polynomial equation. The most significant difference observed was a nearly 30% higher prevalence of brood cells containing a single mite in 2022 compared to 2023.

3.2. *Comparison of Thermal Images of the Brood Nest*

As a result of testing the temperature values, it was observed that the temperatures of the different types of cells are clearly distinguished and show significant variation. It can be concluded that in the late autumn period, active heating is mainly concentrated in the brood chamber. The areas with higher temperatures are generally clustered around a well-defined brood area. A similar patchy, nodular pattern can be observed for the areas that can be characterized by lower temperatures, such as the honey-containing and pollen-containing cells. According to correlation analysis of the pixel-based intensity parameters extracted from the histograms of the images shown in Figure 2, it was found that between the pixel intensity parameters, there are significant similarities between the identities of the thermal images captured on 2 subsequent days (r = 0.999). The evolution of the temperatures of the brood chamber as a function of time shows a significant similarity, which indicates stable temperature-control activity of the workers in the areas concerned, linked to the brood areas. It can be clearly seen from the images that the workers produce most of the thermal energy for the brood (red, orange, and yellow colorization area in Figure 2), whereas there was no active heat production in other areas in the honey-storing cells nor in the pollen-storing cells (blue colorization area in Figure 2).

The brood area was determined to comprise two well-separated parts; these can be seen on the thermal images in Figure 3. The temperature differences are clearly visible; larvae and early-stage pupae (marked with white and white-striped hexagons) exhibit significantly lower temperatures compared to older pupae (marked with black hexagons). Based on the thermal values of the capped brood, the sealed larvae (LS), prepupa (Pp), (mean temperature value: 28.96 ± 0.70 °C) and pupal stages were well separated, which was statistically confirmed (df = 87; $p < 0.001$). The larval and the prepupa stages could be separated on the edge of the brood and in the middle of the brood. The pupae also could be separated based on the capping temperatures that were confirmed by one-way ANOVA statistical probing (df = 5; F = 4.051375; $p = 0.001451$). The temperature differences were calculated for the different developmental stages. The mean values of different developmental stages of pupae were the following: white-eyed (29.96 ± 0.22 °C); pink-eyed (30.21 ± 0.60 °C); red-eyed (30.27 ± 0.80 °C); dark-brown-eyed and dark-brown-eyed with a lightly pigmented thorax (30.58 ± 0.88 °C); dark-brown-eyed with a medium-dark thorax (30.52 ± 0.68 °C); dark-brown-eyed with a dark thorax (30 ± 0.81 °C).

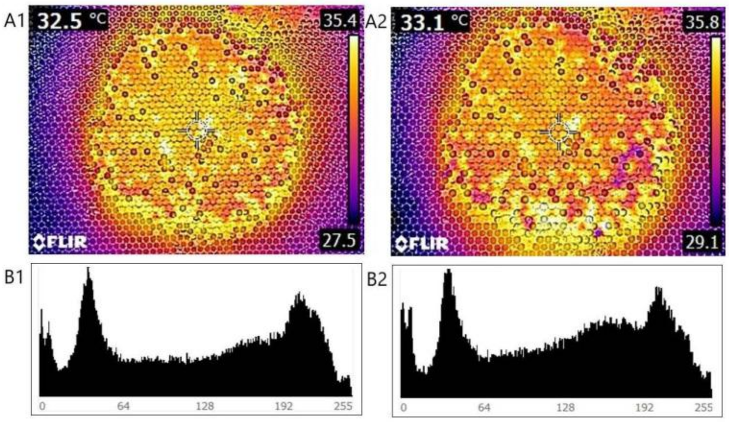

Figure 2. Thermal images of the same hive and frame captured at different time points ((**A1**) 23.10.14; (**A2**) 23.10.15), along with pixel intensity histograms (**B1**,**B2**) generated from digital image processing.

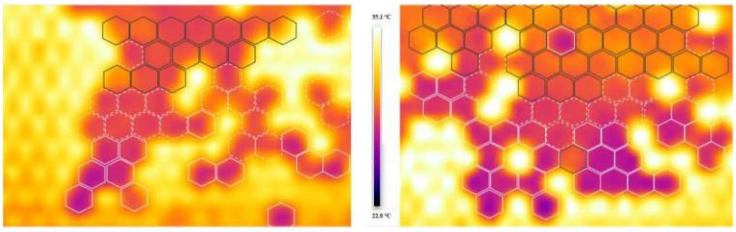

Figure 3. Thermal map of brood with capped larvae (marked white hexagons), pre-pupae (scattered white hexagons), and older pupae (black hexagons).

3.3. Relationship between Temperature Rise and Varroa Mite Presence

The results of infrared (IR) thermal imaging of sealed brood cells of worker bees showed that higher temperatures could be detected on the surface on the wax capping of the developing pupae infested by Varroa mites. The differences can be seen in the thermal images in Figure 4. One of the main findings of the research is that two different heating patterns were recognized on the thermal images, both of which were responsible for the elevated temperature of the parasitized cells. The most common heating pattern is the heating cell, as shown on the left pane in Figure 4(I.). The parasitized cell next to a heating cell, indicated by the hexagon marked with the mite, shows a higher temperature compared to the neighboring cells. A hotspot-elevated temperature pattern can be observed in the right pane in Figure 4(II.). The mite-infested brood cell in the center shows a similar tendency: on average, this cell is 0.65 °C warmer than the neighboring cells. The same tendency was measured during the two years when we compared intact individuals at the same stage of development that were neighboring parasitized individuals. The average temperature of infested individuals was 30.78 ± 0.09 °C, approximately 0.82 °C higher than that of intact worker cells (29.96 ± 0.08 °C) in 2022. The 2023 studies similarly confirmed the fact that parasitized cells had a higher temperature (30.62 ± 0.14 °C) than adjacent, intact individuals (29.86 ± 0.08 °C), averaging 0.76 °C higher. One-way analysis of variance confirmed in both experimental years that brood cells with parasite development alongside individuals of different preimaginal stages had statistically verifiably higher temperatures than those without mites (df = 1; F = 118.76; $p < 0.001$).

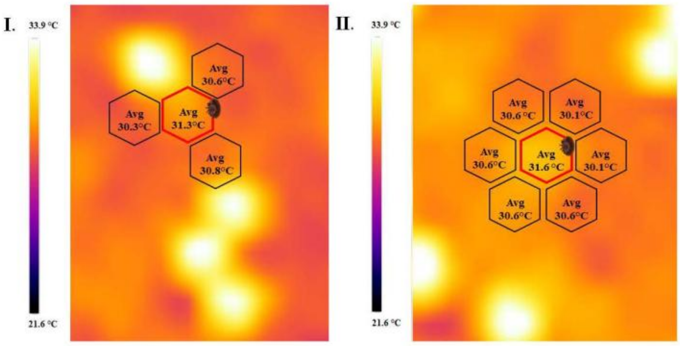

Figure 4. The two most common forms of elevated temperatures caused by Varroa mite. (**I.**) parasitized cell next to a heating cell; (**II.**) A hotspot pattern with the mite-infested brood cell in the center; black hexagon indicates intact; red hexagon indicates parasitized cells.

The temperature values measured on the cap surface, with different numbers of mites in the cell, are shown in Figure 5. Brood cells with a high number of mites/cell (7 (n = 3), 8 (n = 5) and 13 (n = 1)) were excluded from the statistical analyses because of the low number of elements. The single-factor analysis of variance confirmed that there was a statistically valid correlation between the number of mites in a brood cell and the average value of the surface temperatures of the parasitized cells (df = 1; F = 57,919.99; p = 0.001). As the number of mites increases, the confidence interval of the surface temperatures becomes narrower, described by a polynomial decrease in the trend lines drawn at the upper and lower limits of confidence. This verifiable correlation is shown by the result of the statistical analysis of the confidence intervals between the minimum and maximum temperature values measured on brood cells loaded with different numbers of mites. However, it can be observed that the evolution of the mean temperature values with an increasing number of mites per brood cell is stable within a range of 30.0–30.5 °C, representing the mean value. The mean value of the intact cells was 29.98 °C. At a low level of parasitation (one mite/cell: 32.9–27.1 °C; two mites/cell: 33.0–28.4 °C), the mean surface temperatures are within a wide range, whereas at a Varroa load of three mites and above (three mites/cell: 32.4–27.7 °C; four mites/cell: 32.1–29.1 °C; five mites/cell: 31.9–28.5 °C; six mites/cell: 31.1–29 °C), the surface temperatures are continuously narrowing.

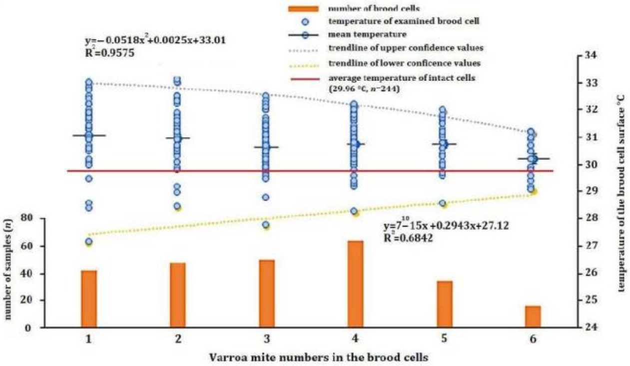

Figure 5. Temperature distribution of the surface of intact and parasitized brood cells as a function of different numbers of Varroa mites (n = 508).

4. Discussion

Monitoring the abundance of *Varroa* mites in different countries and seasons is important for the study of *Varroa* population dynamics [34]. The rapid spread of *Varroa* mites is illustrated by this two-year study: swarms can reach a high mite count in the brood 4 months after establishment. This increase can range from 3.117% to 12.936% [35]. In our experiment, the high infestation levels in both years could be explained by the high bee density in Hungary, which plays a primary role in the distribution of the mite through the drifting of worker bees [36–38]. Our observations on mite population dynamics provided us with indicators that were consistent with those found in the literature, both for larval and pupal stages [39]. The results of the 2022 sampling were atypical for the population dynamics of the mite compared to the 2023 sampling, which represented a normal population dynamics trend [39]. We can confirm that the number of parasites per worker brood cell at the pupal stage was low in 2022: it was predominantly between one and two mites/cell for the pupal stages. Few of the samples analyzed had more than four mites/cell. In contrast, when analyzing samples from 2023, in terms of the mixed-age composition of the dissected pupas, the most dominant number of mites in the cell was four. The differences in the two-year study can be attributed to seasonal patterns of varying nutrition throughout the bee pasture. Thus, colonies' performance can be influenced by weather conditions [39,40].

Our studies have shown that temperature analysis based on infrared imaging can be a suitable method for monitoring temperature changes in a colony of honey bees, even over five days, as continuous experiments show (r = 0.999) [41]. Furthermore, it can be used to detect the presence of possible *Varroa* mite parasitism in brood cells and to isolate the different honey bee developmental stages. Our study employs a new approach to investigate the temperature dynamics of the brood and hive. Since removing frames from the hive affects temperatures, our measurements were conducted within a specified time interval under controlled environmental conditions. This investigation is grounded in the principles of thermodynamics, allowing us to infer the thermal energy of the bodies [42,43]. By ensuring that the measured objects are composed of the same material, we maintain the comparability of the temperature values. In our study, we observed that the larval and pupal stages of honey bees develop at different temperatures. This variation can be attributed to the distinct temperature requirements specific to each developmental stage [21,44], but further detailed research is needed with higher-resolution infrared cameras. Our results confirmed that the mite-parasitized brood has, on average, a 0.79 °C higher temperature over the two-year period, which was statistically demonstrable. The results of Bauer et al. [21] indicated that the increased values could be explained by elevated metabolic processes induced by mite-transmitted bee viruses. In our opinion, the explanation for this phenomenon can be traced back to the intense social behavior of imagoes. The poikilothermic nature of arthropods explains our position, as developmental forms have an environment-dependent and variable body temperature that is independent of exposure to pathogens. Honey bee workers act as homeotherms, according to this point of view, to establish the optimal temperature and humidity for the developing pupae. The concentrated heating of a single cell in a capped brood can be explained by the so-called hotspot phenomenon [15], whereby worker bees release the thermal energy produced by pressing their thorax onto the brood surface in a concentrated manner on a single cell, especially the *Varroa*-parasitized cells. Another concentrated heating technique that plays a role in social fever is the so-called empty hot brood cells concept [45]; this can guarantee the local heating of infested individuals. The possible explanation for social fever is that workers sense the presence of mites in the cell. The workers try to shift the ambient temperature of the parasitic foreign organism out of the optimal range by active heating, thus worsening the biological indicators and living conditions of the parasitic organism [6,20,21]. An interesting observation of our study is that the variance in the temperature values measured on parasitized brood cells varies strongly depending on the number of parasites within the cell. For the parasite number in a cell, higher temperature values with less variability were obtained from our study for a higher number of infested cells (three mites/cell). The narrowing of the temperature confidence intervals with increasing parasite counts occurred in parallel with parasite detection of the infested individuals by workers, as in the case of hygienic behavior. The difference in variance is explained by the fact that workers are expected to detect parasitized cells with a higher success rate; also, the damage to the brood increases with the number of mites. The damage produces various volatile components [46,47] that can trigger social behavior and, thus, social fever. In contrast, brood cells with a low parasite load are less likely to be detected, maybe because they are in the beginning stages of the varroosis infestation. This fact explains the lower temperature variance in brood cells with a higher parasite count and the increasingly narrow range of temperature values on the surface.

Overall, the primary finding of our experimental work is that non-invasive thermal image analysis, utilizing a handheld thermal camera, can effectively locate *Varroa destructor* in a capped honey bee brood. Following further studies, refinement of this method could lead to a widely applicable technique for non-invasive, high-throughput detection of varroosis under field conditions. A significant advantage of this method is its potential for use by beekeepers without requiring specialized knowledge. Notably, the sensitivity of the thermal imaging device used in our study is comparable to that of sensors in most modern high-end smartphones. Consequently, accessible devices could be employed to optimize the timing of mite control in apiaries, aligning with integrated pest management criteria. Additionally, our method could expedite and validate selection efforts for desirable traits in bee breeding, such as *Varroa* sensitive hygiene (VSH) and suppressed mite reproduction (SMR), following further large-scale testing. The drawbacks of this method include the need for the development of AI-based image evaluation software which can reliably identify the target objects after a learning process for the temperature pattern of each brood comb. To isolate infested brood cells, the program must incorporate prior knowledge such as the temperature thresholds of intact and invested cells and specific temperature patterns of the brood, which can be effectively handled by a deep learning model based on artificial intelligence. To ensure the accuracy of this determination, it is essential to consider a combination of factors, including heating patterns and potential measurement errors. Additionally, the method needs to be tested during hot periods in summer to determine the temperature of specific brood cells in bees without active heating. This will provide deeper insights into the biological mechanisms underlying social fever in bees and will help to evaluate the detection method.

5. Conclusions

Our study has demonstrated that a handheld infrared thermal camera, which is easy and simple to use in field conditions, can effectively provide indirect visualization of changes in bee life activities. The thermal energy released by the active muscular activity of worker bees significantly influences the temperature of the brood cells, which is demonstrably related to the parasitization of the brood cells by *Varroa* mites. In the future, this method could be suitable for non-invasive visualization of the spread and presence of *Varroa* mites. The direct outcome of our work is the ability to detect varroosis symptoms without the need for direct dissection of brood cells. For practitioners, this methodology offers a practical opportunity to obtain rapid, non-invasive, and indirect information to assess the number of varroa mites and the health status of bee colonies. However, the method limitations include the costly tool requirements and the lack of a fully developed software support interface, which is essential for optimal performance. Further studies are needed for the summer period, during which bees actively cool the hive to maintain an optimal temperature range. With further improvements in the technique and additional validation trials, this method could become a valuable prognostic tool for large-scale apiaries. The results will contribute to the successful prediction and control of varroosis and may provide a non-invasive, time-efficient tool for varroa research and bee breeding selection works.

Author Contributions: Conceptualization, T.S. (Tamás Sipos) and S.K.; methodology, T.S. (Tamás Sipos), S.K., T.D. and Z.Z.; software, T.S. (Tamás Sipos) and S.F.; validation, T.S. (Tamás Sipos),

T.S. (Tamás Schieszl) and S.O.-G.; formal analysis, S.K. and T.D.; investigation, T.S. (Tamás Sipos), Z.Z. and A.B.; resources, T.S. (Tamás Sipos) and S.K.; data curation, S.K. and T.S. (Tamás Schieszl); writing—original draft preparation, T.S. (Tamás Sipos), T.S. (Tamás Schieszl), Z.Z., S.F., A.B. and S.K.; writing—review and editing, T.S. (Tamás Sipos), S.O.-G., S.F., S.K. and T.D.; visualization, Z.Z.; supervision, S.K.; project administration, T.S. (Tamás Sipos); funding acquisition, T.S. (Tamás Sipos) and S.K. All authors have read and agreed to the published version of the manuscript.

Funding: This research was funded by the ÚNKP-23-3-I New National Excellence Program of the Ministry for Culture and Innovation from the source of The National Research, Development and Innovation Fund.

Data Availability Statement: The raw data supporting the conclusions of this article will be made available by the authors on request.

Conflicts of Interest: Author Tamás Donkó was employed by the company Medicopus Nonprofit Ltd. The remaining authors declare that the research was conducted in the absence of any commercial or financial relationships that could be construed as potential conflicts of interest.

References

1. Cook, C.N.; Kaspar, R.E.; Flaxman, S.M.; Breed, M.D. Rapidly changing environment modulates the thermoregulatory fanning response in honeybee groups. *Anim. Behav.* **2016**, *115*, 237–243. [CrossRef]
2. Jones, J.C.; Benjamin, P.O. Nest thermoregulation in social insects. *Adv. Insect Physiol.* **2006**, *33*, 153–191.
3. Tautz, J.; Maier, S.; Groh, C.; Rössler, W.; Brockmann, A. Behavioral performance in adult honey bees is influenced by the temperature experienced during their pupal development. *Proc. Natl. Acad. Sci. USA* **2003**, *100*, 7343–7347. [CrossRef] [PubMed]
4. Petz, M.; Stabentheiner, A.; Crailsheim, K. Respiration of individual honeybee larvae in relation to age and ambient temperature. *J. Comp. Physiol. B* **2004**, *174*, 511–518. [CrossRef]
5. Stabentheiner, A.; Kovac, H.; Brodschneider, R. Honeybee colony thermoregulation–regulatory mechanisms and contribution of individuals in dependence on age, location and thermal stress. *PLoS ONE* **2010**, *5*, e8967. [CrossRef]
6. Seeley, T.D. *The Wisdom of the Hive: The Social Physiology of Honey Bee Colonies*; Harvard University Press: Cambridge, MA, USA, 2009.
7. Starks, P.T.; Gilley, D.C. Heat shielding: A novel method of colonial thermoregulation in honey bees. *Naturwissenschaften* **1999**, *86*, 438–440. [CrossRef]
8. Groh, C.; Tautz, J.; Rössler, W. Synaptic organization in the adult honey bee brain is influenced by brood-temperature control during pupal development. *Proc. Natl. Acad. Sci. USA* **2004**, *101*, 4268–4273. [CrossRef]
9. Abou-Shaara, H.F.; Owayss, A.A.; Ibrahim, Y.Y.; Basuny, N.K. A review of impacts of temperature and relative humidity on various activities of honey bees. *Insectes Sociaux* **2017**, *64*, 455–463. [CrossRef]
10. Stabentheiner, A.; Kovac, H.; Mandl, M.; Käfer, H. Coping with the cold and fighting the heat: Thermal homeostasis of a superorganism, the honeybee colony. *J. Comp. Physiol. A* **2021**, *207*, 337–351. [CrossRef]
11. Moritz, R.; Southwick, E.E. *Bees as Superorganisms: An Evolutionary Reality*; Springer Science & Business Media: Berlin/Heidelberg, Germany, 2012.
12. Lindauer, M. The water economy and temperature regulation of the honeybee colony. *Bee World* **1955**, *36*, 81–92. [CrossRef]
13. Heinrich, B. The mechanisms and energetics of honeybee swarm temperature regulation. *J. Exp. Biol.* **1981**, *91*, 25–55. [CrossRef]
14. Southwick, E.E.; Heldmaier, G. Temperature control in honey bee colonies. *Bioscience* **1987**, *37*, 395–399. [CrossRef]
15. Bujok, B.; Kleinhenz, M.; Fuchs, S.; Tautz, J. Hot spots in the bee hive. *Naturwissenschaften* **2002**, *89*, 299–301. [CrossRef]
16. Southwick, E.E. Metabolic energy of intact honey bee colonies. *Comp Biochem. Physiol. A* **1982**, *71*, 277–281. [CrossRef]
17. Ivanov, K.P. The development of the concepts of homeothermy and thermoregulation. *J. Therm. Biol.* **2006**, *31*, 24–29. [CrossRef]
18. Starks, P.T.; Blackie, C.A.; Seeley, T. Fever in honeybee colonies. *Naturwissenschaften* **2000**, *87*, 229–231. [CrossRef]
19. De Roode, J.C.; Lefèvre, T. Behavioral immunity in insects. *Insects* **2012**, *3*, 789–820. [CrossRef]
20. Goblirsch, M.; Warner, J.F.; Sommerfeldt, B.A.; Spivak, M. Social fever or general immune response? Revisiting an example of social immunity in honey bees. *Insects* **2020**, *11*, 528. [CrossRef] [PubMed]
21. Bauer, D.; Wegener, J.; Bienefeld, K. Recognition of mite-infested brood by honeybee (*Apis mellifera*) workers may involve thermal sensing. *J. Therm. Biol.* **2018**, *74*, 311–316. [CrossRef]
22. Sipos, T.; Donkó, T.; Jócsák, I.; Keszthelyi, S. Study of Morphological Features in Pre-Imaginal Honey Bee Impaired by *Varroa destructor* by Means of Computer Tomography. *Insects* **2021**, *12*, 717. [CrossRef]
23. Sipos, T.; Glavák, C.; Turbók, J.; Somfalvi-Tóth, K.; Donkó, T.; Keszthelyi, S. Analysis of X-ray irradiation effects on the mortality values and hemolymph immune cell composition of *Apis mellifera* and its parasite, *Varroa destructor*. *J. Invertebr. Pathol.* **2024**, *204*, 108109. [CrossRef] [PubMed]
24. Campbell, A.L.; Naik, R.R.; Sowards, L.; Stone, M.O. Biological infrared imaging and sensing. *Micron* **2002**, *33*, 211–225. [CrossRef] [PubMed]

25. Harrap, M.J.; Hempel de Ibarra, N.; Whitney, H.M.; Rands, S.A. Reporting of thermography parameters in biology: A systematic review of thermal imaging literature. *R. Soc. Open Sci.* **2018**, *5*, 181281. [CrossRef] [PubMed]
26. Kim, J. Skin temperature characteristics of the ligustrum moth (*Brahmaea certhia*) and the hawk moth (*Theretra oldenlandiae*) using IR camera. *J. Mech. Sci. Technol.* **2022**, *36*, 983–990. [CrossRef]
27. Stabentheiner, A.; Kovac, H.; Hetz, S.K.; Käfer, H.; Stabentheiner, G. Assessing honeybee and wasp thermoregulation and energetics—New insights by combination of flow-through respirometry with infrared thermography. *Thermochim. Acta* **2012**, *534*, 77–86. [CrossRef]
28. Bjerge, K.; Frigaard, C.E.; Mikkelsen, P.H.; Nielsen, T.H.; Misbih, M.; Kryger, P. A computer vision system to monitor the infestation level of *Varroa destructor* in a honeybee colony. *Comput. Electron. Agric.* **2019**, *164*, 104898. [CrossRef]
29. Johnson, A.P.; Wallman, J.F. Infrared imaging as a non-invasive tool for documenting maggot mass temperatures. *Aust. J. Forensic Sci.* **2014**, *46*, 73–79. [CrossRef]
30. Hunt, V.L.; Lock, G.D.; Pickering, S.G.; Charnley, A.K. Application of infrared thermography to the study of behavioural fever in the desert locust. *J. Therm. Biol.* **2011**, *36*, 443–451. [CrossRef]
31. Klein, B.A.; Stiegler, M.; Klein, A.; Tautz, J. Mapping sleeping bees within their nest: Spatial and temporal analysis of worker honey bee sleep. *PLoS ONE* **2014**, *9*, e102316. [CrossRef]
32. Rembold, H.; Kremer, J.P.; Ulrich, G.M. Characterization of postembryonic developmental stages of the female castes of the honey bee, *Apis mellifera* L. *Apidologie* **1980**, *11*, 29–38. [CrossRef]
33. Dietemann, V.; Nazzi, F.; Martin, S.J.; Anderson, D.L.; Locke, B.; Delaplane, K.S.; Wauquiez, Q.; Tannahill, C.; Frey, E.; Ziegelmann, B.; et al. Standard methods for varroa research. *J. Apic. Res.* **2013**, *52*, 1–54. [CrossRef]
34. Messan, K.; Messan, M.R.; Chen, J.; DeGrandi-Hoffman, G.; Kang, Y. Population dynamics of *Varroa* mite and honeybee: Effects of parasitism with age structure and seasonality. *Ecol. Model.* **2021**, *440*, 109359. [CrossRef]
35. Giacobino, A.; Miotti, C.; Molineri, A.; Orellano, E.; Signorini, M.; Pacini, A. *Varroa destructor* re-invasion dynamics during autumn and winter in *Apis mellifera* colonies from a temperate climate. *J. Invertebr. Pathol.* **2023**, *197*, 107890. [CrossRef]
36. Farkas, Á.; Zajácz, E. Nectar production for the Hungarian honey industry. *Eur. J. Plant Sci. Biotechnol.* **2007**, *1*, 125–151.
37. Peck, D.T.; Seeley, T.D. Mite bombs or robber lures? The roles of drifting and robbing in *Varroa destructor* transmission from collapsing honey bee colonies to their neighbors. *PLoS ONE* **2019**, *14*, e0218392. [CrossRef] [PubMed]
38. Bava, R.; Castagna, F.; Palma, E.; Ceniti, C.; Millea, M.; Lupia, C.; Britti, D.; Musella, V. Prevalence of *Varroa destructor* in honeybee (*Apis mellifera*) farms and varroosis control practices in Southern Italy. *Microorganisms* **2023**, *11*, 1228. [CrossRef]
39. Rosenkranz, P.; Aumeier, P.; Ziegelmann, B. Biology and control of *Varroa destructor*. *J. Invertebr. Pathol.* **2010**, *103*, S96–S119. [CrossRef]
40. Aronstein, K.A.; Saldivar, E.; Vega, R.; Westmiller, S.; Douglas, A.E. How Varroa parasitism affects the immunological and nutritional status of the honey bee, Apis mellifera. *Insects* **2012**, *3*, 601–615. [CrossRef]
41. Klein, B.A.; Busby, M.K. Slumber in a cell: Honeycomb used by honey bees for food, brood, heatin and sleeping. *PeerJ* **2020**, *8*, e9583. [CrossRef]
42. Fermi, E. *Thermodynamics*; Courier Corporation: North Chelmsford, MA, USA, 2012.
43. Lee, J.H.; Ramamurthi, K. *Fundamentals of Thermodynamics*; CRC Press: Boca Raton, FL, USA, 2022.
44. Czekońska, K.; Tofilski, A. Body mass of honey bee drones developing in constant and in changing temperatures. *Apidologie* **2020**, *51*, 510–518. [CrossRef]
45. Kleinhenz, M.; Bujok, B.; Fuchs, S.; Tautz, J. Hot bees in empty broodnest cells: Heating from within. *J. Exp. Biol.* **2003**, *206*, 4217–4231. [CrossRef] [PubMed]
46. Martin, C.; Provost, E.; Bagnères, A.G.; Roux, M.; Clément, J.L.; Le Conte, Y. Potential mechanism for detection by *Apis mellifera* of the parasitic mite *Varroa destructor* inside sealed brood cells. *Physiol. Entomol.* **2002**, *27*, 175–188. [CrossRef]
47. Light, M.; Shutler, D.; Cutler, G.C.; Hillier, N.K. *Varroa destructor* mite electrophysiological responses to honey bee (*Apis mellifera*) colony volatiles. *Exp. Appl. Acarol.* **2020**, *81*, 495–514. [CrossRef] [PubMed]

5. GENERAL DISCUSSION

In the first study, the effects of *V. destructor* on developing *A. mellifera* pupae were investigated using diagnostic computed tomography. Our results demonstrate that diagnostic CT, as a novel non-invasive imaging technique in apicultural research, is suitable for detecting *V. destructor* within sealed *A. mellifera* brood cells. Importantly, the sensitivity of CT-based detection was strongly dependent on both the number, and the developmental stage of the mites present in the cell. This dependency can be explained by the biological characteristics and reproductive cycle of female Varroa mites (Rosenkranz *et al*., 2010; Warner *et al*., 2024).

CT detection proved to be most reliable at advanced developmental stages of the parasite, particularly once the deutonymphal or deutochrysalis stage had acquired its final body shape and size sufficient for radiological identification, with 0.117 × 0.117 × 0.1 mm3 voxel size (Ifantidis, 1983; Donzé and Guerin, 1994; Rosenkranz *et al*., 2010). The improved detectability of mites on the 16th, 18th, and 20th developmental days of *A. mellifera* development can further be attributed to the concealed lifestyle of the foundress mite during earlier stages, as well as to anatomical changes in the host during pupation (Kanbar and Engels, 2003). Developing mite stages were typically located on the ventral side of the pupa, most often near the fifth abdominal segment and in proximity to the faecal accumulation site at the bottom of the brood cell (Kanbar and Engels, 2003; Dietemann *et al*., 2012). As a consequence, parasites positioned ventrally were more difficult to detect than those located dorsally on the abdomen. At present, CT image evaluation requires manual assessment, and detection efficiency is therefore influenced by the experience of the observer. Nevertheless, a consistent pattern emerged: the later the developmental stage at which scanning was performed, the easier it became to identify mites within sealed brood cells.

Beyond confirming previously described effects of *V. destructor* parasitism, the present findings provide novel insights into how parasite-induced damage manifests structurally during pupae development. In both the first and second studies, CT-based measurements demonstrated that parasitism unequivocally affected the anatomical features of developing *A. mellifera* pupae. According to the first CT-assisted investigation, parasitised pupae largely retained their overall volume and surface area, while a significant reduction in body mass was observed. These findings are consistent with previously published data describing weight loss associated with *V. destructor* infestation (Colin *et al*., 1999; van Engelsdorp *et al*., 2007; Facchini *et al*., 2019). Duay *et al*. (2003) provided the first reliable quantitative evidence of individual drone weight loss, particularly from the red-eyed pupal stage onwards, supporting the present observations.

The second study focused on detailed morphological comparisons of major body regions in intact and parasitised *A. mellifera* specimens during pre-imaginal development. Developmental disorders induced by *V. destructor* were clearly confirmed, with the most pronounced alterations observed in the abdominal region (Bowen-Walker and Gunn, 2001). These results corroborate the findings of Facchini *et al*. (2019), who demonstrated that pupae in infested cells were significantly shorter than those in mite-free cells, with this effect depending on mite number, developmental stage, and spatial position within the comb. The observed abdominal deformations are strongly suggestive of infection with DWV, a relationship that has been firmly established by previous experimental studies identifying *V. destructor* as an efficient vector of this virus (Tentcheva *et al*., 2006; McMenamin and Genersch, 2015; Anguiano-Baez *et al*., 2016; Wipfer *et al*., 2016). In the present dissertation, the second study was reinforced by RT-PCR detection of DWV in parasitised specimens, providing molecular confirmation of viral involvement.

The morphological alterations observed in parasitised pupae – particularly abdominal deformation and altered body proportions – strongly support the concept that *V. destructor* acts not merely as a physical parasite, but as a biological amplifier of viral pathogenesis (Morfin *et al*, 2023). The consistent detection of deformed wing virus (DWV) in parasitised specimens by RT-PCR reinforces the interpretation that structural abnormalities arise from the combined effects of mechanical tissue damage, nutrient depletion, and virus-mediated disruption of developmental pathways (Lanzi *et al*., 2006; Locke *et al*., 2016; Traynor *et al*., 2020).

Our findings corroborate earlier CT-based observations demonstrating that pupae developing in infested cells are significantly shorter than those in mite-free cells, with the magnitude of this effect depending on mite number, developmental stage, and spatial position within the comb (Facchini *et al*., 2019). The temporal emergence of these deviations further supports the role of DWV infection acquired during the pupal stage through Varroa feeding behaviour (Francis *et al*., 2013; McMenamin and Genersch, 2015; Wipfer *et al*., 2016).

An unexpected yet biologically informative observation was the relative enlargement of the thoracic region in infected specimens compared to total body size. Rather than representing true hypertrophy, this pattern likely reflects disproportional development caused by constrained growth of the abdomen and head. Virus-induced deformation of thoracic musculature involved in wing movement may further contribute to this phenomenon (Tentcheva *et al*., 2006; Anguiano-Baez *et al*., 2016; Power *et al*., 2021). The parabolic developmental curves identified at later pupal stages emphasize the importance of exposure duration and cumulative damage. Early infestations may initially exert sublethal effects; however, prolonged parasitic feeding combined with escalating viral replication can push developing individuals beyond critical physiological thresholds (Jeyapriya *et al*., 2025). This dynamic interaction helps explain why overt morphological symptoms often appear abruptly at advanced developmental stages rather than progressing linearly over time.

A key contribution of the present work lies in demonstrating that diagnostic CT can function as an integrative tool linking morphological observation with physiological interpretation on a large scale of brood. Traditional approaches to studying Varroa damage rely largely on destructive sampling, mass measurements, or post-emergence assessments, which obscure the temporal sequence of pathological events (Dietemann *et al*., 2013). In contrast, CT imaging enables non-destructive, in situ detection of developmental perturbations before clinical symptoms become apparent.

The reduced radiodensity observed in the first study of infested pupae can be explained by the depletion of high-density organic components such as proteins and carbohydrates, as well as inorganic constituents, most notably water (Amdam *et al*., 2004; Annoscia *et al*., 2012; Ramsey *et al*., 2019; Han *et al*., 2024). Given that water is present in the highest proportion within insect hemolymph (Shaw and Stobbart, 1963), the observed density changes likely reflect haemolymph depletion and metabolic disruption induced by parasitism. Although direct chemical tissue analyses were beyond the scope of the present study, these structural signatures are consistent with previously described physiological effects of Varroa infestation (Bowen-Walker and Gunn, 2001; Han et al., 2024). Collectively, these findings position diagnostic CT as a powerful complementary approach in Varroa research. By capturing spatially explicit patterns of internal tissue alteration of pupae across defined developmental times, CT-based analysis bridges the gap between morphology and physiology and provides a foundation for integrating imaging data with molecular diagnostics and colony-level health assessments.

Based on the first two studies, human diagnostic computed tomography proved suitable for detecting *V. destructor* within sealed brood cells and for characterizing parasite-associated morphological and tissue alterations in developing pupae. However, to analyse the fine internal architecture of brood cells and pupae anatomy, the spatial resolution of clinical CT becomes a limiting factor. In this context, micro-computed tomography represents a critical methodological extension, enabling high-resolution, three-dimensional visualization and quantitative assessment of brood cell microstructure, and *A. mellifera* anatomy (Bader *et al*., 2022; De Paula *et al*., 2022).

The third study focused on using CT-based imaging, to analyse structural differences in the brood cells and developing pupae. Micro-CT imaging allowed these processes to be examined at an 8.75 µm voxel size level. The findings of the study are consistent with earlier studies demonstrating that repeated usage of combs for years leads to progressive alterations in cell geometry, including reductions in inner volume and diameter, which negatively affect preimaginal development (Berry and Delaplane, 2001; Al-Kahtani and Taha, 2021). As brood generations are reared, cell walls and bottoms gradually darken and become more brittle, a phenomenon previously attributed to comb aging (Hepburn, 1998). The wall thickening can be attributed to the accumulation of organic residues originating from larval metabolism and colony activity, including honey, pollen, propolis, faeces, silken cocoons and pellicle layers (Free and Williams, 1974; Taha *et al.*, 2010). The progressive deposition of these materials results in measurable reductions in brood cell volume and diameter, effects that had previously been inferred indirectly, but are here directly visualised and quantified using μ-CT (Taha and Al-Kahtani, 2021). Previous studies have shown that comb age has profound effects on colony performance (Taha and Al-Kahtani, 2020). Colonies maintained on younger combs produce larger brood areas, heavier emerging workers, and stronger populations, whereas old combs are associated with reduced colony strength and honey yield (Berry and Delaplane, 2001; Taha and El-Sanat, 2007; Al-Kahtani, 2018; Shawer *et al.*, 2021). Interestingly, brood survival has occasionally been reported to be higher in old combs, highlighting the complex trade-offs between structural degradation and colony-level adaptation (Berry and Delaplane, 2001).

Importantly, the present study represents, to our knowledge, the first application of micro-CT for the quantitative analysis of *A. mellifera* brood cells and pupae, and the first to directly calibrate micro-CT data with human diagnostic CT images obtained from the same biological system. From an applied perspective, the combined use of diagnostic CT and micro-CT strongly reinforces the necessity of regular comb replacement in beekeeping practice (Meng *et al.*, 2025). By revealing how structural degradation accumulates within brood cells and constrains larval and pupal development. Micro-CT imaging technique provide objective, quantitative support for management recommendations that were previously based largely on indirect observations and destructive measurements (Al-Kahtani and Taha, 2021). Moreover, this integrative imaging framework establishes a foundation for future studies investigating how comb microarchitecture influences *V. destructor* reproduction, and colony health (Maggi *et al*., 2010).

Ionizing radiation represents a methodological paradox in experimental studies of the *V. destructor-A. mellifera* system. On one hand, ionizing radiation provides a unique physical tool capable of penetrating complex biological structures and enabling non-destructive internal visualization of intact organisms, forming the physical basis of CT and micro-CT imaging (Fazel *et al*., 2009). On the other hand, ionizing radiation itself constitutes a potent abiotic stressor, with well-documented cytological, physiological and immunological consequences (Newcombe, 1971; Yamada *et al*., 2022). Consequently, any interpretation of CT- or micro-CT-based observations must explicitly consider the biological effects induced by irradiation and define the limits within which imaging remains biologically interpretable.

The fourth study of this dissertation demonstrates that X-ray irradiation induces clear dose- and time-dependent mortality in both the host, *A. mellifera*, and its parasite, *V. destructor*, although with markedly different sensitivities. At higher dose levels (≥50 Gy), mortality of adult worker bees approached 100% within 18 days post-irradiation, while *V. destructor* mortality reached approximately 90% over the same period. These results indicate that irradiation at such dose levels cannot be considered selectively detrimental to the parasite without causing severe and ultimately lethal effects on the host (Richardson and Myser, 1973; Matthes *et al*., 1991). This finding is consistent with earlier studies reporting relatively low radiation tolerance in *A. mellifera* compared to many other insect taxa, likely reflecting the vulnerability of complex multicellular systems to cumulative DNA damage and oxidative stress (Richardson and Myser, 1973; Matthes *et al*., 1991; De Guzman *et al*., 2019).

At the lowest tested dose (15 Gy), *V. destructor* exhibited higher relative sensitivity than its host, resulting in a moderate reduction in mite survival while most irradiated worker bees remained viable. Although this effect is far below the threshold required for practical Varroa control, it provides an important methodological insight (Rosenkranz *et al*., 2010; Warner *et al*., 2024). Specifically, it demonstrates that even sublethal irradiation can elicit measurable biological responses in both organisms, underscoring the necessity of carefully defining biologically relevant exposure limits in imaging-based studies (Tilton and Brower, 1983). Importantly, the dose levels applied in diagnostic CT imaging are orders of magnitude lower than those inducing mortality or overt physiological disruption in this experiment, supporting the suitability of these techniques for non-invasive research when applied within appropriate parameters (Kalender, 2014). The potential applications of micro-CT in entomology, including apicultural research, must be approached with careful dose optimization, as radiation exposure can reach several grays under high-resolution scanning conditions (*e.g*. ~5 Gy at 65 µm resolution), depending on the imaging protocol (Clark and Badea, 2014, 2021). Beyond survival effects, X-ray irradiation induced pronounced alterations in the hemolymph immune cell composition of adult worker bees. The observed increase in plasmatocyte and granulocyte proportions, accompanied by a reduction in prohemocytes, is indicative of immune activation and stress-induced shifts in hemocyte differentiation dynamics (Christensen *et al*., 1990; Ling *et al*., 2006).

The irradiation experiments were conducted on adult workers, whereas CT-based imaging focused on pre-imaginal stages. While developmental stage-specific radiation tolerance has been suggested in insect models, the present work does not aim to extrapolate radiobiological thresholds across life stages (Paithankar *et al*., 2017). Instead, the irradiation study serves to define upper biological response limits, whereas diagnostic CT imaging operates several orders of magnitude below these thresholds. Taken together, the irradiation study provides a critical validation framework for the CT imaging-based approaches. By defining dose-dependent biological response thresholds in both host and parasite, it establishes clear boundaries between diagnostically relevant radiation exposure and biologically disruptive irradiation. This distinction is essential for interpreting CT and micro-CT-derived observations with confidence and for integrating structural imaging into a broader, biologically informed framework of bee health research, focusing on *V. destructor* and *A. mellifera* complex.

The final experiment of the dissertation extends the imaging-based investigation of the *V. destructor- A. mellifera* system from structural to functional physiology by introducing infrared thermography as a tool to assess colony-level responses to parasitism under *in vivo* conditions (Bauer *et al.*, 2018). While CT and micro-CT provided detailed insight into the hidden spatial organization of brood cells and parasite-host interactions, infrared imaging uniquely captures the dynamic physiological responses of the superorganism, revealing how colonies actively respond to biotic stress (Bauer *et al.*, 2018; Gobrisch *et al.*, 2020). Based on research by Bauer *et al.* (2018), temperatures 0.1-0.19 °C higher were measured in capped brood cells infected with *V. destructor*. A key conceptual advance of this work is the first *in situ*, field demonstration of elevated capping surface temperature associated with Varroa parasitism. Higher temperatures detected consistently over Varroa-infested brood cells cannot be attributed to only passive thermal effects of the parasite or to the increased metabolism of the developing pupae. Instead, the spatially structured heating patterns manifesting either as localised hotspot heating or as heating cells adjacent to parasitised brood that strongly indicate active, worker-mediated thermoregulation targeted at infected individuals (Bujok *et al.*, 2002; Kleinhenz *et al.*, 2003; Klein *et al.*, 2014; Klein and Busby, 2020). This supports the interpretation of social fever as a form of collective immune defence as Starks *et al.* (2000) described first in the case of *Ascosphaera apis* infection, complementing previously described hygienic and grooming behaviours (Seeley, 2009, 2019). Previous studies have demonstrated that even small deviations from optimal brood temperature can profoundly affect *A. mellifera* development, immune competence, and neural function, while simultaneously imposing physiological stress on parasites (Groh *et al.*, 2004; Kovac és mtsai., 2014; Norrström és mtsai., 2022). The sustained elevation detected in this study is therefore likely sufficient to shift the thermal environment away from the optimum for Varroa reproduction, while remaining within the tolerance limits of the host brood (Aldea-Sánchez *et al.*, 2021; Porporato *et al.*, 2022; Xu *et al.*, 2025).

A particularly informative finding is the relationship between mite load and temperature variance. Cells with higher numbers of mites exhibited narrower temperature confidence intervals and more consistent heating responses, suggesting improved detectability by workers and stronger collective responses. In contrast, low-level infestations showed greater thermal variability, likely reflecting early-stage parasitism that has not yet triggered a full colony-level response. This mirrors patterns known from hygienic behaviour, where detection efficiency increases with the parasite numbers in a single cell, and supports the hypothesis that thermal cues form part of a multimodal detection system involving chemical, mechanical, and thermal signals (Bauer *et al*., 2018; Kim *et al*., 2018; Spivak and Danka, 2021; Piou *et al*., 2023).

From a methodological perspective, infrared thermography complements CT-based approaches by offering a truly non-invasive, field-applicable diagnostic measurement. Unlike X-ray-based techniques, infrared imaging introduces no ionizing radiation and therefore avoids the confounding physiological effects demonstrated in the irradiation experiments. The ability to detect Varroa-associated physiological changes without disturbing brood structure or colony integrity represents a significant advance for both research and applied apiculture. Crucially, the integration of infrared thermography with structural imaging techniques establishes a multi-scale diagnostic framework. CT and micro-CT reveal the location of the parasites and how they alter brood development, while infrared imaging reveals how the colony responds in real time for a biotic stressor. Beyond its immediate research applications, this work highlights the potential of infrared thermography as a practical and scalable tool for beekeeping (Stabentheiner *et al*., 2003; Bauer *et al*., 2018). The sensitivity of the thermal camera applied in this study is comparable to that of modern, commercially available smartphone-based thermal sensors, which are increasingly accessible to beekeepers and researchers alike. Smartphone-based thermal imaging has already been widely adopted in human medicine and veterinary diagnostics for the non-invasive detection of inflammatory processes, circulatory disturbances and localised physiological stress (van Dooremalen *et al*., 2019; Coe and Blackie, 2021). These established applications underscore the robustness and diagnostic relevance of low-cost infrared technologies, supporting their potential transfer to apicultural contexts. The method holds promise for scalable, non-invasive monitoring of Varroa infestation and for supporting selection programs targeting traits such as VSH SMR (Mondet *et al*., 2020). However, the successful deployment of this approach will require the development of AI-based image analysis software capable of learning colony-specific thermal patterns and accounting for seasonal variation, particularly during summer periods dominated by active cooling.

In summary, the infrared thermography study completes the conceptual arc of the dissertation by demonstrating that Varroa parasitism can be detected not only structurally and morphologically, but also functionally at the level of collective physiology. The identification of eusocial fever *in situ* underscores the importance of considering the colony as a thermoregulatory superorganism whose immune responses extend beyond individual-level mechanisms. This insight opens new avenues for understanding host-parasite coevolution and for developing innovative, non-invasive diagnostic strategies in bee health research.

6. CONCLUSIONS AND RECOMMENDATIONS

This dissertation demonstrates that advanced imaging technologies provide fundamentally new perspectives for understanding the complex host-parasite interactions between *A. mellifera* and *V. destructor*. By integrating diagnostic computed tomography, micro-computed tomography, controlled irradiation experiments, and infrared thermography, the present work establishes a multiscale, non-invasive framework that links structural, physiological, and collective-level responses of the *A. mellifera* colony to Varroa parasitism.

The results confirm that human diagnostic CT is a suitable and biologically interpretable tool for the *in situ* detection of *V. destructor* within sealed brood cells and for monitoring parasite associated morphological and tissue-level alterations during pupal development. CT-based imaging revealed that Varroa parasitism induces pronounced structural changes prior to adult emergence, including reduced radiodensity and altered body proportions. These findings position diagnostic CT as a powerful complementary method to traditional destructive sampling approaches in apicultural research.

Micro-computed tomography extended this framework by resolving the fine internal architecture of brood cells and pupae at micrometer-scale resolution. The quantitative visualization of comb aging, wall thickening, and reductions in brood cell volume provides direct structural evidence for long-standing hypotheses regarding the biological consequences of prolonged comb use. The combined calibration of diagnostic CT and micro-CT imaging represents a methodological novelty, allowing structural information to be interpreted across spatial scales from colony-level screening to fine-scale anatomical detail. From an applied perspective, these results offer robust, quantitative support for the practice of regular comb replacement as a key element of sustainable colony management.

The irradiation experiments clarified the biological boundaries within which X-ray-based imaging remains methodologically valid for bee health studies. By demonstrating clear dose- and time-dependent responses in both *A. mellifera* and their ectoparasite, the study establishes that while high radiation doses are biologically disruptive, the exposure levels associated with diagnostic CT imaging remain well below thresholds that induce mortality or severe physiological impairment. These findings underscore the importance of dose optimization for living insects, particularly in high-resolution micro-CT applications, and provide a critical validation framework for the responsible use of ionizing radiation in entomological research.

The introduction of infrared thermography represents a conceptual expansion of imaging-based Varroa research from static structural analysis to dynamic functional assessment. The *in situ* detection of elevated temperatures above Varroa-infested brood cells provides the first field-based evidence for social fever as an active colony-level defence response against this parasite. This finding highlights the colony as a thermoregulatory superorganism whose immune defences extend beyond individual-level mechanisms. Infrared thermography thus emerges as a truly non-invasive, field-applicable tool with significant potential for both research and practical diagnostics.

Taken together, the dissertation establishes that Varroa parasitism can be detected and interpreted across multiple biological levels: structurally within brood cells, physiologically within developing individuals, and functionally at the level of collective colony responses. This integrative approach advances current understanding of *V. destructor* and *A. mellifera* interactions and provides a methodological blueprint for future studies aiming to bridge imaging, molecular diagnostics, and colony health assessment.

Future research should focus on integrating these imaging modalities with molecular and immunological markers to further elucidate the causal links between structural alterations, pathogen dynamics, and colony-level resilience. The development of automated, AI-based image analysis pipelines will be essential for translating CT and infrared thermography into scalable diagnostic tools suitable for large-scale monitoring and selective breeding programs. In particular, infrared thermography holds promise for supporting selection for Varroa-tolerant traits such as Varroa-sensitive hygiene and suppressed mite reproduction under field conditions.

More broadly, the imaging framework presented here has relevance beyond Varroa research. It offers a generalizable model for studying hidden biological processes in eusocial insects and highlights the potential of non-invasive imaging technologies to transform both fundamental research and applied apiculture. By combining methodological rigor with biological interpretability, this work contributes to the development of innovative, evidence-based strategies for improving bee health in the face of ongoing abiotic of biotic stressors.

7. NEW SCIENTIFIC RESULTS

The scientific outcomes presented herein are derived from five distinct studies conducted during this doctoral dissertation:

1. We were the first to demonstrate the applicability of human diagnostic computed tomography (CT) for the *in-situ* detection of *Varroa destructor* within *Apis mellifera* sealed brood cells.
2. Using non-invasive imaging techniques, we were the first to document developmental abnormalities and tissue composition alterations in the preimaginal stages of honey bees, with the mean density change of infested pupae reaching 1.657 HU (1.481%) ($p=0.001$).
3. The dissertation presents the first quantitative micro-CT analysis of intact *Apis mellifera* brood cells and pupae, providing direct structural evidence that comb aging, wall thickening, and reduced cell volume for larval and pupal development (-12.22% in volume ($p<0\ 0.05$)).
4. Dose- and time-dependent high energy X-ray irradiation experiments define biological response thresholds in both *Apis mellifera* and *Varroa destructor* (effect of X-ray on mortality of examined organisms $p<0\ 0.001$). The results provide the first evidence in *Apis mellifera* that ionizing radiation induces dose-dependent shifts in plasmatocyte ($p<0.001$) and prohemocyte counts ($p<0.001$).
5. This work delivers the first *in situ*, field-based demonstration that *A. mellifera* colonies exhibit localised temperature elevation of Varroa-infested brood cells (+0.79 °C), confirming social fever as an active, collective immune defense mechanism ($p=0.001$).

8. SUMMARY

The first study aimed to evaluate the applicability of human diagnostic computed tomography (CT) for the non-invasive detection of *Varroa destructor* within sealed *Apis mellifera* brood cells. Developing *A. mellifera* pupae were examined at different stages of pre-imaginal development (days 14, 16, 18, and 20). CT datasets were used to assess the presence, number, spatial position of mites, and parasite-associated anatomical alterations. The results confirmed that diagnostic CT is suitable for detecting *V. destructor* within sealed brood, although detection sensitivity strongly depended on mite number and developmental stage. Detection was most successful on days 18 and 20, due to the number of the mites in the cells and the developing mite size (deutocrystalis stage) exceeded the resolution threshold of clinical CT. Mites were most frequently located on the ventral side of the abdomen, near the fifth abdominal segment and the faecal accumulation zone. Parasitised pupae exhibited reduced radiodensity and altered body proportions, while no significant differences in external body volume were detected. In contrast, dissections performed on day 20 revealed an average body mass reduction of 16.6 mg in parasitised individuals. These findings demonstrate that diagnostic CT represents an effective complementary tool for studying the spatial and temporal dynamics of the *V. destructor* and *A. mellifera* interaction without destructive sampling.

The second study performed detailed CT-based morphometric analyses of intact and *V. destructor*-parasitised *A. mellifera* pupae at days 14, 16, 18, and 20 of development. In parallel, molecular detection of deformed wing virus (DWV) was conducted. Morphometric comparisons included multiple body region ratios involving the head, thorax, abdomen, and total body length. Non-invasive CT imaging revealed progressively developing morphological abnormalities that became most pronounced at days 18 and 20. Parasitised individuals showed marked changes in body proportions, including reduced head-to-abdomen (-6,86%) and abdomen-to-body length ratios (-3,77%), while relative thorax size increased (+3,33%). These alterations were consistent with known DWV-associated phenotypes and were confirmed by RT-PCR detection. The time-dependent progression of abnormalities indicates that mite feeding and viral replication act cumulatively, supporting the interpretation that *V. destructor* functions not only as a physical parasite but also as a biological amplifier of viral pathogenesis. The results explain the frequently observed threshold-like, non-linear developmental damage associated with Varroa-DWV interactions.

The third study evaluated the applicability of micro-computed tomography (micro-CT) for high-resolution structural analysis of sealed brood cells and developing pupae of *A. mellifera*.

Micro-CT enabled quantitative, micrometer-scale visualization of internal cell architecture previously accessible only through destructive methods. The study demonstrated that prolonged comb use results in progressive wall thickening and a significant reduction in brood cell volume (-35.41%), driven by the accumulation of metabolic residues, silk layers, and organic deposits. Reduced cell volume imposed direct physical constraints on developing pupae, leading to decreased body size (-12.22%) and altered body proportions. This study represents the first direct calibration of human diagnostic CT and micro-CT within the same biological system, linking microstructural changes at the cell level with colony-level consequences. The findings provide strong quantitative evidence supporting regular comb replacement as a biologically justified management practice.

The fourth study investigated the biological effects of ionizing X-ray radiation on adult *A. mellifera* workers and phoretic *V. destructor* mites. The experiments aimed to define biologically safe exposure limits for X-ray-based imaging and to evaluate radiation as a potential alternative mite control strategy. Clear dose- and time-dependent mortality was observed in both host and parasite. High doses (50, 100, 150 Gy) resulted in complete worker mortality by day 18, while lower doses (15 Gy) revealed relatively higher sensitivity in *V. destructor* compared to the host. Hemolymph analyses showed significant radiation-induced shifts in immune cell composition, characterised by increased proportions of plasmatocytes and granulocytes and reduced prohemocyte abundance. This study provides the first hemolymph-level immunological assessment of X-ray exposure in *A. mellifera* and establishes reference values for safe radiation doses applicable in CT and micro-CT studies.

The fifth study introduced infrared thermography as a tool for assessing colony-level physiological responses to *V. destructor* infestation under field conditions. Using a portable thermal camera, consistently elevated surface temperatures were detected above *V. destructor* infested sealed brood cells capping. Spatially structured heating patterns hot spot heating, and heating cell indicate that temperature elevation represents an active, worker-mediated response rather than a passive consequence of parasitism. This study provides the first *in situ* field evidence of social fever associated with *V. destructor* infestation. Elevated temperatures likely create suboptimal conditions for mite reproduction while remaining within host tolerance limits. Infrared thermography thus emerges as a truly non-invasive, radiation-free, field-applicable method with significant potential for Varroa diagnostics and the selection of tolerant *A. mellifera* colonies.

9. ÖSSZEFOGLALÁS

Az első vizsgálat célja a humán diagnosztikai komputertomográfia (CT) alkalmazhatóságának értékelése volt, a *Varroa destructor* nem invazív kimutatása céljából, fedett *Apis mellifera* fiasításban. A fejlődő méhbábok különböző fejlődési időpontokban kerültek vizsgálatra, az egyedfejlődésük 14, 16, 18, 20 napján. Az eltérő időben készített CT-felvételek alapján értékeltük az atkák jelenlétét, számát, térbeli elhelyezkedését, valamint a parazitáltsághoz köthető fejlődő bábokon érzékelhető anatómiai elváltozásokat.

Az eredmények igazolták, hogy a diagnosztikai CT alkalmas a *V. destructor* kimutatására a fedett fiasításban, azonban az érzékenység nagymértékben függ az atkák számától és fejlődési stádiumától. Az atkák kimutatása a lépsejtek belül az egyedfejlődés 18 és 20. napján volt a legeredményesebb, amikor a fejlődő nőstény atkák mérete elérte a diagnosztikai CT érzékenységi szintjét. A felvételeken látható atkák leggyakrabban a báb potrohának hasi oldalán, az ötödik potrohszelvény környezetében és a bélsár-akkumulációs zóna közelében helyezkedtek el.

A parazitált bábok esetében a megfigyelhet csökkent radiodenzitás és megváltozott testtömeg voltak statisztikailag igazolható eltérések, miközben a testtérfogat és felszín esetében a parazitizmus függvényében mérhető statisztikai eltérés nem volt kimutatható. Az egyedfejlődés 20. napján végzett lépsejt boncolás során, a parazitált egyedek testtömege átlagosan 16,6 mg-al volt kevesebb az intakt egyedekhez viszonyítva. A vizsgálat eredményei megerősítik, hogy a diagnosztikai CT hatékony kiegészítő eszköz lehet a Varroa-méh kapcsolat időbeli és térbeli dinamikájának vizsgálatában, különösen nagyszámú minta destruktív feldolgozása nélkül.

A második vizsgálat során részletes humán diagnsoztikai CT alapú morfometriai elemzést végeztünk ép és parazitált méhbábokon, az egyedfejlődés 14, 16, 18, és 20. napján. A vizsgált egyedek tekintetében a deformált szárny vírus (DWV) molekuláris kimutatását is elvégeztük. A fő testtájak több eltérő időpontban a 14, 16, 18 és 20. napon és módon kerültek összehasonlításra: fej, tor és potroh hossz, fej-tor, fej-potroh, fej-teljes testhossz, tor-teljes testhossz, potroh-teljes testhossz.

A CT által biztosított non-invazív felvételezési mód, az egyedfejlődés során folyamatosan kialakuló fejlődési rendellenességeket támasztotta alá, melyek a 18. és a 20. napon fejeződtek ki leginkább. A parazitált egyedeknél markáns testarány-változások jelentkeztek, elsősorban fej-potroh (-6,86%) és a potroh-teljes testhossz csökkenése (-3,77%) volt megfigyelhető, miközben a tor relatív mérete megnövekedett (+3,33%). Ezek a morfológiai eltérések összhangban állnak a DWV fertőzés ismert tüneteivel, amit RT-PCR vizsgálatokkal is megerősítettünk.

Az eltérések időben fokozódó jellege arra utal, hogy az atka táplálkozása és a vírus replikációja kumulatív módon károsítja a fejlődő egyedeket. Az eredmények alátámasztják, hogy a *V. destructor* nem pusztán ektoparazita, hanem az immunszupresszív hatásának okán a vírus patogenezis „biológiai katalizátora". A parazita által kiváltott táplálkozási stressz és immunszuppresszió, lehetővé teszi a vírus gyors replikációját, amely a fejlődés késői szakaszában hirtelen megjelenő, súlyos morfológiai elváltozásokhoz vezet.

A harmadik tanulmány a micro-CT alkalmazhatóságát vizsgálta az *A. mellifera* fedett fiasításos lépsejtjeinek és a fejlődő bábjainak nagyfelbontású szerkezeti elemzésére. A micro-CT lehetővé tette a lépsejtek belső struktúrájának mikrométeres pontosságú kvantitatív vizsgálatát, amely korábban csak destruktív módszerekkel volt elérhető.
A vizsgálat kimutatta, hogy az évekig használt lépekben a sejtfalak és sejtfelületek fokozatosan megvastagodnak, a sejttérfogat pedig szignifikánsan csökkent (-35,41%). Ezek a változások szoros kapcsolatban állnak a lárvák anyagcseretermékeinek, bábing, ürülékének és egyéb szerves maradványainak akkumulációjával. A csökkent sejttérfogat közvetlen fizikai korlátozást jelent a fejlődő bábok számára, ami testméret csökkenést (-12,22%) és testarány változást eredményezett. Az elhasználódott, beszűkült sejtek hosszú távon a kolónia teljesítményének romlásához, és a család népességének csökkenéséhez, a dolgozók méretének törpüléséhez vezethet.
A tanulmány újdonsága, hogy elsőként történt meg a humán diagnosztikai CT és a micro-CT adatok közvetlen kalibrálása ugyanazon biológiai rendszerben. Ez lehetővé tette a lépsejt-szintű mikrostruktúrák és a kolónia-szintű folyamatok összekapcsolását, és erős, kvantitatív bizonyítékot szolgáltatott a rendszeres lépcsere biológiai indokoltságára.

A negyedik vizsgálat az ionizáló Röntgen-sugárzás biológiai hatásait elemezte felnőtt *A. mellifera* dolgozókon és a foretikus nőstény *V. destructor* egyedeken. A kísérlet célja kettős volt: egyrészt a röntgenalapú képalkotás biológiai biztonságának meghatározása, másrészt a sugárzás, mint lehetséges alternatív atka gyérítő módszer értékelése.
Az eredmények egyértelmű dózis- és időfüggő mortalitást mutattak mind a gazdaszervezet, mind a parazita esetében. Magas dózisok (50, 100, 150 Gy) mellett a gazda szerezet a kísérlet 18. napra teljes mortalitást mutattak, míg az alacsonyabb dózisnál (15 Gy) melyre a *V. desturctor* nagyobb érzékenységet mutatott, mint a gazdaszervezet. A differenciált hemocita vizsgálatok kimutatták, hogy a Röntgen-sugárzás jelentősen módosítja az immunsejtek összetételét: nőtt a plazmatociták és granulociták aránya, miközben csökkent a prohemociták száma. A Duncan post-hoc teszt kimutatta, hogy a hemolimfa arányok jól elkülöníthetők az alacsony dózis, már akár a kontroll csoporttól is.

Ez a tanulmány az *A. mellifera* esetében elsőként dokumentálta a Röntgen-sugárzás differenciált hemocita számra gyakorolt hatásait, és alapvető referenciaértékeket szolgáltatott a CT- és micro-CT-vizsgálatok során alkalmazható biztonságos dózistartományok meghatározásához. Emellett a tanulmány először vizsgálta a gazda-parazita nagy energiájú Röntgen-sugár tűrőképességét. Mindamellett kiemelendő, hogy a kívánt aktagyérítő hatást a kísérletek nem érték el.

Az ötödik vizsgálat az infravörös termográfia alkalmazását elemzi terepi körülmények között, a *V. destructorral* parazitált fiasítás kolónia-szintű élettani válaszainak vizsgálatára. A mérések során hordozható kézi hőkamerával sikerült kimutatni, hogy a parazitált lépsejtek felszíni hőmérséklete tartósan magasabb, az intakt szomszédos sejtek értékeihez képest.

A térben strukturált melegedési mintázatok a károsított lépsejtek esetében arra utalnak, hogy a hőmérséklet-emelkedés nem passzív jelenség. A család hőháztartásában fontos szerepet játszó mintázatok ismerhetők fel a hőképeken, így a dolgozó méhek által kiváltott aktív válasz feltételezhető. Ez a megfigyelés az első *in situ*, terepi bizonyítéka az ún. szociális láz jelenségének *V. destructor* parazitizmus esetén. A hőmérséklet-emelkedés valószínűsíthetően kedvezőtlen feltételeket teremt az atka szaporodása számára, miközben a méhbábok toleranciahatárán belül marad, viszont ezen megállapítások jobb megértéséhez további vizsgálatok szükségesek.

A vizsgálat rávilágított arra, hogy az infravörös termográfia valóban non-invazív, káros sugárzásoktól mentes és terepen is alkalmazható módszer, amely új távlatokat nyithat a *V. destructor* vizsgálatában akár az atka toleráns méhcsaládok szelekciójában.

10. REFERENCES

Abou-Shaara, H. F., Owayss, A. A., Ibrahim, Y. Y., & Basuny, N. K. (2017). A review of impacts of temperature and relative humidity on various activities of honey bees. Insectes Sociaux, 64(4), 455-463.

Akimov, I. A., Benedyk, S. V., & Zaloznaya, L. M. (2004). Complex analysis of morphological characters of Gamasid mite *Varroa destructor* (Parasitiformes, Varroidae). Vestnik zoologii, 38(5), 57-66,

Alba-Alejandre, I., Alba-Tercedor, J., & Vega, F. E. (2019). Anatomical study of the coffee berry borer (*Hypothenemus hampei*) using micro-computed tomography. Scientific Reports, 9(1), 1-16.

Alba-Tercedor, J., & Alba-Alejandre, I. (2017). Comparing micro-CT results of insects with classical anatomical studies: The European honey bee (*Apis mellifera* Linnaeus, 1758) as a benchmark (Insecta: Hymenoptera, Apidae). In Bruker Micro-CT Users Meeting, June 11-15, 2017 (Brussels, Belgium) (pp. 147-167).

Alberti, G., & Zeck-Kapp, G. (1986). The nutrimentary egg development of the mite, *Varroa jacobsoni* (Acari, Arachnida), an ectoparasite of honey bees. Acta Zoologica, 67(1), 11-25.

Aldea-Sánchez, P., Ramírez-Cáceres, G. E., Rezende, E. L., & Bozinovic, F. (2021). Heat tolerance, energetics, and thermal treatments of honeybees parasitized with Varroa. Frontiers in Ecology and Evolution, 9, 656504.

Alghamdi, A. A., & Alattal, Y. Z. (2023). Expression levels of heat-shock proteins in *Apis mellifera jemenetica* and *Apis mellifera carnica* foragers in the desert climate of Saudi Arabia. Insects, 14(5), 432.

AL-Kahtani, S. N. (2018). Morphometric characteristics of carniolan honeybee workers in relation to age of comb. Scientific Journal of King Faisal University (Basic and Applied Sciences), 19(2), 1440H.

AL-Kahtani, S. N. (2018). Morphometric characteristics of carniolan honeybee workers in relation to age of comb. Scientific Journal of King Faisal University (Basic and Applied Sciences), 19(2), 1440H.

Al-Kahtani, S. N., & Taha, E. K. A. (2021). Effect of comb age on cell measurements and worker body size. PLoS One, 16(12), e0260865.

Allen, M. F. & Ball, B. V. (1995). Characterisation and serological relationships of strains of Kashmir bee virus. Annals of Applied Biology, 126(3), 471-484.

Alves, T. S., Pinto, M. A., Ventura, P., Neves, C. J., Biron, D. G., Junior, A. C., Pedro, L., de Paula, F., & Rodrigues, P. J. (2020). Automatic detection and classification of honey bee comb cells using deep learning. Computers and Electronics in Agriculture, 170(1), 105244.

Amdam, G.V., Hartfelder, K., Norberg, K., Hagen, A., Omholt, S.W., (2004). Altered physiology in worker honey bees (Hymenoptera: Apidae) infested with the mite *Varroa destructor* (Acari: Varroidae): a factor in colony loss during overwintering? Journal of Economic Entomology 97 (3), 741-747.

Amiri, E., Strand, M. K., Tarpy, D. R., & Rueppell, O. (2020). Honey bee queens and virus infections. Viruses, 12(3), 322.

Anderson, D.L., (1994). Non-reproduction of *Varroa jacobsoni* in *Apis mellifera* colonies in Papua New Guinea and Indonesia. Apidologie 25(4), 412-421

Anderson, D.L., Trueman, J.W.H., (2000). *Varroa jacobsoni* (Acari: Varroidae) is more than one species. Experimental and Applied Acarology 24, 165-189.

Anguiano-Baez, R.; Guzman-Novoa, E.; Hamiduzzaman, M.M.; Espinosa-Montaño, L.G.; Correa-Benítez, (2016) A. *Varroa destructor* (Mesostigmata: Varroidae) parasitism and climate differentially influence the prevalence, levels and overt infections of deformed wing virus in honey bees (Hymenoptera: Apidae). Journal of Insect Science 16, 44.

Annoscia, D., Del Piccolo, F., & Nazzi, F. (2012). How does the mite *Varroa destructor* kill the honeybee *Apis mellifera*? Alteration of cuticular hydrcarbons and water loss in infested honeybees. Journal of Insect Physiology, 58(12), 1548-1555.

Astuti, P. K., Hegedűs, B., Oleksa, A., Bagi, Z., & Kusza, S. (2024). Buzzing with intelligence: Current issues in apiculture and the role of artificial intelligence (AI) to tackle it. Insects, 15(6), 418.

Bader, C., Costa, J., Lee, N., Smith, R., Ri, R., Weaver, J. C., & Oxman, N. (2022). Computational methods for the characterization of *Apis mellifera* comb architecture. Communications Biology, 5(1), 468.

Bai, W. F., Lin, Z. G., Yan, W. Y., Zhang, L. Z., Evans, J. D., & Huang, Q. (2021). Haplotype Analysis of *Varroa destructor* and Deformed Wing Virus Using Long Reads. Frontiers in Insect Science, 1, 756886.

Batz, P., Ruttor, A., Thiel, S., Wegener, J., Zautke, F., Schwekendiek, C., & Bienefeld, K. (2022). Semi-automatic detection of honeybee brood hygiene – an example of artificial learning to facilitate ethological studies on social insects. Biology Methods and Protocols, 7(1), bpac005.

Bauer, D., Wegener, J., & Bienefeld, K. (2018). Recognition of mite-infested brood by honeybee (*Apis mellifera*) workers may involve thermal sensing. Journal of Thermal Biology, 74, 311-316.

Becher, M. A., Hildenbrandt, H., Hemelrijk, C. K., & Moritz, R. F. (2010). Brood temperature, task division and colony survival in honeybees: A model. Ecological Modelling, 221(5), 769-776.

Bell, G. D., Corps, N., Mortimer, D., Gretton, S., & Bury, N. R. (2023a). Visualising fat reserves in an insect: A method using X-ray micro-computerised tomography of the Common Wasp (*Vespula vulgaris*). Zoology, 158, 126092.

Bell, G. D., Corps, N., Mortimer, D., Gretton, S., Bury, N., & Connett, G. J. (2023b). The tracheal system of the Common Wasp (*Vespula vulgaris*)-A micro-CT study. Journal of Insect Physiology, 149, 104547.

Belsky, J., & Joshi, N. K. (2019). Impact of biotic and abiotic stressors on managed and feral bees. Insects, 10(8), 233.

Berényi, O.; Bakonyi, T.; Derakhshifar, I.; Köglberger, H.; Nowotny, N. (2006) Occurrence of Six Honeybee Viruses in Diseased Austrian Apiaries. Applied Environmental Microbiology 72, 2414-2420.

Berkaya, S. K., Gunal, E. S., & Gunal, S. (2021). Deep learning-based classification models for beehive monitoring. Ecological Informatics, 64, 101353.

Berry, J. A., & Delaplane, K. S. (2001). Effects of comb age on honey bee colony growth and brood survivorship. Journal of Apicultural Research, 40(1), 3-8.

Bianchi, E. M., Ferrari, C., Aguirre, N. C., Filippi, C. V., Vera, P. A., Puebla, A. F., Gennari, P. G., Rodriguez, A. G., Scannapieco, C., A., Acuña, V. C., & Lanzavecchia, S. B. (2023). Phenotypic and genetic characterization of Africanized *Apis mellifera* colonies with natural tolerance to *Varroa destructor* and contrasting defensive behaviour. Frontiers in Insect Science, 3, 1175760.

Bloch, G., Toma, D. P., & Robinson, G. E. (2001). Behavioural rhythmicity, age, division of labor and period expression in the honey bee brain. Journal of Biological Rhythms, 16(5), 444-456.

Boecking, O., & Genersch, E. (2008). Varroosis-the ongoing crisis in bee keeping. Journal of Consumer Protection and Food Safety, 3(2), 221-228.

Boecking, O., & Spivak, M. (1999). Behavioural defenses of honey bees against *Varroa jacobsoni* Oud. Apidologie, 30(2-3), 141-158.

Boot, W. J., Calis, J. N., & Beetsma, J. (1992). Differential periods of Varroa mite invasion into worker and drone cells of honey bees. Experimental & Applied Acarology, 16(4), 295-301.

Bowen-Walker, P. L., & Gunn, A. (2001). The effect of the ectoparasitic mite, *Varroa destructor* on adult worker honeybee (*Apis mellifera*) emergence weights, water, protein, carbohydrate, and lipid levels. Entomologia Experimentalis et Applicata, 101(3), 207-217.

Brodschneider, R., & Crailsheim, K. (2010). Nutrition and health in honey bees. Apidologie, 41(3), 278-294.

Büchler, R., Andonov, S., Bernstein, R., Bienefeld, K., Costa, C., Du, M., Gabel, M., Given, K., Hatjina, F., Harpur, A. B., Hoppe, A., Kezic, N., Kovačić, M., Kryger, P., Mondet, F., Spivak, M., Uzunov, A., Wegener, J., & Wilde, J. (2025). Standard methods for rearing and selection of *Apis mellifera* queens 2.0. Journal of Apicultural Research, 64(2), 555-611.

Bujok, B., Kleinhenz, M., Fuchs, S., & Tautz, J. (2002). Hot spots in the bee hive. The Science of Nature, 89(7), 299-301.

Buscarlet, L.A. (1982) Effects of γ irradiation on respiration and on food consumption measured through 22Na in *Tribolium confusum* J. du V. (Coleoptera: Tenebrionidae). Journal of Stored Product Research, 19, 19-24.

Calderone, N. W., & Kuenen, L. P. S. (2001). Effects of western honey bee (Hymenoptera: Apidae) colony, cell type, and larval sex on host acquisition by female *Varroa destructor* (Acari: Varroidae). Journal of Economic Entomology, 94(5), 1022-1030.

Campbell, J., Kessler, B., Mayack, C., & Naug, D. (2010). Behavioural fever in infected honeybees: parasitic manipulation or coincidental benefit? Parasitology, 137(10), 1487-1491.

Castejón, D., Alba-Tercedor, J., Rotllant, G., Ribes, E., Durfort, M., & Guerao, G. (2018). Micro-computed tomography and histology to explore internal morphology in decapod larvae. Scientific Reports, 8(1), 1-11.

Castilhos, D., Polesso, A. M., da Silva, A. C. F., dos Santos, A. B., de Carvalho Lopes, A. T., de Oliveira Filho, da Cunha, A. F. S., Puker, A., Matioli, A. L., Serrado Campos, A. A., de Morais, A. L., Modro, A. F. H., Neto, A. A. S., Pires, A. S. M., Biasi, C., Peixoto, C. M., Mercês C. C.,, de Carvalho, C. A. L., Paiva, C. S., Pereira, D. S., Freire, D. S., Souza, D. C., De Jong D., Soares D. A. M., & de Medeiros, V. F. (2023). *Varroa destructor* infestation levels in

Africanized honey bee colonies in Brazil from 1977 when first detected to 2020. Apidologie, 54(1), 5.

Chen Y., Evans J., Feldlaufer M., (2006a) Horizontal and vertical transmission of viruses in the honey bee, *Apis mellifera*, Journal of Invertebrate Pathology, 92(3), 152-159.

Chen, Y. P., Pettis, J. S., Collins, A., & Feldlaufer, M. F. (2006b). Prevalence and transmission of honeybee viruses. Applied and Environmental Microbiology, 72(1), 606-611.

Christensen, B. M., Huff, B. M., & Li, J. (1990). Effect of γ irradiation on the hemocyte-mediated immune response of *Aedes aegypti* against microfilariae. Journal of Invertebrate Pathology, 56(1), 123-127.

Clark, D. P., & Badea, C. T. (2014). Micro-CT of rodents: state-of-the-art and future perspectives. Physica medica, 30(6), 619-634.

Clark, D. P., & Badea, C. T. (2021). Advances in micro-CT imaging of small animals. Physica Medica, 88, 175-192.

Coe, A., & Blackie, N. (2022). Comparison of low-and high-cost infrared thermal imaging devices for the detection of lameness in dairy cattle. Veterinary Sciences, 9(8), 414.

Cook, C. N., Kaspar, R. E., Flaxman, S. M., & Breed, M. D. (2016). Rapidly changing environment modulates the thermoregulatory fanning response in honeybee groups. Animal Behaviour, 115, 237-243.

Copeland, D. C., Mott, B. M., Kortenkamp, O. L., Erickson, R. J., Allen, N. O., & Anderson, K. E. (2025). Image-based honey bee larval viral and bacterial diagnosis using machine learning. Scientific Reports, 15(1), 30717.

Corby-Harris, V., Snyder, L., & Meador, C. (2019). Fat body lipolysis connects poor nutrition to hypopharyngeal gland degradation in *Apis mellifera*. Journal of Insect Physiology, 116, 1-9.

Crane, E. (1999). The world history of beekeeping and honey hunting (1st ed.). Taylor and Francis, Routledge. New York, Part II: Opportunistic Honey Hunting by Man, Chapter 6, pp. 35-42.

Csaba, Gy. (1983). *Varroa jacobsoni* (Oudemans, 1904), a mézelő méh (*Apis mellifera*) atkája és a varroosis. Parasitologia Hungarica, 16(2), 31-38.

Csóka, Á., Kovács, G., Ács, V., Matics, Z., Gerencsér, Z., Szendrő, Zs., Nagy I., Petneházy, Ö., Repa, I., Moizs, M. & Donkó, T. (2022). A general technique for the estimation of farm animal body part weights from CT scans and its applications in a rabbit breeding program. Computers and Electronics in Agriculture, 196, 106865.

Daisley, B. A., Pitek, A. P., Mallory, E., Chernyshova, A. M., Allen-Vercoe, E., Reid, G., & Thompson, G. J. (2023). Disentangling the microbial ecological factors impacting honey bee susceptibility to *Paenibacillus larvae* infection. Trends in Microbiology, 31(5), 521-534.

Damayo, J. E., McKee, R. C., Buchmann, G., Norton, A. M., Ashe, A., & Remnant, E. J. (2023). Virus replication in the honey bee parasite, *Varroa destructor*. Journal of Virology, 97(12), e01149-23.

Dams, L. R. (1978). Bees and honey-hunting scenes in the Mesolithic rock art of eastern Spain. Bee World, 59(2), 45-53.

De Guzman L.I., Delfinado-Baker M., (1996). A new species of *Varroa (Acari: Varroidae*) associated with *Apis koschevnikovi (Apidae: Hymenoptera*) in Borneo. International Journal of Acarology. 22, 23-27

De Guzman, L. I., Rinderer, T. E., & Frake, A. M. (2007). Growth of *Varroa destructor* (Acari: Varroidae) populations in Russian honey bee (Hymenoptera: Apidae) colonies. Annals of the Entomological Society of America, 100(2), 187-195

De Guzman, L. I., Rinderer, T. E., & Frake, A. M. (2008). Comparative reproduction of *Varroa destructor* in different types of Russian and Italian honey bee combs. Experimental and Applied Acarology, 44(3), 227-238.

De Guzman, L. I., Simone-Finstrom, M., Frake, A. M., & Tokarz, P. (2019). Comb irradiation has limited, interactive effects on colony performance or pathogens in bees, *Varroa destructor* and wax based on two honey bee stocks. Insects, 10(1), 15.

De Jong, D., De Jong, P.H., Gonçalves, L.S., (1982). Weight loss and other damage to developing worker honeybees from infestation with *Varroa jacobsoni*. Journal of Apicultural Results 21, 165-216.

De Paula, J. C., Doello, K., Mesas, C., Kapravelou, G., Cornet-Gómez, A., Orantes, F. J., Martínez, R., Linares, F., Prados, C. J., Porres, J. M., Osuna, A., & de Pablos, L. M. (2022). Exploring honeybee abdominal anatomy through micro-CT and novel multi-staining approaches. Insects, 13(6), 556

Del Piccolo F., Nazzi, F., Della Vedova G., & Milani, N. (2010). Selection of *Apis mellifera* workers by the parasitic mite *Varroa destructor* using host cuticular hydrocarbons. Parasitology, 137(6), 967-973.

Delfinado-Baker, M., Aggarwal, K., (1987). A new *Varroa* (*Acari: Varroidae*) from the nest of *Apis cerana (Apidae).* International Journal of Acarology. 13, 233-237.

Dietemann, V., Nazzi, F., Martin, S. J., Anderson, D. L., Locke, B., Delaplane, K. S., Wauqiuez, Q., Tanahill, C., Frey, E., Ziegelmann, B., Rosenkranz, P., & Ellis, J. D. (2013). Standard methods for varroa research. Journal of Apicultural Research, 52(1), 1-54.

Dietemann, V., Pflugfelder, J., Anderson, D., Charrière, J. D., Chejanovsky, N., Dainat, B., de Miranda, J., Delaplane, K., Dillier, F-X., Gallmann, S. F. P., Gauthier, L., Imdorf, A., Koeniger, N., Kralj, J., Meikle, W., Pettis J., Rosenkranz, P., Sammataro, D., Smith, D., Yañez, O., & Neumann, P. (2012). *Varroa destructor*: research avenues towards sustainable control. Journal of Apicultural Research, 51(1), 125-132.

Donkó, T., Petneházy, Ö., Fajtai, D., & Keszthelyi, S. (2022). A conceptualisation of computed tomography outputs in entomological research by step by step displaying trough the CT-based visualization of a wood-boring larvae. Acta Phytopathologica et Entomologica Hungarica, 57(2), 127-138.

Donzé, G., & Guerin, P. M. (1994). Behavioural attributes and parental care of Varroa mites parasitizing honeybee brood. Behavioural Ecology and Sociobiology, 34(5), 305-319.

Doublet, V., Oddie, M. A., Mondet, F., Forsgren, E., Dahle, B., Furuseth-Hansen, E., Williams, G. L., de Smet, L., Natsopoulou, M. E., Murray, T. E., Semberg, E., Yañez, O., de Graaf, C. D., Le Conte, Y., Neumann, P., Rimstad, E., Paxton, R. J., & de Miranda, J. R. (2024). Shift in virus composition in honeybees (*Apis mellifera*) following worldwide invasion by the parasitic mite and virus vector *Varroa destructor*. Royal Society Open Science, 11(1), 231529.

Duay P., de Jong D., Engels W., (2003). Weight loss in drone pupae (*Apis mellifera*) multiply infested by *Varroa destructor* mites. Apidologie 34, 61-65.

Dynes, T. L., Berry, J. A., Delaplane, K. S., Brosi, B. J., & de Roode, J. C. (2019). Reduced density and visually complex apiaries reduce parasite load and promote honey production and overwintering survival in honey bees. PLoS One, 14(5), e0216286.

Easton, S. (2012). Practical Veterinary Diagnostic Imaging (2nd ed.). John Wiley & Sons Ltd., Chichester United Kingdoom. Chapter 12. 127-128.

Eliash, N., Singh, N. K., Kamer, Y., Pinnelli, G. R., Plettner, E., & Soroker, V. (2014). Can we disrupt the sensing of honey bees by the bee parasite *Varroa destructor*? PLoS One, 9(9), e106889.

Eliash, N., Suenaga, M., & Mikheyev, A. S. (2022). Vector-virus interaction affects viral loads and co-occurrence. BMC Biology, 20(1), 284.

Emsen, B., Guzman-Novoa, E., & Kelly, P. G. (2014). Honey production of honey bee (Hymenoptera: Apidae) colonies with high and low *Varroa destructor* (Acari: Varroidae) infestation rates in eastern Canada. The Canadian Entomologist, 146(2), 236-240.

Evans, J. D., Aronstein, K., Chen, Y. P., Hetru, C., Imler, J. L., Jiang, H., Kanost, M., Thompson, G. J., Zou, Z., & Hultmark, D. (2006). Immune pathways and defence mechanisms in honey bees *Apis mellifera*. Insect Molecular Biology, 15(5), 645-656.

Evans, J. D., & Spivak, M. (2010). Socialized medicine: individual and communal disease barriers in honey bees. Journal of Invertebrate Pathology, 103, S62-S72.

Evans, J. D., & Wheeler, D. E. (1999). Differential gene expression between developing queens and workers in the honey bee, *Apis mellifera*. Proceedings of the National Academy of Sciences, 96(10), 5575-5580.

Evans, J.D. and Chen, Y. (2021). Colony Collapse Disorder and Honey Bee Health. In Honey Bee Medicine for the Veterinary Practitioner, Edited by Kane. R. T and Faux M. C., John Wiley & Sons, Inc. Hoboken, Chapter 19, 229-234

Eyer, M., Neumann, P., & Dietemann, V. (2016). A look into the cell: honey storage in honey bees, *Apis mellifera*. PLoS One, 11(8), e0161059.

Facchini, E.; Nalon, L.; Andreis, M.E.; Andreis, M.A.; Di Giancamillo, M.; Rizzi, R.; Mortarino, M. (2019) Honeybee pupal length assessed by CT-scan technique: Effects of Varroa infestation, developmental stage and spatial position within the brood comb. Scientific Reports, 9, 10614.

Fahrenholz, L., Lamprecht, I., & Schricker, B. (1989). Thermal investigations of a honey bee colony: thermoregulation of the hive during summer and winter and heat production of members of different bee castes. Journal of Comparative Physiology B, 159, 551-560.

Farkas, Á., & Zajácz, E. (2007). Nectar production for the Hungarian honey industry. European Journal of Plant Science and Biotechnology, 1(2), 125-151.

Fazel, R., Krumholz, H. M., Wang, Y., Ross, J. S., Chen, J., Ting, H. H., Shah, N. D., Nasir, K., Einstein, J., A., & Nallamothu, B. K. (2009). Exposure to low-dose ionizing radiation from medical imaging procedures. New England Journal of Medicine, 361(9), 849-857.

Feketéné Ferenczi, A., Kovácsné Soltész, A., Szűcs, I., & Bauerné Gáthy, A. (2024). Current Situation of Honey-Producing Apiaries – Quantitative Study of Honey Production Characteristics Based on a Questionnaire Survey in Hungary. Agriculture, 14(12), 2100.

Feketéné Ferenczi, A., Szűcs, I., & Bauerné Gáthy, A. (2023). Evaluation of the pollination ecosystem service of the honey bee (*Apis mellifera*) based on a beekeeping model in Hungary. Sustainability, 15(13), 9906.

Foster, F. (2020). Bees and vultures: Egyptian hieroglyphs is Ammianus Marcellinus. The Classical Quarterly, 70 (2), 884-890.

Francis, R. M., Nielsen, S. L., & Kryger, P. (2013). Varroa-virus interaction in collapsing honey bee colonies. PLoS One, 8(3), e57540.

Free, J. B., & Williams, I. H. (1974). Factors determining food storage and brood rearing in honeybee (*Apis mellifera* L.) comb. Journal of Entomology Series A, General Entomology, 49(1), 47-63.

Frey, E., & Rosenkranz, P. (2014). Autumn invasion rates of *Varroa destructor* (Mesostigmata: Varroidae) into honey bee (Hymenoptera: Apidae) colonies and the resulting increase in mite populations. Journal of Economic Entomology, 107(2), 508-515.

Fries, I., & Camazine, S. (2001). Implications of horizontal and vertical pathogen transmission for honey bee epidemiology. Apidologie, 32(3), 199-214.

Fries, I., Camazine, S., & Sneyd, J. (1994). Population dynamics of *Varroa jacobsoni*: a model and a review. Bee World, 75(1), 5-28.

Fries, I., Huazhen, W., Wei, S., & Jin, C. S. (1996). Grooming behaviour and damaged mites (*Varroa jacobsoni*) in *Apis cerana cerana* and *Apis mellifera ligustica*. Apidologie, 27(1), 3-11.

Fuchs, A., Schreyer, A., Feuerbach, S., Korb, J. (2004). A new technique for termite monitoring using computer tomography and endoscopy. International Journal of Pest Management, 50 (1), 63-66.

Fuchs, S. (1990). Preference for drone brood cells by *Varroa jacobsoni* Oud in colonies of *Apis mellifera carnica*. Apidologie, 21(3), 193-199.

Gabel, M., Hoppe, A., Scheiner, R., Obergfell, J., & Büchler, R. (2023). Heritability of *Apis mellifera* recapping behaviour and suppressed mite reproduction as resistance traits towards *Varroa destructor*. Frontiers in Insect Science, 3, 1135187.

Garrido C., Rosenkranz P., Stürmer M., Rübsam R., Büning J., (2000). Toluidine blue staining as a rapid measure for initiation of oocyte growth and fertility in *Varroa jacobsoni* Oud. Apidologie 31, 559-566.

Garrido, C., & Rosenkranz, P. (2003). The reproductive program of female *Varroa destructor* mites is triggered by its host, *Apis mellifera*. Experimental and Applied Acarology, 31(3), 269-273.

Gábor, E., Cinege, G., Csordás, G., Rusvai, M., Honti, V., Kolics, B., Török, T., Williams, J. M., Kurucz, É., & Andó, I. (2020). Identification of reference markers for characterizing honey bee (*Apis mellifera*) hemocyte classes. Developmental & Comparative Immunology, 109, 103701.

Geffre, A. C., Gernat, T., Harwood, G. P., Jones, B. M., Morselli Gysi, D., Hamilton, A. R., Bonning, C. B., Toth, L. A., Robinson, E. G., & Dolezal, A. G. (2020). Honey bee virus causes context-dependent changes in host social behaviour. Proceedings of the National Academy of Sciences, 117(19), 10406-10413.

Genersch, E., Von Der Ohe, W., Kaatz, H., Schroeder, A., Otten, C., Büchler, R., Berg, S., Ritter, W., Mühlen, W., Gisder, S., Meixner, D. M., Liebig, G., & Rosenkranz, P. (2010). The German bee monitoring project: a long term study to understand periodically high winter losses of honey bee colonies. Apidologie, 41(3), 332-352.

Glass, J. R., & Harrison, J. F. (2024). A thermal performance curve perspective explains decades of disagreements over how air temperature affects the flight metabolism of honey bees. Journal of Experimental Biology, 227(7).

Goblirsch, M., Warner, J. F., Sommerfeldt, B. A., & Spivak, M. (2020). Social fever or general immune response? Revisiting an example of social immunity in honey bees. Insects, 11(8), 528.

Goodwin, R. M., Taylor, M. A., Mcbrydie, H. M., & Cox, H. M. (2006). Drift of *Varroa destructor*-infested worker honey bees to neighbouring colonies. Journal of Apicultural Research, 45(3), 155-156.

Grindrod, I., & Martin, S. J. (2023). Varroa resistance in *Apis cerana*: a review. Apidologie, 54(2), 14.

Groh, C., Tautz, J., & Rössler, W. (2004). Synaptic organization in the adult honey bee brain is influenced by brood-temperature control during pupal development. Proceedings of the National Academy of Sciences, 101(12), 4268-4273.

Guzman-Novoa, E., Corona, M., Alburaki, M., Reynaldi, F. J., Invernizzi, C., Fernández de Landa, G., & Maggi, M. (2024). Honey bee populations surviving *Varroa destructor* parasitism in Latin America and their mechanisms of resistance. Frontiers in Ecology and Evolution, 12, 1434490.

Hadisoesilo S., Otis G.W., (1998). Differences in drone cappings of *Apis cerana* and *Apis nigrocincta*. Journal of Apicultural Research 37, 11-15

Hall, M.J., Martín-Vega, D. (2019) Visualization of insect metamorphosis. Philosophical Transactions of the Royal Society B, 374, 20190071.

Hallman, G.J. (2013) Control of stored product pests by ionizing radiation. Journal of Stored Products Research, 52, 36-41.

Han, B., Wu, J., Wei, Q., Liu, F., Cui, L., Rueppell, O., & Xu, S. (2024). Life-history stage determines the diet of ectoparasitic mites on their honey bee hosts. Nature Communications, 15(1), 725.

Harbo, J. R., & Harris, J. W. (1999a). Selecting honey bees for resistance to *Varroa jacobsoni*. Apidologie, 30(2-3), 183-196.

Harbo, J. R., & Harris, J. W. (1999b). Heritability in honey bees (Hymenoptera: Apidae) of characteristics associated with resistance to *Varroa jacobsoni* (Mesostigmata: Varroidae). Journal of Economic Entomology, 92(2), 261-265.

Haydak, M. H. (1970). Honey bee nutrition. Annual Review of Entomology, 15(1), 143-156.

Hepburn, H. R. (1998). Reciprocal interactions between honeybees and combs in the integration of some colony functions in *Apis mellifera* L. Apidologie, 29(1-2), 47-66.

Hernández López, J., Schuehly, W., Crailsheim, K., & Riessberger-Gallé, U. (2014). Trans-generational immune priming in honeybees. Proceedings of the Royal Society B: Biological Sciences, 281(1785), 20140454.

Hung, K. L. J., Kingston, J. M., Albrecht, M., Holway, D. A., & Kohn, J. R. (2018). The worldwide importance of honey bees as pollinators in natural habitats. Proceedings of the Royal Society B: Biological Sciences, 285(1870), 20172140.

Hystad, E. M., Salmela, H., Amdam, G. V., & Münch, D. (2017). Hemocyte-mediated phagocytosis differs between honey bee (*Apis mellifera*) worker castes. PLoS One, 12(9), e0184108.

Ifantidis, M. D. (1983). Ontogenesis of the mite *Varroa jacobsoni* in worker and drone honeybee brood cells. Journal of Apicultural Research, 22(3), 200-206.

Ifantidis, M. D. (1988). Some aspects of the process of *Varroa jacobsoni* mite entrance into honey bee (*Apis mellifera*) brood cells. Apidologie, 19(4), 387-396.

IRAC, (2026). Insecticide Resistance Action Committee. The IRAC Mode of Action Classification URL: https://irac-online.org/mode-of-action/ (accessed: 19. 01. 2026)

Ilyasov, R. A., Lee, M. L., Takahashi, J. I., Kwon, H. W., & Nikolenko, A. G. (2020). A revision of subspecies structure of western honey bee *Apis mellifera*. Saudi Journal of Biological Sciences, 27(12), 3615-3621.

Jack, C. J., & Ellis, J. D. (2021). Integrated pest management control of *Varroa destructor* (Acari: Varroidae), the most damaging pest of (*Apis mellifera* L. (Hymenoptera: Apidae)) colonies. Journal of Insect Science, 21(5), 6.

Jeyapriya, G., Sumathi, E., Saminathan, V. R., Renukadevi, P., Sasikala, R., Priya, S. S., Kowiska, S., & Pradeep, S. (2025). Parasitic Mites of Honey Bees (Apis Spp.): A Detailed Review of *Varroa destructor* in Parasitism, Pathogen Transmission and its Management. Acta Parasitologica, 70(5), 1-25.

Johnson, B. R. (2008). Within-nest temporal polyethism in the honey bee. Behavioural Ecology and Sociobiology, 62(5), 777-784.

Jones, J. C., Helliwell, P., Beekman, M., Maleszka, R., & Oldroyd, B. P. (2005). The effects of rearing temperature on developmental stability and learning and memory in the honey bee, *Apis mellifera*. Journal of Comparative Physiology A, 191, 1121-1129.

Jonsson, T. (2023). Micro-CT and deep learning: Modern techniques and applications in insect morphology and neuroscience. Frontiers in Insect Science, 3, 1016277.

Kakumanu, M. L., Reeves, A. M., Anderson, T. D., Rodrigues, R. R., & Williams, M. A. (2016). Honey bee gut microbiome is altered by in-hive pesticide exposures. Frontiers in Microbiology, 7, 1255.

Kalender, W. A. (2014). Dose in x-ray computed tomography. Physics in Medicine & Biology, 59(3), R129.

Kanbar, G., & Engels, W. J. P. R. (2003). Ultrastructure and bacterial infection of wounds in honey bee (*Apis mellifera*) pupae punctured by Varroa mites. Parasitology Research, 90(5), 349-354.

Kast, C., Droz, B., & Kilchenmann, V. (2023). Toxicity of coumaphos residues in beeswax foundation to the honey bee brood. Environmental Toxicology and Chemistry, 42(8), 1816-1822.

Kastberger, G., & Stachl, R. (2003). Infrared imaging technology and biological applications. Behaviour Research Methods, Instruments, & Computers, 35(3), 429-439.

Keszthelyi, S., Glavak, C., & Pal-Fam, F. (2015). Mortality and sterility consequences of X-ray radiation on the granary weevil, *Sitophilus granarius*. Bulletin of Insectology, 68, (1), 7-11.

Keszthelyi, S., Pónya, Z., Csóka, Á., Bázár, G., Morschhauser, T., & Donkó, T. (2020). Non-destructive imaging and spectroscopic techniques to investigate the hidden-lifestyle arthropod pests: A review. Journal of Plant Diseases and Protection, 127(3), 283-295.

Kevill, J. L., de Souza, F. S., Sharples, C., Oliver, R., Schroeder, D. C., & Martin, S. J. (2019). DWV-A lethal to honey bees (*Apis mellifera*): a colony level survey of DWV variants (A, B, and C) in England, Wales, and 32 states across the US. Viruses, 11(5), 426.

Kim, S. H., Mondet, F., Hervé, M., & Mercer, A. (2018). Honey bees performing varroa sensitive hygiene remove the most mite-compromised bees from highly infested patches of brood. Apidologie, 49(3), 335-345.

Kirrane, M. J., de Guzman, L. I., Rinderer, T. E., Frake, A. M., Wagnitz, J., & Whelan, P. M. (2012). Age and reproductive status of adult Varroa mites affect grooming success of honey bees. Experimental and Applied Acarology, 58(4), 423-430.

Klein, B. A., & Busby, M. K. (2020). Slumber in a cell: honeycomb used by honey bees for food, brood, heating… and sleeping. PeerJ, 8, e9583.

Klein, B. A., Stiegler, M., Klein, A., & Tautz, J. (2014). Mapping sleeping bees within their nest: spatial and temporal analysis of worker honey bee sleep. PLoS One, 9(7), e102316.

Klein, S., Cabirol, A., Devaud, J. M., Barron, A. B., & Lihoreau, M. (2017). Why bees are so vulnerable to environmental stressors. Trends in Ecology & Evolution, 32(4), 268-278.

Kleinhenz, M., Bujok, B., Fuchs, S., & Tautz, J. (2003). Hot bees in empty broodnest cells: heating from within. Journal of Experimental Biology, 206(23), 4217-4231.

Koleoglu, G., Goodwin, P. H., Reyes-Quintana, M., Hamiduzzaman, M. M., & Guzman-Novoa, E. (2018). *Varroa destructor* parasitism reduces hemocyte concentrations and prophenol oxidase gene expression in bees from two populations. Parasitology Research, 117(4), 1175-1183.

Kolics, É., Parrag, T., Házi, F., Szepesi, K., Heltai, B., Mátyás, K., Kutasy, B., Virág, E., Taller, J., & Kolics, B. (2020). An alternative, high throughput method to identify csd alleles of the honey bee. Insects, 11(8), 483.

Kolics, É., Sajtos, Z., Mátyás, K., Szepesi, K., Solti, I., Németh, G., Taller, J., Baranyai, E., Specziár, A., & Kolics, B. (2021). Changes in Lithium Levels in Bees and Their Products Following Anti-Varroa Treatment Insects, 12(7), 579.

Kovac, H., Käfer, H., Stabentheiner, A., & Costa, C. (2014). Metabolism and upper thermal limits of *Apis mellifera carnica* and *A. m. ligustica*. Apidologie, 45, 664-677.

Kuenen, L. P. S., & Calderone, N. W. (1997). Transfers of Varroa mites from newly emerged bees: Preferences for age-and function-specific adult bees (Hymenoptera: Apidae). Journal of Insect Behaviour, 10(2), 213-228.

Kühnholz, S., & Seeley, T. D. (1997). The control of water collection in honey bee colonies. Behavioural Ecology and Sociobiology, 41, 407-422.

Kulhanek, K., Steinhauer, N., Wilkes, J., Wilson, M., Spivak, M., Sagili, R. R., Tarpy, D. R., McDermott, E., Garavito, A., Rennich, K., & VanEngelsdorp, D. (2021). Survey-derived best management practices for backyard beekeepers improve colony health and reduce mortality. PLoS One, 16(1), e0245490.

Lanzi, G., De Miranda, J. R., Boniotti, M. B., Cameron, C. E., Lavazza, A., Capucci, L., Camazine, M. S., & Rossi, C. (2006). Molecular and biological characterization of deformed wing virus of honeybees (*Apis mellifera* L.). Journal of Virology, 80(10), 4998-5009.

Le Conte, Y., Arnold, G., & Desenfant, P. H. (1990). Influence of brood temperature and hygrometry variations on the development of the honey bee ectoparasite *Varroa jacobsoni* (Mesostigmata: Varroidae). Environmental Entomology, 19(6), 1780-1785.

Le Conte, Y., De Vaublanc, G., Crauser, D., Jeanne, F., Rousselle, J. C., & Bécard, J. M. (2007). Honey bee colonies that have survived *Varroa destructor*. Apidologie, 38(6), 566-572.

Le Conte, Y., Meixner, M. D., Brandt, A., Carreck, N. L., Costa, C., Mondet, F., & Büchler, R. (2020). Geographical distribution and selection of European honey bees resistant to *Varroa destructor*. Insects, 11(12), 873.

Leonhardt, S. D., Gallai, N., Garibaldi, L. A., Kuhlmann, M., & Klein, A. M. (2013). Economic gain, stability of pollination and bee diversity decrease from southern to northern Europe. Basic and Applied Ecology, 14(6), 461-471.

Ling, E., Shirai, K., Kanekatsu, R., Kiguchi, K., Kobayashi, Y., Funayama, T., & Watanabe, H. (2006). Contribution of circulating hemocytes to the regeneration of heavy ion beams (12C5+) irradiated hematopoietic organs in the silkworm, *Bombyx mori,* through the way of phagocytosis of injured cells after invasion. Developmental & Comparative Immunology, 30(6), 531-543.

Liu, J., Zhang, R., Tang, R., Zhang, Y., Guo, R., Xu, G., Chen, D., Huang, Y. Z., Chen, Y., & Li, W. (2022). The role of honey bee derived aliphatic esters in the host-finding behaviour of *Varroa destructor*. Insects, 14(1), 24.

Locke, B., Semberg, E., Forsgren, E., & De Miranda, J. R. (2017). Persistence of subclinical deformed wing virus infections in honeybees following Varroa mite removal and a bee population turnover. PLoS One, 12(7), e0180910.

Locke, B., Thaduri, S., Stephan, J. G., Low, M., Blacquière, T., Dahle, B., LeConte, Y., Neumann, P., & de Miranda, J. R. (2021). Adapted tolerance to virus infections in four geographically distinct *Varroa destructor*-resistant honeybee populations. Scientific Reports, 11(1), 12359.

Maggi, M., Damiani, N., Ruffinengo, S., De Jong, D., Principal, J., & Eguaras, M. (2010). Brood cell size of *Apis mellifera* modifies the reproductive behaviour of *Varroa destructor*. Experimental and Applied Acarology, 50(3), 269-279.

Mallory, E., Freeze, G., Daisley, B. A., & Allen-Vercoe, E. (2024). Revisiting the role of pathogen diversity and microbial interactions in honeybee susceptibility and treatment of *Melissococcus plutonius* infection. Frontiers in Veterinary Science, 11, 1495010.

Martin, S. J. (1994). Ontogenesis of the mite *Varroa jacobsoni* Oud. in worker brood of the honeybee *Apis mellifera* L. under natural conditions. Experimental & Applied Acarology, 18(2), 87-100.

Martin, S. J., Highfield, A. C., Brettell, L., Villalobos, E. M., Budge, G. E., Powell, M., Nikaido, S., & Schroeder, D. C. (2012). Global honey bee viral landscape altered by a parasitic mite. Science, 336(6086), 1304-1306.

Matthes, H. F., Hübner, M., Hiepe, T., Boehme, R., & Proesch, U. (1991). Ionizing radiation for control of *Varroa jacobsoni* infestation. Tierärztliche Umschau, 46, (1), 20-23.

Mattila, H. R., & Seeley, T. D. (2007). Genetic diversity in honey bee colonies enhances productivity and fitness. Science, 317(5836), 362-364.

Mazar, A., Panitz-Cohen, N., & Bloch, G. (2022). The Apiary at Tel Reḥov: An Update. Near Eastern Archaeology, 85(2), 126-131.

Mazonakis, M., & Damilakis, J. (2016). Computed tomography: What and how does it measure? European Journal of Radiology, 85(8), 1499-1504.

McMenamin, A. J., & Genersch, E. (2015). Honey bee colony losses and associated viruses. Current Opinion in Insect Science, 8, 121-129.

Medrzycki, P., Sgolastra, F., Bortolotti, L., Bogo, G., Tosi, S., Padovani, E., Claudio, P., & Sabatini, A. G. (2010). Influence of brood rearing temperature on honey bee development and susceptibility to poisoning by pesticides. Journal of Apicultural Research, 49(1), 52-59.

Meng, Q., Huang, R., Yang, S., Jiang, W., Tian, Y., & Dong, K. (2025). An Overview of the Adverse Impacts of Old Combs on Honeybee Colonies and Recommended Beekeeping Management Strategies. Insects, 16(4), 351.

Metscher, B. D. (2009). MicroCT for comparative morphology: simple staining methods allow high-contrast 3D imaging of diverse non-mineralized animal tissues. BMC Physiology, 9(1), 11.

Mitton, G. A., Meroi Arcerito, F., Cooley, H., Fernandez de Landa, G., Eguaras, M. J., Ruffinengo, S. R., & Maggi, M. D. (2022). More than sixty years living with *Varroa destructor*: a review of acaricide resistance. International Journal of Pest Management, 1-18.

Mondet, F., Beaurepaire, A., McAfee, A., Locke, B., Alaux, C., Blanchard, S., Alaux, C., Blanchard, S., Danka, B., & Le Conte, Y. (2020). Honey bee survival mechanisms against the parasite *Varroa destructor*: a systematic review of phenotypic and genomic research efforts. International Journal for Parasitology, 50(6-7), 433-447.

Mordecai, G. J., Brettell, L. E., Martin, S. J., Dixon, D., Jones, I. M., & Schroeder, D. C. (2016). Superinfection exclusion and the long-term survival of honey bees in Varroa-infested colonies. The ISME journal, 10(5), 1182-1191.

Mordecai, G.J.; Brettell, McMenamin, A.J.; Genersch, E. (2015) Honey bee colony losses and associated viruses. Current Opinion in Insect Science, 8, 121-129.

Morfin, N., Anguiano-Baez, R., & Guzman-Novoa, E. (2021). Honey bee (*Apis mellifera*) immunity. Veterinary Clinics: Food Animal Practice, 37(3), 521-533.

Morfin, N., Goodwin, P. H., & Guzman-Novoa, E. (2020). Interaction of field realistic doses of clothianidin and *Varroa destructor* parasitism on adult honey bee (*Apis mellifera* L.) health and neural gene expression, and antagonistic effects on differentially expressed genes. PLoS One, 15(2), e0229030.

Morfin, N., Goodwin, P. H., & Guzman-Novoa, E. (2023). *Varroa destructor* and its impacts on honey bee biology. Frontiers in Bee Science, 1, 1272937.

Muijres, F. T., Van Dooremalen, C., Lankheet, M., Lugt, H., De Vries, L. J., & Van Langevelde, F. (2020). *Varroa destructor* infestation impairs the improvement of landing performance in foraging honeybees. Royal Society Open Science, 7(9), 201222.

Naug, D. (2008). Structure of the social network and its influence on transmission dynamics in a honeybee colony. Behavioural Ecology and Sociobiology, 62(11), 1719-1725.

Nazzi, F., & Le Conte, Y. (2016). Ecology of *Varroa destructor,* the major ectoparasite of the western honey bee, *Apis mellifera*. Annual Review of Entomology, 61(1), 417-432.

Negri, P., Maggi, M., Ramirez, L., Szawarski, N., De Feudis, L., Lamattina, L., & Eguaras, M. (2016). Cellular immunity in *Apis mellifera*: studying hemocytes brings light about bees skills to confront threats. Apidologie, 47(3), 379-388.

Neov, B., Georgieva, A., Shumkova, R., Radoslavov, G., & Hristov, P. (2019). Biotic and abiotic factors associated with colonies mortalities of managed honey bee (*Apis mellifera*). Diversity, 11(12), 237.

Newcombe, H. B. (1971). The genetic effects of ionizing radiations. Advances in Genetics, 16, 239-303.

Nolan IV, M. P., & Delaplane, K. S. (2017). Distance between honey *bee Apis mellifera* colonies regulates populations of *Varroa destructor* at a landscape scale. Apidologie, 48(1), 8-16.

Norrström, N., Niklasson, M., & Leidenberger, S. (2021). Winter weight loss of different subspecies of honey bee *Apis mellifera* colonies (Linnaeus, 1758) in southwestern Sweden. PLoS One, 16(10), e0258398.

Odemer, R. (2020). Reproductive capacity of *Varroa destructor* in four different honey bee subspecies. Saudi Journal of Biological Sciences, 27(1), 247-250.

Ory, F., Duchemin, V., Kilchenmann, V., Charrière, J. D., Dainat, B., & Dietemann, V. (2022). Lack of evidence for trans-generational immune priming against the honey bee pathogen *Melissococcus plutonius*. PLoS One, 17(5), e0268142.

O'Sullivan, J. D., Behnsen, J., Starborg, T., MacDonald, A. S., Phythian-Adams, A. T., Else, K. J., Cruickshank, M. S., & Withers, P. J. (2018). X-ray micro-computed tomography (μCT): an emerging opportunity in parasite imaging. Parasitology, 145(7), 848-854.

Oudemans A.C., (1904). On a new genus and species of parasitic acari. Notes from the Leyden Museum 24, 216-222.

Paithankar, J. G., Deeksha, K., & Patil, R. K. (2017). Gamma radiation tolerance in different life stages of the fruit fly *Drosophila melanogaster*. International Journal of Radiation Biology, 93(4), 440-448.

Palmer-Young, E. C., Ryabov, E. V., Markowitz, L. M., Boncristiani, D. L., Grubbs, K., Pawar, A., Peterson, R., & Evans, J. D. (2023). Host-driven temperature dependence of Deformed wing virus infection in honey bee pupae. Communications Biology, 6(1), 333.

Papp M., Békési L., Farkas R., Makrai L., Judge M. F., Maroti G., Tőzsér D., & Solymosi N. (2022). Natural diversity of the honey bee (*Apis mellifera*) gut bacteriome in various climatic and seasonal states. PLoS One, 17(9), e0273844.

Panziera, D., van Langevelde, F., & Blacquière, T. (2017). Varroa sensitive hygiene contributes to naturally selected varroa resistance in honey bees. Journal of Apicultural Research, 56(5), 635-642.

Pasho, D. J., Applegate, J. R., & Hopkins, D. I. (2021). Diseases and pests of honey bees (*Apis mellifera*). Veterinary Clinics: Food Animal Practice, 37(3), 401-412.

Pätzold, S., & Ritter, W. (1989). Studies on the behaviour of the honey-bee mite, *Varroa jacobsoni* O., in a temperature gradient. Journal of Applied Entomology, 107(1-5), 46-51.

Paxton, R. J. (2005). Male mating behaviour and mating systems of bees: an overview. Apidologie, 36(2), 145-156.

Peck, D. T. (2021). The parasitic mite *Varroa destructor*: history, biology, monitoring, and management. in Honey Bee Medicine for the Veterinary Practitioner, Edited by Kane. R. T and Faux M. C., John Wiley & Sons, Inc., Hoboken, Chapter 20. 235-251.

Peck, D. T., & Seeley, T. D. (2019). Mite bombs or robber lures? The roles of drifting and robbing in *Varroa destructor* transmission from collapsing honey bee colonies to their neighbors. PLoS One, 14(6), e0218392.

Petneházy, Ö., Rück, S., Sós, E., & Reinitz, L. Z. (2023). 3D Reconstruction of the blood supply in an elephant's forefoot using fused CT and MRI sequences. Animals, 13(11), 1789.

Piou, V., Arafah, K., Bocquet, M., Bulet, P., & Vétillard, A. (2024). The proteomic content of *Varroa destructor* gut varies according to the developmental stage of its host. PLoS Pathogens, 20(12), e1012802.

Piou, V., Vilarem, C., Rein, C., Sprau, L., & Vétillard, A. (2021). Standard methods for dissection of *Varroa destructor* Females. Insects, 13(1), 37.

Plate, M., Bernstein, R., Hoppe, A., & Bienefeld, K. (2020). Long-term evaluation of breeding scheme alternatives for endangered honeybee subspecies. Insects, 11(7), 404.

Poinapen, D., Konopka, J. K., Umoh, J. U., Norley, C. J., McNeil, J. N., & Holdsworth, D. W. (2017). Micro-CT imaging of live insects using carbon dioxide gas-induced hypoxia as anesthetic with minimal impact on certain subsequent life history traits. BMC Zoology, 2(1), 9.

Polatto, L. P., Chaud-Netto, J., & Alves-Junior, V. V. (2014). Influence of abiotic factors and floral resource availability on daily foraging activity of bees: influence of abiotic and biotic factors on bees. Journal of Insect Behaviour, 27, 593-612.

Popescu, A., Dinu, T. A., Stoian, E., & Şerban, V. (2021). Honey production in the European Union in the period 2008-2019-a statistical approach. Scientific Papers Series Management, Economic Engineering in Agriculture and Rural Development, 21(2), 461-474

Porporato, M., Manino, A., Cuttini, D., Lorenzon, S., Ciaudano, S., & Parodi, V. (2022). Varroa control by means of a hyperthermic device. Applied Sciences, 12(16), 8138.

Potts, S. G., Imperatriz-Fonseca, V., Ngo, H. T., Aizen, M. A., Biesmeijer, J. C., Breeze, T. D., Dicks, L. V., Garibaldi, A. L., Hill, R., Settele, J., & Vanbergen, A. J. (2016). Safeguarding pollinators and their values to human well-being. Nature, 540(7632), 220-229.

Power, K., Martano, M., Altamura, G., Piscopo, N., & Maiolino, P. (2021). Histopathological features of symptomatic and asymptomatic honeybees naturally infected by deformed wing virus. Pathogens, 10(7), 874.

Ramsey S.D., Ochoa R., Bauchan G, Gulbronson C, Joseph D. Mowery, Cohen A., Lim D., Joklik J., Cicero M. J., Ellis D. J., Hawthorne D., van Engelsdorp D., (2019). *Varroa destructor* feeds primarily on honey bee fat body tissue and not hemolymph; PNAS January 29, 116 (5)

Rath, W. (1999). Co-adaptation of *Apis cerana* Fabr. and *Varroa jacobsoni* Oud. Apidologie, 30(2-3), 97-110.

Rathore, N., & Agrawal, D. (2024). Automated precision beekeeping for accessing bee brood development and behaviour using deep CNN. Bulletin of Entomological Research, 114(1), 77-87.

Reams, T., & Rangel, J. (2022). Understanding the enemy: a review of the genetics, behaviour and chemical ecology of *Varroa destructor*, the parasitic mite of *Apis mellifera*. Journal of Insect Science, 22(1), 18.

Reams, T., Rueppell, O., & Rangel, J. (2024). Honey bee (*Apis mellifera*) nurse bee visitation of worker and drone larvae increases *Varroa destructor* mite cell invasion. Journal of Insect Science, 24(3), 16.

Rembold, H., Kremer, J. P., & Ulrich, G. M. (1980). Characterization of postembryonic developmental stages of the female castes of the honey bee, *Apis mellifera* L. Apidologie, 11(1), 29-38.

Remnant, E. J., Shi, M., Buchmann, G., Blacquière, T., Holmes, E. C., Beekman, M., & Ashe, A. (2017). A diverse range of novel RNA viruses in geographically distinct honey bee populations. Journal of Virology, JVI. 00158-00117.

Ribière, M., Ball, B., & Aubert, M. (2008). Natural history and geographical distribution of honey bee viruses. Virology and the honey bee, 6th Framework. EC Publications, Brussels, 15-84.

Richardson, B. L., & Myser, W. C. (1973). Radiation effects on the hemolymph free amino acid pool of the honeybee prepupa (*Apis mellifera*) and the waxmoth larva (*Galleria mellonella*). Radiation Research, 54(2), 274-283.

Rittschof, C. C., & Nieh, J. C. (2021). Honey robbing: could human changes to the environment transform a rare foraging tactic into a maladaptive behaviour? Current Opinion in Insect Science, 45, 84-90.

Rosengaus, R. B., Traniello, J. F., Chen, T., Brown, J. J., & Karp, R. D. (1999). Immunity in a social insect. The Science of Nature, 86(12), 588-591.

Rosenkranz P., Aumeier P, Ziegelmann B., (2010). Biology and control of *Varroa destructor*, Journal of Invertebrate Pathology, 103, 96-119

Rosenkranz, P. (1993). A Bioassay for the Investigation of Host-finding Behaviour in *Varroa jacobsoni*. Apidologie, 24(5).

Sadd, B. M., Kleinlogel, Y., Schmid-Hempel, R., & Schmid-Hempel, P. (2005). Trans-generational immune priming in a social insect. Biology Letters, 1(4), 386-388.

Seeley, T. D. (1989). The Honey Bee Colony as a Superorganism. American Scientist, 77(6), 546-553.

Seeley, T. D. (2009). The Wisdom of the Hive: The Social Physiology of Honey Bee Colonies. Harvard University Press. United States of America

Seeley, T. D. (2019). The Lives of Bees: The Untold Story of the Honey Bee in the Wild. Princeton University Press. United States of America

Severson, D. W., & Erickson Jr, E. H. (1990). Quantification of cluster size and low ambient temperature relationships in the honey bee. Apidologie, 21(2), 135-142.

Sharma, A., Agrawal, A. K., Singh, B., Kumar, S., Brockmann, A., & Bala, M. (2025). Micro-CT based internal morphological analysis of blowfly (*Chrysomya megacephala*): a potential tool to age blowfly pupae having forensic implications. International Journal of Tropical Insect Science, 1-11.

Shawer, D. M., Rakha, O. M., Taha, E. K. A., Al-Kahtani, S. N., & Elnabawy, E. M. (2021). The impact of caging the queens during the flow season on some biological activities of honeybee colonies. Saudi Journal of Biological Sciences, 28(5), 2975-2979.

Shik, J. Z., Hou, C., Kay, A., Kaspari, M., & Gillooly, J. F. (2012). Towards a general life-history model of the superorganism: predicting the survival, growth and reproduction of ant societies. Biology Letters, 8(6), 1059-1062.

Simone-Finstrom, M. (2017). Social immunity and the superorganism: Behavioural defenses protecting honey bee colonies from pathogens and parasites. Bee World, 94(1), 21-29.

Smith, D. B., Bernhardt, G., Raine, N. E., Abel, R. L., Sykes, D., Ahmed, F., Pedroso, I., & Gill, R. J. (2016). Exploring miniature insect brains using micro-CT scanning techniques. Scientific Reports, 6(1), 21768.

Smith, M. L., & Peck, D. T. (2023). Dynamics of honey bee colony death and its implications for *Varroa destructor* mite transmission using observation hives. Apidologie, 54(1), 13.

Smoliński, S., Langowska, A., & Glazaczow, A. (2021). Raised seasonal temperatures reinforce autumn *Varroa destructor* infestation in honey bee colonies. Scientific Reports, 11(1), 22256.

Southwick, E. E., & Heldmaier, G. (1987). Temperature control in honey bee colonies. Bioscience, 37(6), 395-399.

Spivak, M., & Danka, R. G. (2021). Perspectives on hygienic behaviour in *Apis mellifera* and other social insects. Apidologie, 52(1), 1-16.

Spötter, A., Gupta, P., Nürnberg, G., Reinsch, N., & Bienefeld, K. (2012). Development of a 44K SNP assay focussing on the analysis of a varroa-specific defence behaviour in honey bees (*Apis mellifera carnica*). Molecular Ecology Resources, 12(2), 323-332.

Sprau, L., Gessler, B., Liebsch, M., Traynor, K., Rosenkranz, P., & Hasselmann, M. (2024a). The selection traits of mite non-reproduction (MNR) and Varroa sensitive hygiene (VSH) show high variance in subsequent generations and require intensive time investment to evaluate. Apidologie, 55(5), 68.

Sprau, L., Traynor, K., Gessler, B., Hasselmann, M., & Rosenkranz, P. (2024b). Mite non-reproduction is not a consequence of the brood removal behaviour of varroa sensitive hygiene honey bee colonies (*Apis mellifera*). Ecology and Evolution, 14(6), e11595.

Stabentheiner, A., Kovac, H., & Brodschneider, R. (2010). Honeybee colony thermoregulation–regulatory mechanisms and contribution of individuals in dependence on age, location and thermal stress. PLoS One, 5(1), e8967.

Stabentheiner, A., Kovac, H., Mandl, M., & Käfer, H. (2021). Coping with the cold and fighting the heat: thermal homeostasis of a superorganism, the honeybee colony. Journal of Comparative Physiology A, 207(3), 337-351.

Stabentheiner, A., Nagy, J. M., Kovac, H., Käfer, H., Petrocelli, I., & Turillazzi, S. (2022). Effect of climate on strategies of nest and body temperature regulation in paper wasps, *Polistes biglumis* and *Polistes gallicus*. Scientific Reports, 12(1), 3372.

Stabentheiner, A., Pressl, H., Papst, T., Hrassnigg, N., & Crailsheim, K. (2003). Endothermic heat production in honeybee winter clusters. Journal of Experimental Biology, 206(2), 353-358.

Starks, P. T., Blackie, C. A., & Seeley, T. D. (2000). Fever in honeybee colonies. The Science of Nature, 87(5), 229-231.

Sumpter, D. J. T., & Broomhead, D. S. (2000). Shape and dynamics of thermoregulating honey bee clusters. Journal of Theoretical Biology, 204(1), 1-14.

Swart, P., Wicklein, M., Sykes, D., Ahmed, F., & Krapp, H. G. (2016). A quantitative comparison of micro-CT preparations in Dipteran flies. Scientific Reports, 6(1), 39380.

Taha E.K.A. & El-Sanat S.I. 2007: Effect of combs age on honey production and its physical and chemical properties. Bulletin of Entomology Society Egypt 2, 9-18.

Taha, E. K. A., & Al-Kahtani, S. N. (2020). The relationship between comb age and performance of honey bee (*Apis mellifera*) colonies. Saudi Journal of Biological Sciences, 27(1), 30-34.

Taha, E. K. A., Manosur, H. M., & Shawer, M. B. (2010). The relationship between comb age and the amounts of mineral elements in honey and wax. Journal of Apicultural Research, 49(2), 202-207.

Tarpy, D. R., Vanengelsdorp, D., & Pettis, J. S. (2013). Genetic diversity affects colony survivorship in commercial honey bee colonies. The Science of Nature, 100(8), 723-728.

Tautz, J., Maier, S., Groh, C., Rössler, W., & Brockmann, A. (2003). Behavioural performance in adult honey bees is influenced by the temperature experienced during their pupal development. Proceedings of the National Academy of Sciences, 100(12), 7343-7347.

Tentcheva, D., Gauthier, L., Bagny, L., Fievet, J., Dainat, B., Cousserans, F., Colin, E. M., & Bergoin, M. (2006). Comparative analysis of deformed wing virus (DWV) RNA in *Apis mellifera* and *Varroa destructor*. Apidologie, 37(1), 41-50.

Tilton, E.W., and Brower, J. H., 1983. Radiation effects on arthropods. In: Josephson, E. S., Peterson, M.S., editors. Preservation of food by ionizing radiation, CRC Press Inc. Chapter 2, 269-316.

Tome, H. V., Schmehl, D. R., Wedde, A. E., Godoy, R. S., Ravaiano, S. V., Guedes, R. N., Martins, F. G., & Ellis, J. D. (2020). Frequently encountered pesticides can cause multiple disorders in developing worker honey bees. Environmental Pollution, 256, 113420.

Toulkeridou, E., Gutierrez, C. E., Baum, D., Doya, K., & Economo, E. P. (2023). Automated segmentation of insect anatomy from micro-CT images using deep learning. Natural Sciences, 3(4), e20230010.

Traynor, K. S., Mondet, F., de Miranda, J. R., Techer, M., Kowallik, V., Oddie, M. A., Chantawannakul, P., & McAfee, A. (2020). *Varroa destructor*: A complex parasite, crippling honey bees worldwide. Trends in Parasitology, 36(7), 592-606.

Tucker, K. W. (1978). Honey Bee Pests, Predators, and Diseases, edited by Morse, A. R., Cornell University Press, Ithaca, NY, Chapter 16, 410-411.

U.S. Department of Agriculture, Natural Resources Conservation Service (USDA-NRCS). Insects and Pollinators: Pollinators by the Numbers. (2016). Available online: www.nrcs.usda.gov/wps/portal/nrcs/main/national/plantsanimals/pollinate (accessed on 5 July 2021).

Urban, M., & Chlebo, R. (2024). Current Status and Future Outlooks of Precision Beekeeping Systems and Services. Reviews in Agricultural Science, 12, 165-181.

Utaipanon, P., Holmes, M. J., Chapman, N. C., & Oldroyd, B. P. (2019). Estimating the density of honey bee (*Apis mellifera*) colonies using trapped drones: area sampled and drone mating flight distance. Apidologie, 50(4), 578-592.

Van Dooremalen C., E.Stam, L. Gerritsen, B. Cornelisen, J. van der Steen, F. van Langevelde, T. Blacquiére, (2013). Interactive effect of reduced pollen availability and *Varroa destructor* infestation limits growth and protein content of young honey bees. Journal of Insect Physiology, 59 (4), 487-493.

Van Dooremalen, C., & van Langevelde, F. (2021). Can colony size of honeybees (*Apis mellifera*) be used as predictor for colony losses due to *Varroa destructor* during winter? Agriculture, 11(6), 529.

Van Dooremalen, C., Gerritsen, L., Cornelissen, B., van der Steen, J. J., van Langevelde, F., & Blacquiere, T. (2012). Winter survival of individual honey bees and honey bee colonies depends on level of *Varroa destructor* infestation. PLoS One, 7(4), e36285.

Van Doremalen, R. F. M., Van Netten, J. J., Van Baal, J. G., Vollenbroek-Hutten, M. M. R., & van der Heijden, F. (2019). Validation of low-cost smartphone-based thermal camera for diabetic foot assessment. Diabetes Research and Clinical Practice, 149, 132-139.

Walsh, E. M., Sweet, S., Knap, A., Ing, N., & Rangel, J. (2020). Queen honey bee (*Apis mellifera*) pheromone and reproductive behaviour are affected by pesticide exposure during development. Behavioural Ecology and Sociobiology, 74, 1-14.

Warner, S., Pokhrel, L. R., Akula, S. M., Ubah, C. S., Richards, S. L., Jensen, H., & Kearney, G. D. (2024). A scoping review on the effects of Varroa mite (*Varroa destructor*) on global honey bee decline. Science of the Total Environment, 906, 167492.

Winston, M. L. (1991). The Biology of the Honey Bee. Harvard University Press, Cambridge. MA, Chapter 3, 15-18.

Wipfler, B., Pohl, H., Yavorskaya, M.I. & Beutel, R.G. (2016) A review of methods for analysing insect structures the role of morphology in the age of phylogenomics. Current Opinion in Insect Science, 18, 60-68

Xie, X., Huang, Z. Y., & Zeng, Z. (2016). Why do Varroa mites prefer nurse bees? Scientific Reports, 6(1), 28228.

Xu, X., Zhou, S., Huang, J., Geng, F., Zhu, X., & Abou-Shaara, H. F. (2025). Influence of hyperthermia treatment on varroa infestation, viral infections, and honey bee health in beehives. Insects, 16(2), 168.

Yamada, H., Dias, V. S., Parker, A. G., Maiga, H., Kraupa, C., Vreysen, M. J., Mamai, W., Schetelig, F. M., Somda, N. S. B., & Bouyer, J. (2022). Radiation dose-rate is a neglected critical parameter in dose–response of insects. Scientific Reports, 12(1), 6242.

Yañez, O., Piot, N., Dalmon, A., De Miranda, J. R., Chantawannakul, P., Panziera, D., Amiri, E., Smagghe, G., Schroeder, D., & Chejanovsky, N. (2020). Bee viruses: routes of infection in hymenoptera. Frontiers in Microbiology, 11, 943.

Yue, C., Schröder, M., Bienefeld, K., & Genersch, E. (2006). Detection of viral sequences in semen of honeybees (*Apis mellifera*): evidence for vertical transmission of viruses through drones. Journal of Invertebrate Pathology, 92(2), 105-108.

Zhukovskaya, M., Yanagawa, A., & Forschler, B. T. (2013). Grooming behaviour as a mechanism of insect disease defense. Insects, 4(4), 609-630.

Ziegelmann, B., Lindenmayer, A., Steidle, J., & Rosenkranz, P. (2013). The mating behaviour of *Varroa destructor* is triggered by a female sex pheromone: Part 1: Preference behaviour of male mites in a laboratory bioassay. Apidologie, 44(3), 314-323.

ACKNOWLEDGEMENT

I would also like to acknowledge and thank all those individuals who contributed to this research and made the completion of this dissertation possible.

First and foremost, I would like to express my profound gratitude to Professor Sándor Keszthelyi and Dr. Tamás Donkó for giving me the opportunity to work as a PhD student under their supervision. I am deeply thankful for their continuous support, encouragement, and trust throughout this period, regardless of the circumstances.

I am also deeply grateful to my co-authors for their valuable contributions, collaboration, and support:
Dr. Ádám Csóka, Dr. Katalin Somfalvi-Tóth, Dr. Ildikó Jócsák, Dr. Janka Turbók, Dr. Sándor Farkas, Szilvia Orsi-Gibicsár, Csaba Glavák, Tamás Schieszl, Zsombor Zakk, Tamás Kiss and Antal Binder.

Finally, I would like to express my heartfelt gratitude to my family for their continuous support throughout my doctoral studies, particularly for their invaluable assistance with the practical aspects of the beekeeping-related research. I would like to extend my special thanks to my wife, Dr. Szabina Simon, for her unwavering support, patience, and encouragement during this period.

PUBLICATIONS AND PRESENTATIONS

Peer-reviewed papers relevant to the dissertation

Keszthelyi, S., **Sipos, T**., Csóka, Á., & Donkó, T. (2021), CT-supported analysis of the destructive effects of *Varroa destructor* on the pre-imaginal development of honey bee, *Apis mellifera*. Apidologie, 52(1), 155-162.

Sipos, T., Donkó, T., Jócsák, I., & Keszthelyi, S. (2021), Study of Morphological Features in Pre-Imaginal Honey Bee Impaired by *Varroa destructor* by Means of Computer Tomography. Insects, 12(8), 717.

Sipos, T., Donko, T., Csoka, A., Kiss, T., & Keszthelyi, S. (2023), Comparative micro-computed tomographic analysis of the structure of brood cells and its effect on the development of the pupae of honey bee (*Apis mellifera*). European Journal of Entomology, 120.

Sipos, T., Glavák, C., Turbók, J., Somfalvi-Tóth, K., Donkó, T., & Keszthelyi, S. (2024), Analysis of X-ray irradiation effects on the mortality values and hemolymph immune cell composition of *Apis mellifera* and its parasite, *Varroa destructor*. Journal of Invertebrate Pathology, 204, 108109.

Sipos, T., Orsi-Gibicsár, S., Schieszl, T., Donkó, T., Zakk, Z., Farkas, S., Binder, A., & Keszthelyi, S. (2024). Tracking Varroa Parasitism Using Handheld Infrared Cameras: Is Eusocial Fever the Key? Insects, 15(9), 693.

Oral presentations and conference abstracts

Sipos T., Donkó T., Keszthelyi S., (2022), Mézelő méh ázsiai méhatka által okozott morfológiai és szervi elváltozásainak diagnosztikai CT-vel történő elemzése, EFOP 3.6.3-VEKOP-16-2017-00008, Kaposvár, 2022. 04.27., Kaposvár

Sipos T., Donkó T., Glavák Cs., Turbók J., Keszthelyi S., (2023), Röntgen sugárzáson alapuló módszer fejlesztése az ázsiai méhatka (*Varroa destructor*) elleni védekezésben, Magyar Agrár-és Élettudományi Egyetem ÚNKP konferencia, 2023. 03.29. Kaposvár

Sipos T., Donkó T., Keszthelyi S., (2023), A modern képalkotási technikák nyújtotta lehetőségek a beporzók védelmében, II. Alkalmazott Növénytudományi Konferencia: Roncsolásmentes képalkotó technológiák a növénytermesztésben: legújabb eredmények és alkalmazási lehetőségek 2023. 09. 28. Kaposvár: Konferencia-összefoglaló. (pp. 43-44).

Sipos T., Donkó T., Zakk Zs., Orsi-Gibicsár S. Keszthelyi S., (2024), Az ázsiai méhatka kaptáron belüli elhelyezkedésének meghatározása infravörös képelemzéssel, Magyar Agrár-és Élettudományi Egyetem ÚNKP konferencia, 2024. 03.20. Kaposvár

Sipos T., Lukács H., Keszthelyi S., Donkó T., Csóka Á., Orsi-Gibcsar Sz., (2024), Application of human diagnostic computed tomography in the field of entomological research at Kaposvár Campus, In XXVII. Tavaszi Szél Konferencia 2024 - Absztrakt kötet (pp. 639-641).

Sipos T., (2024), Szántóföldi peszticides kezelések valamint biotikus és abiotikus befolyásoló tényezők hatása a mézelő méh egészségügyi állapotára, Magyar Tudomány Ünnepe növényvédelmi rendezvény, MTA VEAB Növényvédelmi Munkabizottság, 2024.11.18., Keszthely

Sipos T., (2025), Entomológiai vonatkozás képalkotó vizsgálatok, VI. Országos Röntgentomográfiás Fórum, Pannon Egyetem, 2025.06.19-20., Veszprém